*REPORT NO.*
*UCD/CGM-95/02*

*CENTER FOR GEOTECHNICAL MODELING*

# INVESTIGATION AND EVALUATION OF LIQUEFACTION RELATED GROUND DISPLACEMENTS AT MOSS LANDING DURING THE 1989 LOMA PRIETA EARTHQUAKE

**BY**

**ROSS W. BOULANGER**
**IZZAT M. IDRISS**
**LELIO H. MEJIA**

*Research supported by the U. S. Geological Survey (USGS), Department of the Interior, under USGS award number 1434-93-G-2337.*


*DEPARTMENT OF CIVIL & ENVIRONMENTAL ENGINEERING*
*COLLEGE OF ENGINEERING*
*UNIVERSITY OF CALIFORNIA AT DAVIS*

*MAY 1995*

# INVESTIGATION AND EVALUATION OF LIQUEFACTION RELATED GROUND DISPLACEMENTS AT MOSS LANDING DURING THE 1989 LOMA PRIETA EARTHQUAKE

by

Ross W. Boulanger, Izzat M. Idriss, and Lelio H. Mejia

Research supported by the U.S. Geological Survey (USGS), Department of the Interior, under USGS award number 1434-93-G-2337. The views and conclusions contained in this document are those of the authors and should not be interpreted as necessarily representing the official policies, either expressed or implied, of the U.S. Government.

Report No. UCD/CGM-95/02

Center for Geotechnical Modeling
Department of Civil & Environmental Engineering
University of California
Davis, California

May 1995

## ABSTRACT

The 1989 Loma Prieta earthquake caused extensive liquefaction in the area of Moss Landing, located midway between Santa Cruz and Monterey on Monterey Bay. The results of an investigation and evaluation of liquefaction-related ground displacements at select locations in the Moss Landing area are presented in this report. Effects of the earthquake ranged from no observable deformation or damage at some locations, to more than 2 m of liquefaction-induced lateral spreading at the nearly collapsed, $6 million Moss Landing Marine Laboratory. This study provides information regarding the range of earthquake effects and ground displacements observed, the various soils encountered, the detailed stratigraphy at several sites, the different insitu testing methods used, and a unique set of inclinometer data within a laterally spreading shoreline. Analyses of these data provide insight into the application of commonly used methodologies for predicting the occurrence and effects of earthquake-induced liquefaction. These data are also compared against current semi-empirical correlations between cyclic strength and the results of standard penetration test (SPT), cone penetration test (CPT), and shear wave velocity measurements. Lessons are drawn regarding the influence of thin soil strata on overall site behavior, the use of SPT, CPT and shear wave velocity measurements to identify critical strata, and the distribution of deformations within a lateral spread as described by inclinometer measurements. It is hoped that the data and results presented in this report will provide a basis for further development of design methodologies for predicting the potential for liquefaction-related damage during earthquakes.

## ACKNOWLEDGEMENTS

This research project has benefitted from the assistance and contributions of many individuals and organizations. The local merchants, organizations, and people of Moss Landing were extremely helpful in the execution of this research project. Our appreciation is extended to the Moss Landing Harbor Master's Office (Larry P. Steffen, Ron Souza, Annelies and Niel), Woodward Marine (Richard Woodward), Gravelle's Boatyard (Ron Gravelle), Phil's Market (Phil DiGirolamo), the Monterey Bay Aquarium Research Institute (Derek Baylis, Gary Burkhart), the Moss Landing Marine Laboratory (James Nybakken, John Oliver, Gary Greene, Larry Jones), the State Parks (Ken Gray), the Monterey County Public Works (Ronald J. Lundquist, Don Collins), Robert F. Barminski of Lee & Pierce Inc., and long-time Moss Landing resident "Whitey."

Gyimah Kasali and John C. Burton of Rutherford and Chekene graciously provided a wealth of field data from geotechnical studies for the Monterey Bay Aquarium Research facilities, and were extremely helpful with their discussions of and assistance on this research project. Data from past field studies were also generously provided by Robert F. Barminski of Lee & Pierce Inc. and by Harding Lawson Associates.

Photographs and documentation of earthquake-induced damage were provided by Leslie F. Harder of the Department of Water Resources, State of California, Bruce L. Kutter of the University of California at Davis, and John Tinsley of the USGS. Dr. Harder's participation in some early field reconnaissance trips is also greatly appreciated. Scott Jones, an undergraduate student at U.C. Davis, compared the pre- and post-earthquake CPT soundings. Peter Gathungu and Mark Meyers, both graduate students at U. C. Davis, assisted with the field work and performed the laboratory testing. Their assistance with this portion of this research is greatly appreciated.

VBI In-Situ Testing, Inc., provided additional support for this research, enabling significantly more CPT soundings to be performed than otherwise would have been possible. Our deepest gratitude is extended to Virgil Baker of VBI for this support. Woodward-Clyde Consultants contributed to the preparation of this report through their professional development program.

Primary support for this research was provided by the U.S. Geological Survey (USGS), Department of the Interior, under USGS award number 1434-93-G-2337. The views and conclusions contained in this document are those of the authors and should not be interpreted as necessarily representing the official policies, either expressed or implied, of the U.S. Government.

## TABLE OF CONTENTS

# 1. INTRODUCTION

## 1.1 Earthquake Damage at Moss Landing

The Loma Prieta earthquake occurred at 5:04 p.m. on October 17, 1989 along a 45 km long segment of the San Andreas fault beneath the Santa Cruz Mountains of California. The earthquake was assigned a surface wave magnitude, $M_s$=7.1, and a moment magnitude, $M_w$=7.0. Sixty-two people were killed, 3,757 were injured, and more than 12,000 were left homeless (EERI 1990). Total damage resulting from this earthquake was estimated to be about $10 billion, making it one of the most costly U.S. disasters at that time.

The Loma Prieta earthquake caused extensive liquefaction at several locations within the area of Moss Landing located on Monterey Bay about 21 km from the earthquake source (Figs. 1-1 and 1-2). Perhaps the most widely known example of liquefaction related damage in the Moss Landing area is the near collapse of the $6 million Moss Landing Marine Laboratory which was damaged beyond repair by liquefaction-induced lateral spreading of its foundation. Liquefaction related deformations were observed along the entire length of the Moss Landing spit, a 150-300 m wide shoreline peninsula, upon which the Marine Laboratory was located. The magnitude of the deformations along the spit varied widely, with structural damage occurring at several locations while at others, the facilities were essentially undamaged. Water and sewer services on the spit could not be fully restored for over three months, thereby severely affecting operation of several commercial fisheries, the Monterey Bay Aquarium Research Institute, and the Moss Landing Harbor.

Liquefaction related deformations and damage was also observed at locations off the spit, including across the harbor at the Moss Landing Harbor Master's Office, at the approach fills to the Highway No. 1 bridge across Elkhorn Slough, and farther north at the Moss Landing State Beach. In contrast, no evidence of liquefaction or significant soil movements was observed in the area of the main facilities of the 2,000 MW Pacific Gas and Electric Power Plant located on the eastern side of Highway No. 1 across from Moss Landing. Overviews of damage in the Moss Landing area can be found in Tuttle et al. (1990), Greene et al (1991), Mejia (1992), and Barminski (1993).

Extensive liquefaction was also observed at Moss Landing following the 1906 San Francisco earthquake (Lawson 1908, and Youd and Hoose 1978). Reports of liquefaction and lateral spreading in the Moss Landing area suggest that liquefaction was more extensive and ground deformations larger during that earthquake than during the Loma Prieta earthquake. The difference in damage between the two earthquakes is consistent with the higher intensity and longer duration of the ground motions likely to have occurred during the 1906 earthquake.

## 1.2 Objective of Study

The objective of this study was to investigate and evaluate liquefaction-related ground displacements in the Moss Landing area during the 1989 Loma Prieta earthquake. Toward this objective, the primary tasks of this research project were the characterization of selected sites and the documentation of their behavior during the Loma Prieta earthquake. This characterization effort provided information regarding the range of earthquake effects and ground displacements observed, the various soils encountered, the detailed characterization of several sites, the different insitu testing

methods used, and the rare set of inclinometer data within a laterally spreading shoreline.

Evaluation of the compiled data included examining the conditions which affected triggering of liquefaction and post-triggering deformations within the framework of common engineering design methodologies. Common engineering design methodologies are semi-empirical correlations that relate the cyclic strength of soil with insitu test data based on case histories of field performance during earthquakes. Many older case histories used to develop the current correlations are of very limited detail, and only a few involved cone penetration test or shear wave velocity measurements. Thus, more well-defined and well-documented case histories using current methods and standards of insitu testing are needed. Accordingly, it is hoped that the data and results presented in this report will provide a basis for further development of semi-empirical correlations for predicting the potential for liquefaction-related damage during earthquakes.

## 1.3 Study Approach

Characterization of the selected sites included compiling existing field and subsurface information and performing additional field exploration. An abundance of existing field and subsurface information was generously provided by consulting engineers who have worked in the Moss Landing area. Additional field exploration included performing rotary wash borings, standard penetration tests (SPT) with energy measurements, cone penetration tests (CPT), seismic cone penetration tests (SCPT), and laboratory tests. Laboratory tests included cyclic triaxial tests on Osterberg tube samples of a clayey silt suspected of having liquefied, and classification tests such as Atterberg Limits and grain size analyses. Documentation of observed field behavior included interviewing local residents and businesses and collecting earthquake damage reports and photographs. Historical records of dredging operations, aerial photographs, and geological reports for the Moss Landing area were also obtained.

Analyses of the compiled data followed two approaches. First, the data for each site were analyzed using relationships that are widely used in practice for predicting the triggering of liquefaction. The SPT data were analyzed using the simplified procedure originally developed by Seed and Idriss (1971) and subsequently updated by the relationships derived by Seed et al. (1985), as shown in Fig. 1-3. The CPT data were analyzed using the relationships proposed by Seed and De Alba (1986) which were derived from the SPT-based curves shown in Fig. 1-3 using the correlation between the ratio $q_c/N_{60}$ and median grain size ($D_{50}$) shown in Fig. 1-4. For this study, SPT and CPT penetration resistances were normalized to an equivalent overburden stress of 1 bar (0.96 tsf) using the correction factor ($C_N$) proposed by Liao and Whitman (1985). The value of $C_N$ was limited to a maximum value of 1.60 and a minimum value of 0.50 as a matter of practice. The results of these analyses allow a comparison between observed occurrences/nonoccurrences of liquefaction and the predictions of liquefaction potential by these widely used relationships.

Second, the field data were used to obtain critical combinations of normalized CPT tip resistance and earthquake-induced cyclic stress ratio for each site. It is important to note that only the actual field evidence (e.g., comparison of surface ejecta with subsurface strata characteristics; penetration resistance profiles, ground deformations) was used to classify a site as having liquefied or not and to subsequently select the critical stratum and depth for potential triggering of liquefaction. The SPT- and CPT-based triggering analyses were not used to make these determinations, nor

allowed to influence the interpretation of the field evidence.

As will be shown, the critical combinations of CPT tip resistance and cyclic stress ratio were not always in good agreement with the relationships proposed by Seed and De Alba (1986). Subsequently, the critical combinations of CPT tip resistance and cyclic stress ratio are compared to the relationships proposed by Mitchell and Tseng (1990) which were derived from cyclic laboratory tests and CPT calibration chamber studies and favorably compared with the results of cyclic laboratory tests on field samples from other studies (Fig. 1-5). Mitchell and Tseng's curves in Fig. 1-5 suggest that cyclic strengths for a given normalized tip resistance are lower than would be predicted by Seed and De Alba's curves in Fig. 1-4. The data from this study will be shown to be in better agreement with the relationships proposed by Mitchell and Tseng (1990) than with those proposed by Seed and De Alba (1986).

In selecting the critical value of normalized CPT penetration resistance for each CPT sounding (for use in liquefaction triggering correlations), several guidelines were adopted to reduce the potential differences in values that may be obtained by different individuals. First, if the critical depth occurred within a thick stratum of similar material, then the critical value was taken as the average tip resistance over a 0.6 m interval. If the 0.6 m interval contained spikes in the tip resistance profile, then the highest and lowest two individual tip resistance measurements were omitted; Note, for CPTs performed in this study, a 0.6 m interval contains 12 individual tip resistance measurements at 0.05 m sampling intervals. Second, if the critical depth occurred near a contact between soft and stiff soils (i.e., clay over sand), then the tip resistance within 0.15 m of the contact was considered to be strongly affected by the adjacent layer and thus omitted from any averaging. While this guideline appeared reasonable in many situations, the actual zone of influence around a CPT tip is likely larger than provided for by this guideline and thus judgement must be exercised on a case by case basis. Third, if the critical stratum was less than 0.6 m thick (excluding zones influenced by adjacent contacts), then the average value was taken over an appropriately narrower interval (but never less than 0.15 m thick). This guideline was useful for sand lenses between overlying and underlying softer clays, and essentially accounts for the fact that a minimum sand layer thickness of about 0.45 m is required to get a reasonably representative tip resistance.

Shear wave velocities were measured at several sites, and normalized to an equivalent overburden stress of 1 bar using the expression (Robertson et al. 1992):

$$V_{s\text{-}1} = V_s (P_a/\sigma_v')^{0.25}$$

where $V_{s\text{-}1}$ is the normalized shear wave velocity in m/s, $V_s$ is the measured shear wave velocity in m/s, $P_a$ is the reference stress of 1 bar (100 kpa), and $\sigma_v'$ is the effective vertical overburden stress in the same units as $P_a$. Critical combinations of normalized shear wave velocity and cyclic stress ratio from each site were compared to the relationship proposed by Robertson et al. (1992) in Fig. 1-6. In Section 11.3, the compiled data from this study will also be compared to the relationship proposed by Tokimatsu et al. (1991) in Fig. 1-7, for which the normalized shear wave velocity is calculated as:

$$V_{s\text{-}1} = V_s (P_a/\sigma_m')^{0.33}$$

where $\sigma_m'$ is the mean effective stress in the same units as $P_a$, and $\sigma_m'$ is calculated as $(1+2K_o)\sigma_v'/3$ where $K_o$ is the earth pressure coefficient at rest. Note that the profiles of $V_{s\text{-}1}$ shown in this report were normalized using the expression recommended by Robertson et al. (1991). Issues affecting the representativeness of shear wave velocity measurements, particularly for thin strata, are discussed on

a case by case basis.

This report is structured as follows: Chapters 2, 3, and 4 provide background on the geologic setting, ground motions, and methods of field investigation; Chapters 5, 6, 7, 8, 9 and 10 cover individual sites within the Moss Landing area; Chapter 11 presents the discussion and major findings of this study; and Chapter 12 contains some concluding remarks.

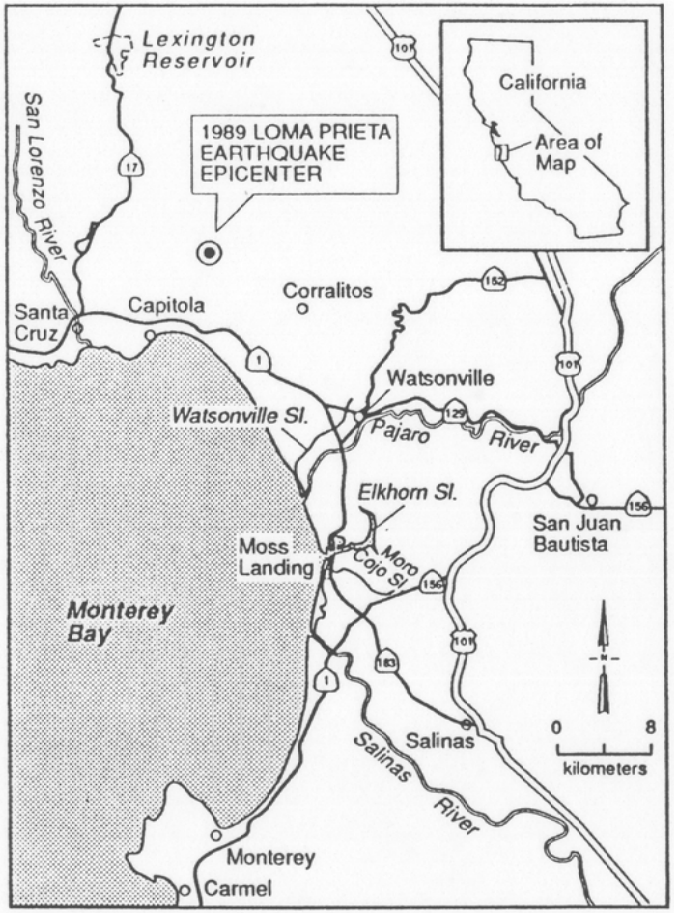


FIG. 1-1. Location of Moss Landing

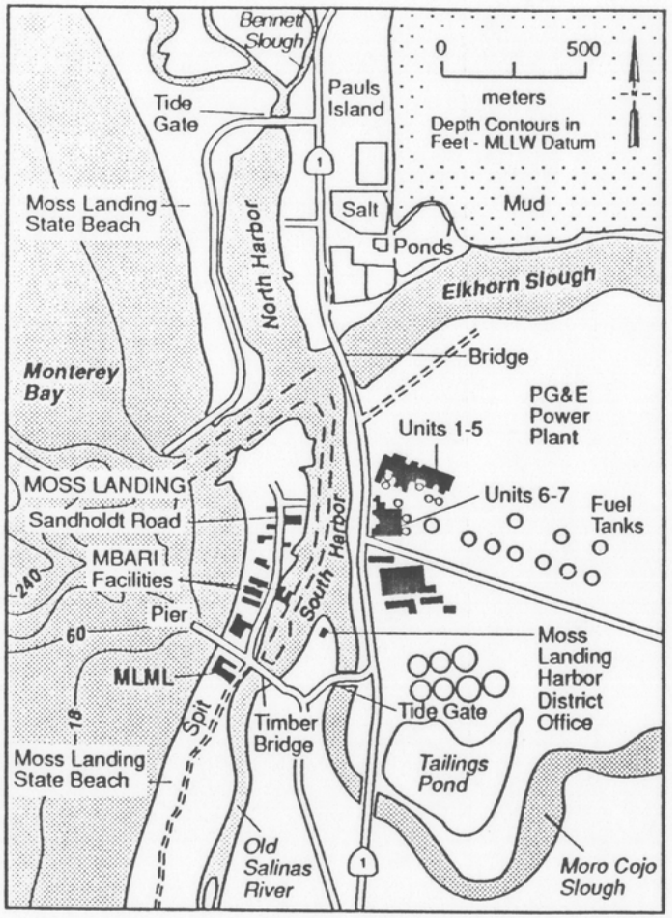


FIG. 1-2. Site Map of the Moss Landing Area

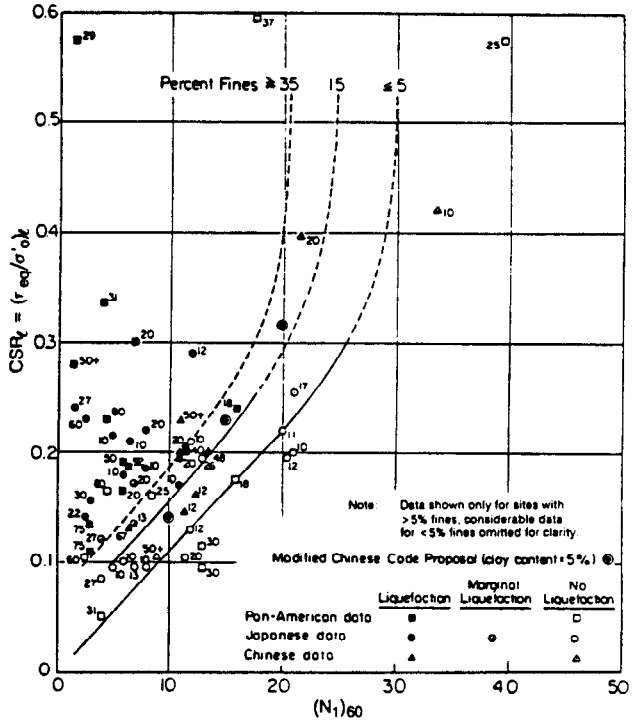


FIG. 1-3. Proposed Relationship Between Corrected SPT Blow Count and Cyclic Stress Ratio Required to Cause Liquefaction (Seed et al. 1985)

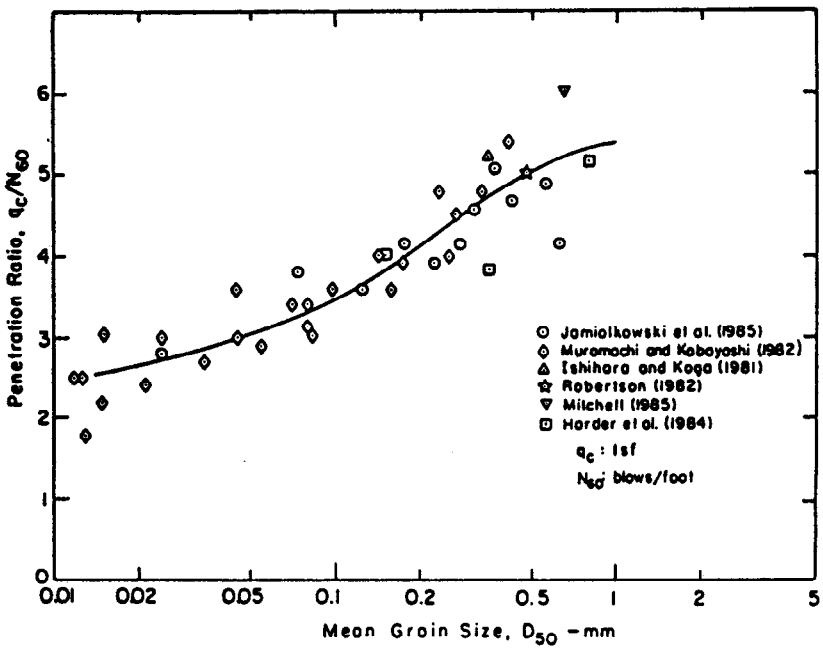


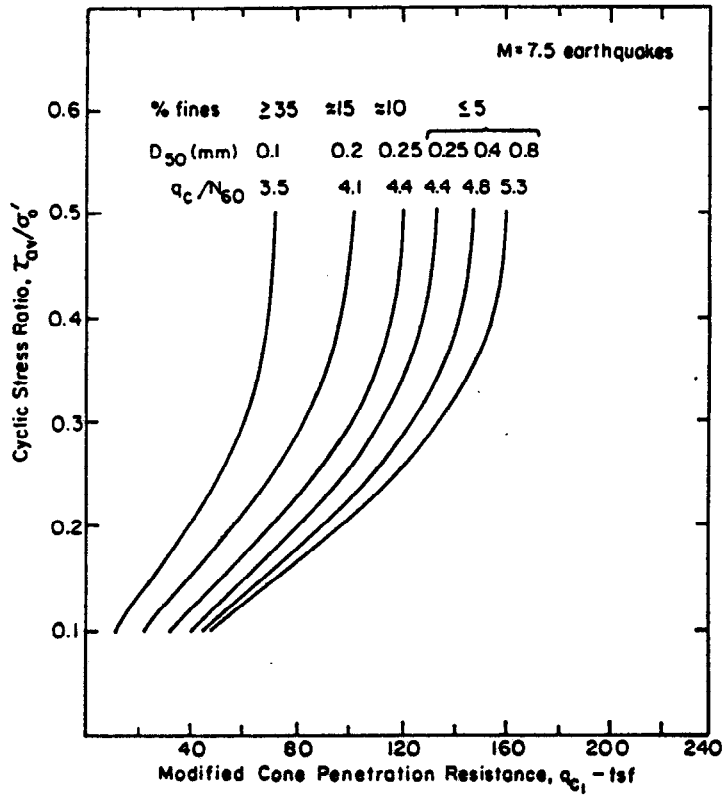


FIG. 1-4. Proposed Relationships Between Normalized CPT Tip Resistance and Cyclic Stress Ratio Required to Cause Liquefaction: Seed and De Alba (1986)

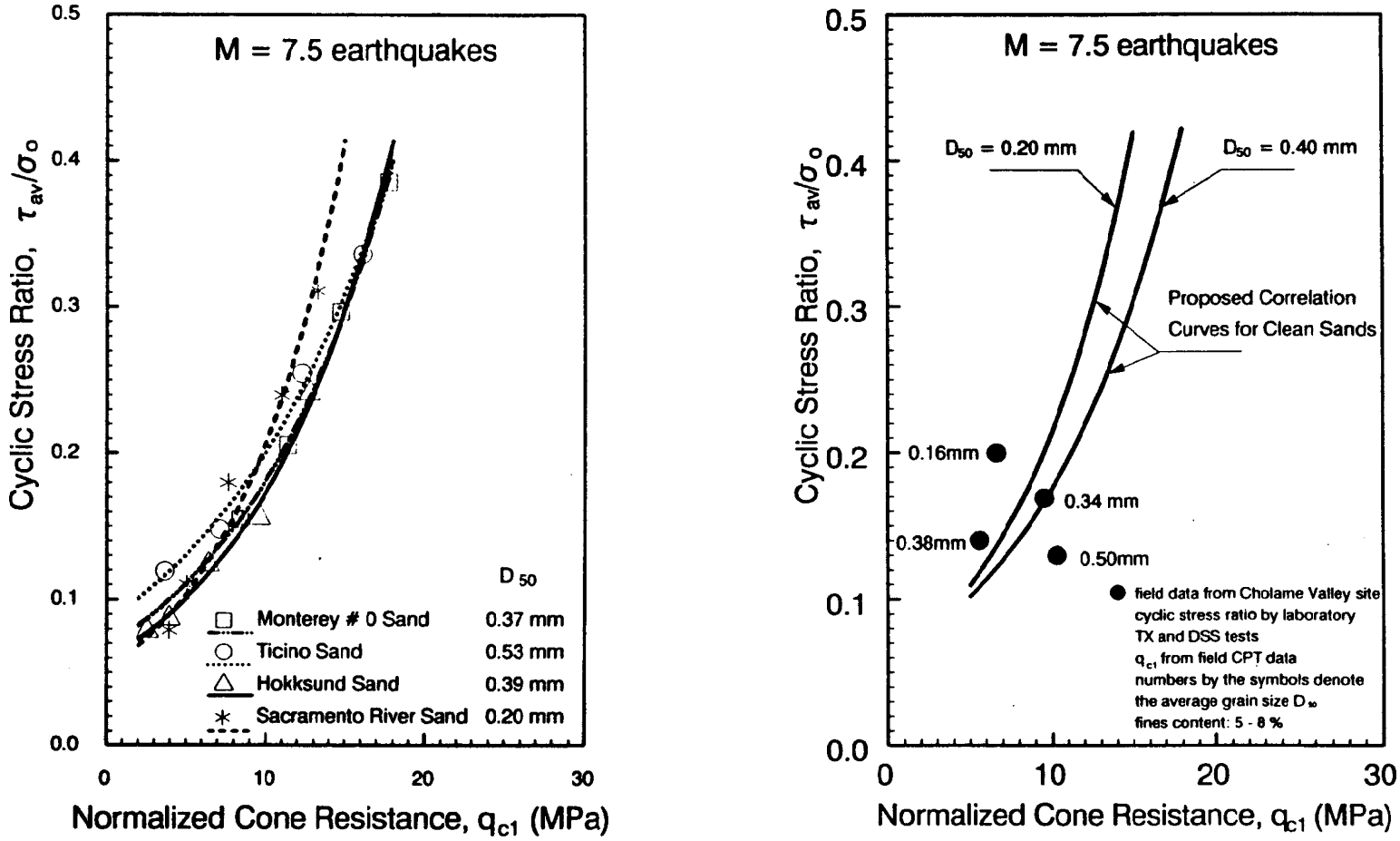


FIG. 1-5. Proposed Relationships Between Normalized CPT Tip Resistance and Cyclic Stress Ratio Required to Cause Liquefaction: Mitchell and Tseng (1990)

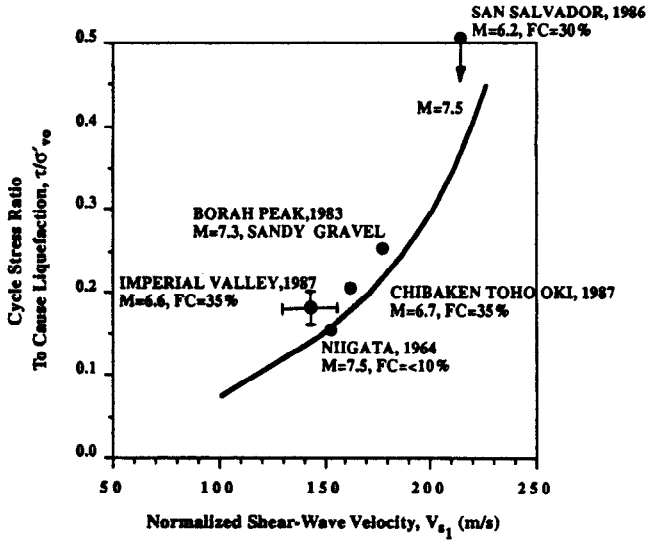


FIG. 1-6. Proposed Correlation Between Normalized Shear Wave Velocity and Cyclic Stress Ratio to Cause Liquefaction for M=7.5 Earthquakes (Robertson et al. 1992)

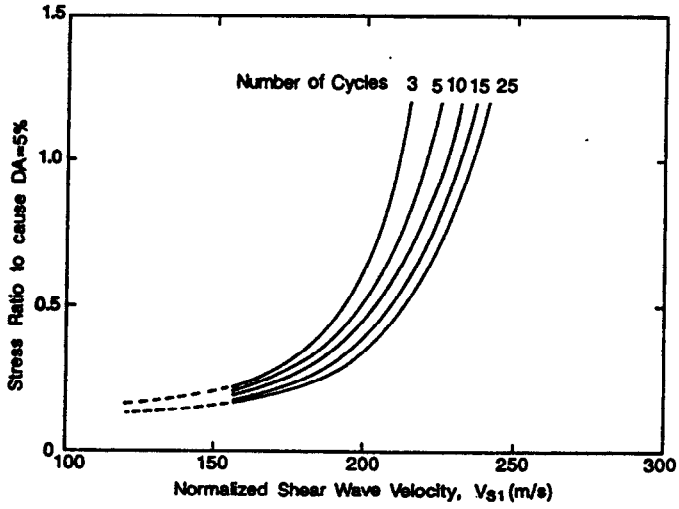


FIG. 1-7. Proposed Correlation Between Normalized Shear Wave Velocity and Cyclic Stress Ratio to Cause DA=5% in 15 Cycles of Loading for Clean Sand (Tokimatsu et al. 1991)

## 2. GEOLOGIC SETTING

Moss Landing is located on Monterey Bay about midway between Santa Cruz and Monterey. The area is a focal point for regional surface drainage entering Monterey Bay through the Elkhorn Slough, the Pajaro River located about 5 km to the north, and the Salinas River located about 7 km to the south. The Salinas River flowed into Monterey Bay through an outlet about 2.5 km north of Moss Landing prior to between 1906 and 1910, after which it shifted to its present outlet about 7 km to the south (Gordon 1977; Griggs 1990), as shown in Fig. 2-1. The harbor now occupies part of the old river channel (Fig. 2-1). Evolution of the shoreline in the harbor is summarized in Fig. 2-2, as summarized by Barminski (1993) based on U.S. Department of Commerce survey maps from 1854, 1910, and 1933. An aerial photo of the Moss Landing Harbor from 1952, looking north, is shown in Fig. 2-3.

The area is underlain by Holocene deposits consisting of relatively thick sands offshore and estuarine and fluvial deposits onshore up to about 60 m deep (Dupre and Tinsley 1980). Moss Landing spit is underlain by littoral soils comprising eolian, fluvial, estuarine, and beach deposits of gravel, sand, silt, and clay deposited in a shoreline environment within the zone of tidal fluctuation. Wood encountered at a depth of about 33 m in a boring drilled at the Pacific Gas and Electric Power Plant was estimated to be about 7,000 years old using radio-carbon dating techniques (Dames and Moore 1963). Radio-carbon dating of shell fragments in the sand at a depth of 6.1 m near Woodward Marine suggested an uncorrected age of about 2,000 years (Tinsley 1993). Pleistocene and Miocene deposits extend to a depth of about 2,000 m at which oil exploration logs show Mesozoic granite is encountered (Cooper Clark and Associates 1978).

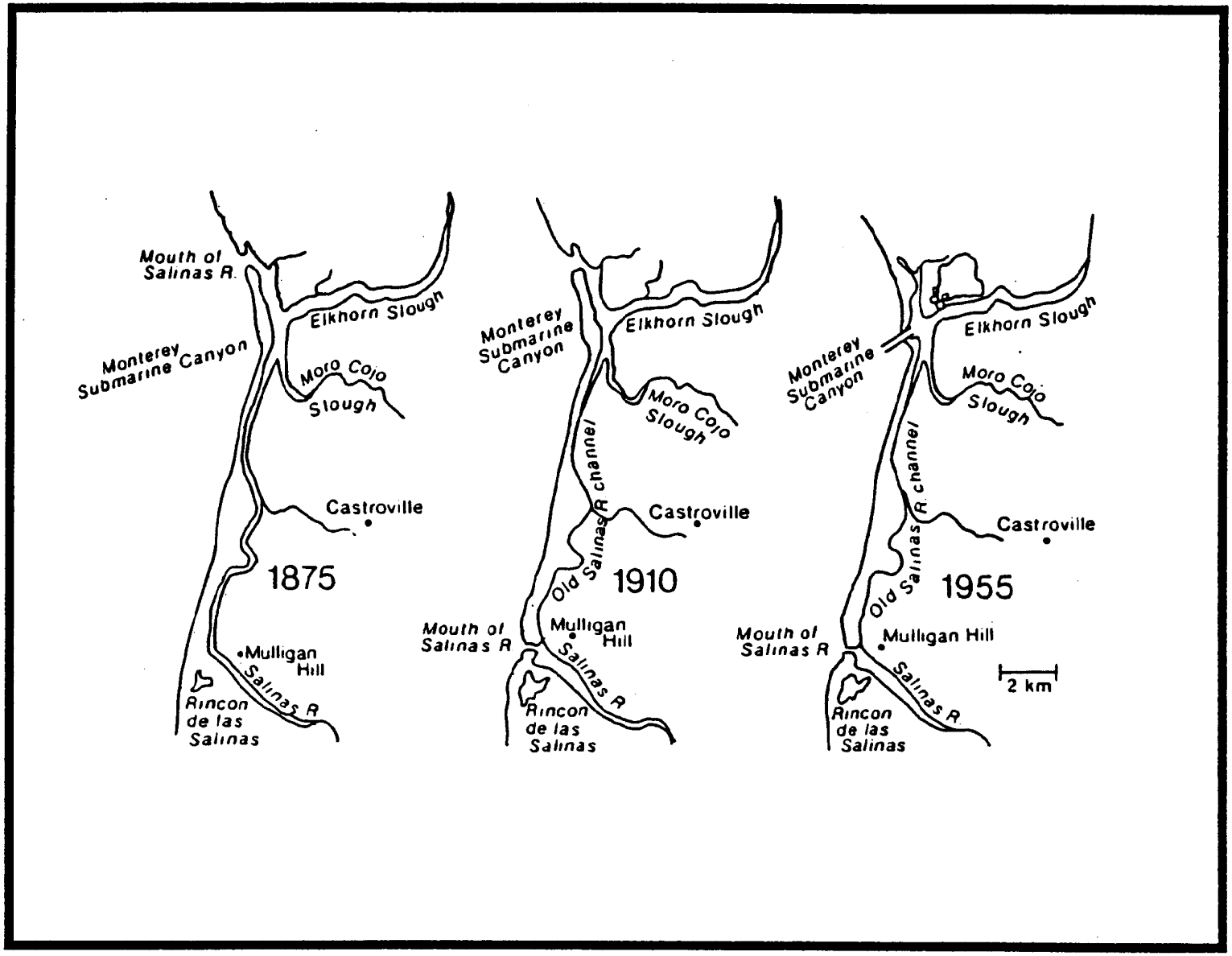


FIG. 2-1. History the Salinas River Mouth (Gordon 1979)

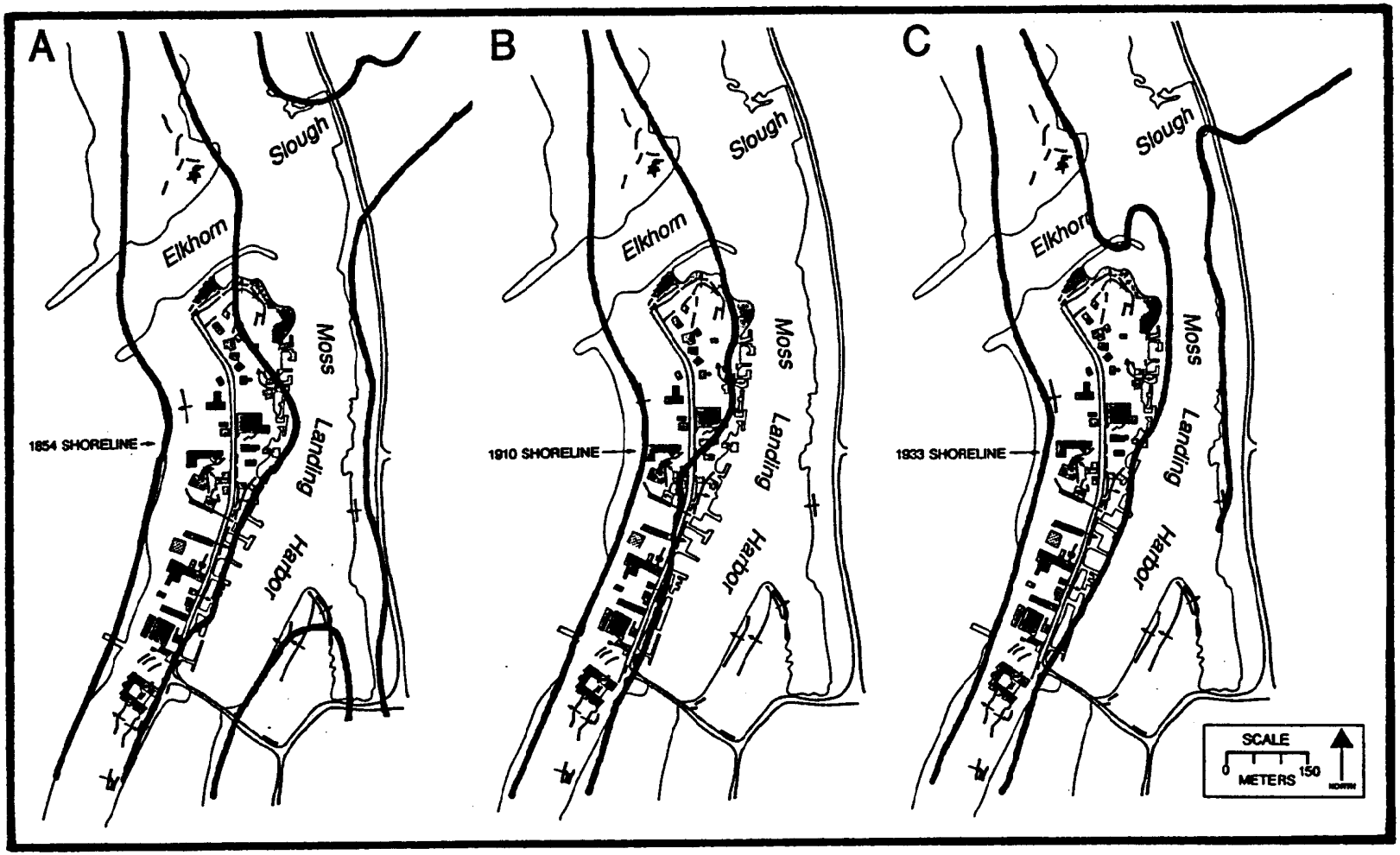


FIG. 2-2. Shoreline Locations from 1854, 1910, and 1933 Surveys (Barminski 1993, based on U.S. Department of Commerce maps)

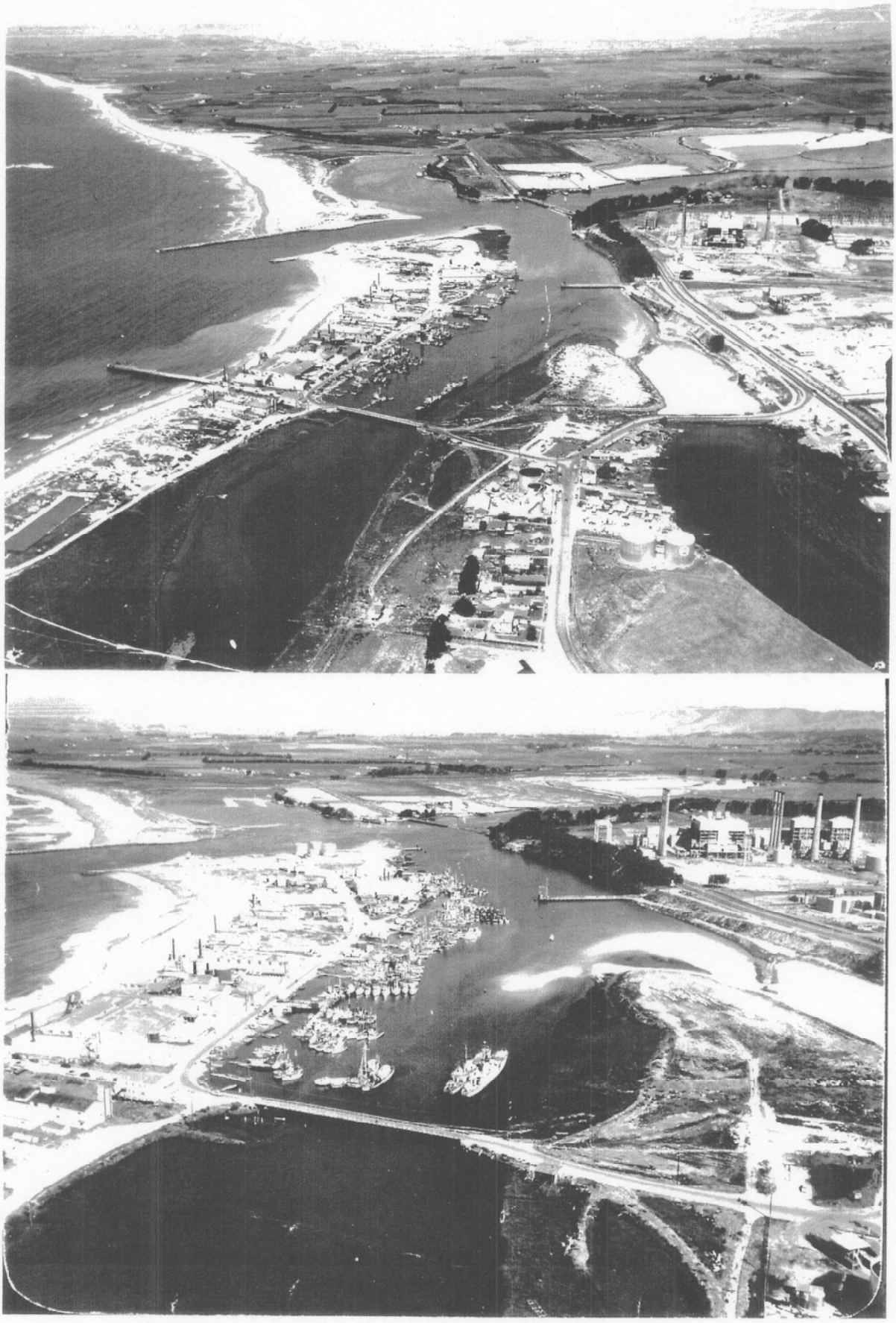

FIG. 2-3. Aerial Photographs of Moss Landing Harbor from 1952.

# 3. GROUND MOTIONS DURING LOMA PRIETA EARTHQUAKE

No ground motion recording instruments were operating near Moss Landing at the time of the 1989 Loma Prieta earthquake. However, several instruments from the California Strong Motion Instrumentation Program (CSMIP) recorded the earthquake motions in the region (Shakal et al. (1989). The peak horizontal accelerations recorded at several stations close to Moss Landing are presented in Table 3-1. The Watsonville and San Juan Bautista stations are not considered free-field ground motions because they involve structures, but are included due to their proximity to Moss Landing. This Table also summarizes the approximate closest distance to the earthquake source and the site conditions for each recording station.

Table 3-1.Strong Motion Records in the Region of Moss Landing

| Recording Station | Distance to Source (km) | Site Condition | Recording location | Peak Horizontal Accelerations (g) | |
|---|---|---|---|---|---|
| | | | | Strong Component, H1 | Weak Component, H2 |
| Watsonville | 8 | Alluvium | 4-story building; ground floor. | 0.39 | 0.28 |
| Capitola - Fire Station | 17 | Alluvium | 1-story building. | 0.54 | 0.47 |
| Santa Cruz - UCSC | 20 | Limestone | 1-story building. | 0.47 | 0.44 |
| San Juan Bautista | 20 | Stiff Alluvium | Bridge overpass; base of column at ground surface. | 0.15 | 0.14 |
| Hollister - South St. & Pine | 29 | Alluvium | Instrument shelter. | 0.38 | 0.18 |
| Sago South - Hollister | 35 | Granite | Instrument shelter. | 0.07 | 0.07 |
| Salinas | 36 | Alluvium | 1-story building; ground floor. | 0.12 | 0.09 |
| Monterey | 47 | Rock | 1-story building; ground floor. | 0.07 | 0.07 |

Based on a review of the strong motion recordings from the Loma Prieta earthquake, the peak horizontal acceleration in the Moss Landing area, located about 21 km from the earthquake source, would have been about 0.15 g if it were underlain by rock or stiff alluvium. However, because the area is underlain by deep alluvium which is generally soft near the surface, the peak horizontal acceleration probably was significantly higher than this value. A peak horizontal acceleration of about 0.20 to 0.30 g would be expected at Moss Landing based on the relationship between peak horizontal accelerations on rock and on soft soils proposed by Idriss (1991).

Numerical simulations using the techniques developed by Wald et al. (1988) and the source and crustal models described by Somerville and Yoshimura (1990) for the 1989 Loma Prieta earthquake suggest that the peak acceleration on a hypothetical rock outcrop at Moss Landing would

have been about 0.15 g (Woodward-Clyde Consultants, 1990). This value is in good agreement with that estimated based on the available recordings and thus supports the above estimate of 0.20 to 0.30 g for the peak horizontal acceleration at Moss Landing.

On a qualitative basis, the estimated range of peak ground acceleration appears consistent with the level of damage to contents of buildings not affected by soil liquefaction and lateral spreading, and with the felt intensity of ground motions by people in the area during the earthquake.

It may be concluded that a peak horizontal acceleration between 0.20 and 0.30 g, say 0.25 g, is a reasonable estimate for evaluating the effects of soil behavior during the 1989 Loma Prieta earthquake at Moss Landing based on the ground motions recorded in the region and the results of the numerical simulations. In particular, a value of 0.25 g would probably represent a median or slightly lower estimate of peak acceleration at this site during the Loma Prieta earthquake, and was thus selected to provide a reasonably conservative assessment of the liquefaction phenomena at this site.

# 4. METHODS OF FIELD INVESTIGATION

Field and subsurface information at Moss Landing were obtained primarily from field investigations by: (1) the University of California at Davis (UCD) under the present research project; (2) Rutherford and Chekene; (3) Harding Lawson and Associates; (4) Woodward-Clyde Consultants; (5) USGS; and (6) Fugro, Inc. Except for UCD, the other investigators were concerned primarily with only one specific location and thus their field investigation methods are described within the relevant sections of this report. The field investigation methods used by UCD in this research project are described below.

Cone penetration tests (CPTs) were performed by VBI In-Situ Testing, Inc., using a 20-ton Hogentogler piezo-electric cone with a 10-$cm^2$ tip, a 20-cm-long friction sleeve, and a pore pressure sensor behind the tip. Shear wave velocity measurements were performed using a Hogentogler piezo-electric seismic cone of similar design. Shear wave velocity measurements were generally performed at intervals of 1.0-2.0 m. Logs of the CPT soundings and shear wave velocity measurements are presented in Appendix A.

Rotary wash borings were performed with a Central Mine Equipment (CME) CME-750 drill rig. A 9.84-cm drag bit was used, after being modified by welding a washer behind the drag bit's teeth to ensure side-discharge of the bentonite drilling fluid. Standard Penetration Tests (SPT) were performed at about 0.76-m intervals (2.5 feet) in the upper portions of the borings and at larger intervals below. A CME 623 N (140-pound) automatic trip hammer was used to drive a 5.08-cm (2-inch) outside diameter, 3.49-cm (1 $^3/_8$-inch) constant inside diameter SPT split spoon sampler (no room for liners). Osterburg tube samples were obtained at select sites using both stainless steel and galvanized steel tubes. Borehole logs are presented in Appendix B. Grain size analyses and Atterberg Limits were performed on select SPT samples. The results of these tests are presented in Appendix C, and summarized on the borehole logs where appropriate.

Energy measurements for the CME rig and hammer used at this site were later performed while drilling at the Moss Landing Marine Laboratory. The energy measurements were performed by George Goble of Goble, Rausch and Likins using both the wave equation method and the ASTM standard method. The energy ratio for this CME automatic trip hammer was estimated to be about 75%.

Aerial photographs of the Moss Landing Harbor area in 1953 and 1967 were obtained from the U.S. Geological Survey, Western Mapping Center, Earth Science Info Center, Menlo Park, California. Additional aerial photographs from 1952 (and other unmarked, but similar dates) were obtained from the archives of the Moss Landing Harbor District.

# 5. MOSS LANDING STATE BEACH ACCESS ROAD

## 5.1 Site Description

Access to the Moss Landing State Beach is provided by a road exiting west off Highway No. 1 just to the north of Elkhorn Slough. This access road, as shown on Figs. 1-2 and 5-1, crosses a tide gate to Bennett Slough and then turns southward along the perimeter of the North Harbor. An entrance kiosk operated by the State Park Service is located to the west of the tide gate, as shown in Fig. 5-1 (adapted from State of California 1990). A pathway to the beach connects off the access road just as the road makes its southward turn. A 1952 aerial photo showing the access road is presented in Fig. 2-3.

## 5.2 Observations of Earthquake Effects

Liquefaction-induced lateral spreading caused extensive damage to the access road, particularly between the tide gate to Bennett Slough and the pathway to the beach. The tide gate was destroyed because of a liquefaction flow slide that resulted in the road surface slumping about 1.3 m across the full tide gate span (Fig. 5-2a). Tidal water movements subsequently eroded the slide debris.

At the entrance kiosk, deformations due to lateral spreading were roughly 0.3 to 0.6 m horizontal with vertical offsets of up to 0.3 m (Fig. 5-2b). Near the entrance to the beach pathway, lateral spreading deformations were about 0.1 to 0.3 m horizontal with vertical offsets of up to 0.05 to 0.10 m (Fig. 5-3). On the tidal flats on the north side of the access road, sand boils occurred at several locations and a series of ground cracks extended along the tide flat near the base of the dunes. About 130 m south of the beach pathway entrance, visible evidence of ground deformations essentially ceased. The above estimates of ground deformations are based on photographs of the site (Gray 1993; Harder 1993; Kutter 1993) and by the field notes of Tinsley (1993).

Significant damage also occurred to the State Beach parking lot at the southern terminus of the access (or Jetty) road. This parking lot is situated on the northern side of the entrance channel to the harbor from Monterey Bay (Figs. 1-2 and 5-1). No field explorations were performed at this location.

## 5.3 Field Investigations

Field investigations were performed in three locations: near the entrance kiosk, near the entrance to the beach pathway, and about 120 m south of the beach pathway. These three locations experienced magnitudes of ground displacement ranging from 0.6 m to no visible movement, as summarized above.

Five cone penetration test (CPT) soundings and two rotary wash borings were performed at the locations shown on Fig. 5-1. Two CPT soundings (UC-15 and UC-16) included shear wave velocity measurements. Appendix A contains the logs of the CPT soundings which were performed on August 19th, 1994. Appendix B contains the logs of the borings which were performed on August 17th and 18th, 1994. Appendix C contains the results of grain size analyses and Atterberg Limit tests.

The procedures and equipment used are described in Section 4.

The positions of the CPT soundings and borings relative to the old Salinas River channel can be seen by comparing the site plan (Fig. 5-1) with Figs. 2-1 and 2-2. The entrance kiosk is located on the access road as it crosses the old Salinas River channel. Fill for the road was apparently placed over the alluvial and estuarine deposits within this old channel. The portion of the access road near the beach pathway is where the roadway transitions into beach and dune deposits. The third location explored, about 120 m south of the beach pathway, appears to be primarily within the beach and dune deposits that separate the harbor from Monterey Bay.

## 5.4 Subsurface Soil Conditions

Subsurface conditions along the access road are shown by the profile in Fig. 5-4. At the locations explored, the upper 10-m of soils encountered were clean sands to gravelly sands having no more than 3% fines (passing the No. 200 sieve). Underlying these sands was a complex sequence of interlayered clay, sand, and gravelly sand.

At the entrance kiosk, the upper 5 m of sand is poorly graded, fine- to medium-grained with a typical $D_{50}$ of about 0.28 mm, and classifying as SP by the Unified Soil Classification System (USCS). The next 3 m of soil consists of interlayered sand and sand with gravel, with $D_{50}$ values ranging from 0.6 to 4.0 mm, and classifying as SP.

Near the entrance to the beach pathway, the upper 6 m of sand was slightly coarser and denser than at the entrance kiosk: typical $D_{50}$ values of about 0.4 mm, and classifying as SP. The next 3 m of soil also consisted of interlayered sand and sand with gravel, with $D_{50}$ values ranging from 0.4 to 3.0 mm, and classifying as SP.

About 120 m south of the beach pathway entrance, the upper 10 m of sands is denser than at the other locations, as indicated by the higher CPT tip resistances. It is possible that the median particle size is also slightly larger than at the other locations, since the geologic profile would suggest that CPT UC-18 may have encountered predominantly beach deposits while the other CPTs encountered predominantly alluvial and estuarine deposits in the abandoned Salinas River channel.

Groundwater levels are expected to fluctuate in response to the changing tide level in the north harbor. At the time of the Loma Prieta earthquake, there was a low tide in the harbor. Referring to the 1989 tide tables (Department of Commerce 1988), the expected water level in the harbor would have been at elevation -0.98 m (NGVD) at the time of the Loma Prieta earthquake (5:07 p.m.). The preceding high tide would have been about elevation 1.0 m at 11:17 a.m. and the following low tide would have been about elevation -1.2 m at 6:24 p.m.. The actual rate of groundwater response to tide fluctuations is not known, but it seems reasonable to estimate the groundwater levels as having been at elevation 0 m at the locations of the exploratory borings and soundings at the time of the earthquake.

## 5.5 Evaluation of Liquefaction Based on SPT and CPT Data

The potential for triggering of liquefaction in the site soils was evaluated using the semi-

empirical procedures described in Section 1.3. Results of the liquefaction analysis for boring UC-B1 and CPT sounding UC-14, located 3-m apart near the entrance kiosk, are shown in Fig. 5-5. The cyclic stress ratio required to cause liquefaction ($CSR_{liq}$) and the cyclic stress ratio induced by the earthquake ($CSR_{eq}$) are shown in the right part of this Figure. From these values a Factor of Safety against liquefaction can be calculated as $FS_{liq}=CSR_{liq}/CSR_{eq}$. The analyses of the SPT data suggest that liquefaction occurred: (1) between the depths of about 1.8 and 5.3 m in the clean sand where the $N_{1-60}$ values range between 7 and 14, and (2) between the depths of about 10.0 and 12.0 m in the silty sand where the $N_{1-60}$ values range between 9 and 13. The analysis of the CPT data is in general agreement with the analysis of the SPT data, but does suggest somewhat higher cyclic strengths (cyclic stress ratio required to cause liquefaction) and thus less extensive liquefaction (particularly in the upper sand layer).

Results of the liquefaction analysis for boring UC-B2 and CPT sounding UC-16, located 3-m apart, near the entrance to the beach pathway are shown in Fig. 5-6. The analysis of the SPT data suggests that liquefaction occurred between the depths of about 4.5 and 6.7 m in the clean sand where the $N_{1-60}$ values ranged between about 17 and 19. The analysis of the CPT data suggests, however, that liquefaction would not have been triggered, and that the factor of safety against liquefaction was at least 1.4 in this depth interval.

The difference in analysis results obtained using the SPT and CPT data is a direct consequence of the value of $q_c/N_{60}$ used to convert the CPT tip resistances to equivalent $N_{60}$ values for use in the liquefaction analyses. For boring UC-B2 and CPT UC-16, the data between depths of 1.5 and 8.5 m suggest that $q_c/N_{60}$ is about 6.6, while the grain size data and the correlation proposed by Seed and De Alba (1986) would suggest $q_c/N_{60}$ values between 4.6 and 5.1. Similarly, for boring UC-B1 and CPT UC-14, the data between depths of 1.5 and 8.5 m suggest that $q_c/N_{60}$ is between 5.1 and 6.9, while the grain size data and the correlation proposed by Seed and De Alba (1986) would suggest $q_c/N_{60}$ values between 4.4 and 5.4. This difference in measured and predicted values of $q_c/N_{60}$ is not unusual since the measured data are within the scatter of correlations relating SPT and CPT penetration resistances to median particle size. The results in Fig. 5-6 illustrate how liquefaction analyses which require (explicitly or implicitly) converting CPT tip resistances to SPT blow counts are sensitive to the assumed $q_c/N_{60}$ values.

The SPT and CPT data show significant differences in penetration resistances at the three sites investigated, and in a pattern consistent with the observed differences in ground deformations. Field evidence clearly indicates that the upper layer of sand liquefied near the entrance kiosk and beach pathway while no apparent liquefaction occurred farther down the Jetty Road (at CPT UC-18). The SPT data shows significantly lower blow counts over a thicker depth interval near the kiosk than near the beach pathway, which is consistent with the deformations being larger near the kiosk than near the beach pathway. The CPT data shows the lowest tip resistances over the thickest depth interval near the kiosk, intermediate tip resistances near the beach pathway, and the greatest tip resistances down the Jetty Road near UC-18. These differences in CPT tip resistances among the three locations is consistent with observed differences in ground deformations.

Critical combinations of earthquake-induced cyclic stress ratio and normalized CPT tip resistance at each of the five CPT soundings are shown in Fig. 5-7. Critical CPT tip resistances were estimated using the guidelines previously described in Section 1.3. Cyclic stress ratios are adjusted

to equivalent cyclic stress ratios for M=7.5 earthquakes based on the ratios presented by Seed and Idriss (1982). For reference purposes, Fig. 5-7 also shows the boundary between conditions of liquefaction and non-liquefaction proposed by Mitchell and Tseng (1990) for clean sands with $D_{50}$ equal to 0.20 mm and 0.40 mm. The boundaries proposed by Mitchell and Tseng (1990) are generally consistent with the observed behavior at this site, except for one point (CPT UC-16) near the beach path which is slightly outside the proposed boundary for a clean sand with a $D_{50}$ of 0.40 mm.

## 5.6 Correlation With Shear Wave Velocity Measurements

Profiles of normalized shear wave velocity ($V_{s-1}$) near the entrance kiosk and the beach pathway are shown in Fig. 5-8. Variations in normalized shear wave velocity versus depth show reasonable agreement with the profiles interpreted from the CPT tip resistances.

The critical value of $V_{s-1}$ is 131 m/s at the entrance kiosk and 156 m/s at the beach pathway. Lower values of $V_{s-1}$ at the entrance kiosk compared to those at the beach pathway are consistent with the larger liquefaction-induced deformations at the entrance kiosk. The induced cyclic stress ratios at the entrance kiosk and beach pathway are estimated to be about 0.19 and 0.24, respectively. These cyclic stress ratios are based on a peak ground acceleration of 0.25 g, and are adjusted to an equivalent M=7.5 earthquake based on the ratios presented by Seed and Idriss (1982). The above critical combinations of normalized shear wave velocity and earthquake-induced cyclic stress ratio are consistent with the relationship in Fig. 1-6 proposed by Robertson et al. (1992).

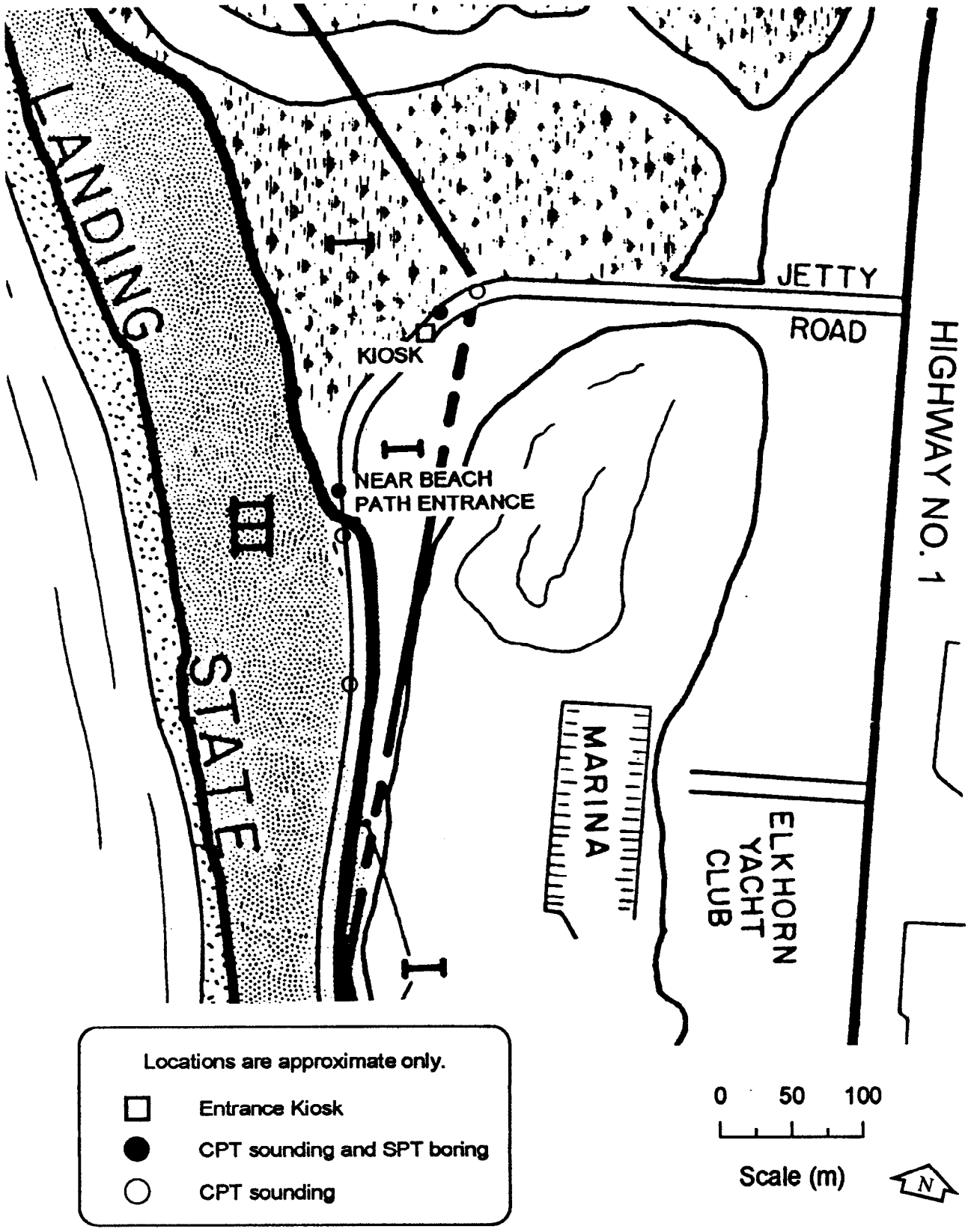


FIG. 5-1. Map Showing the Jetty Road to the Moss Landing State Beach

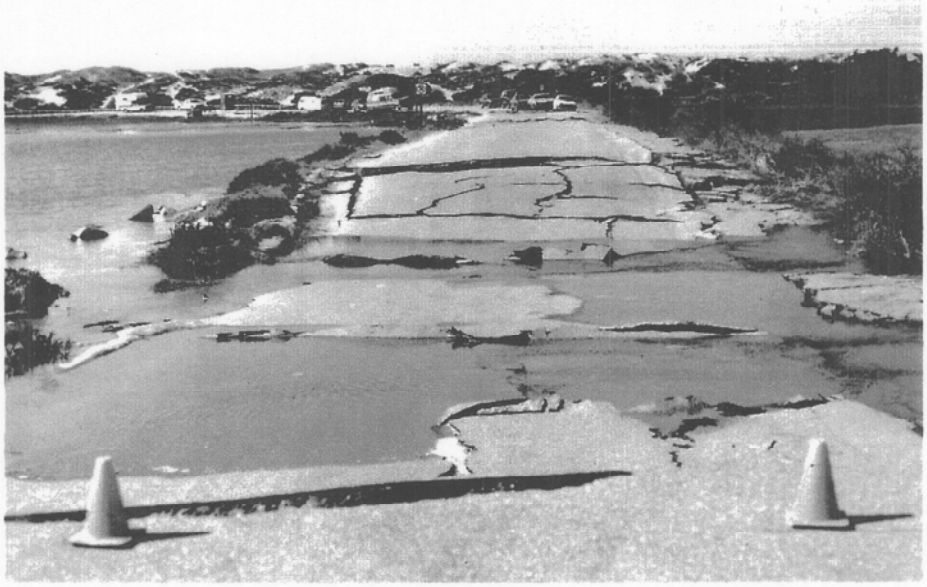

FIG. 5-2(a). Collapse of the Tide Gate Across Jetty Road to Moss Landing State Beach (Note: the Entrance Kiosk is visible in the distance).

FIG. 5-2(b). Entrance Kiosk at Moss Landing State Beach.

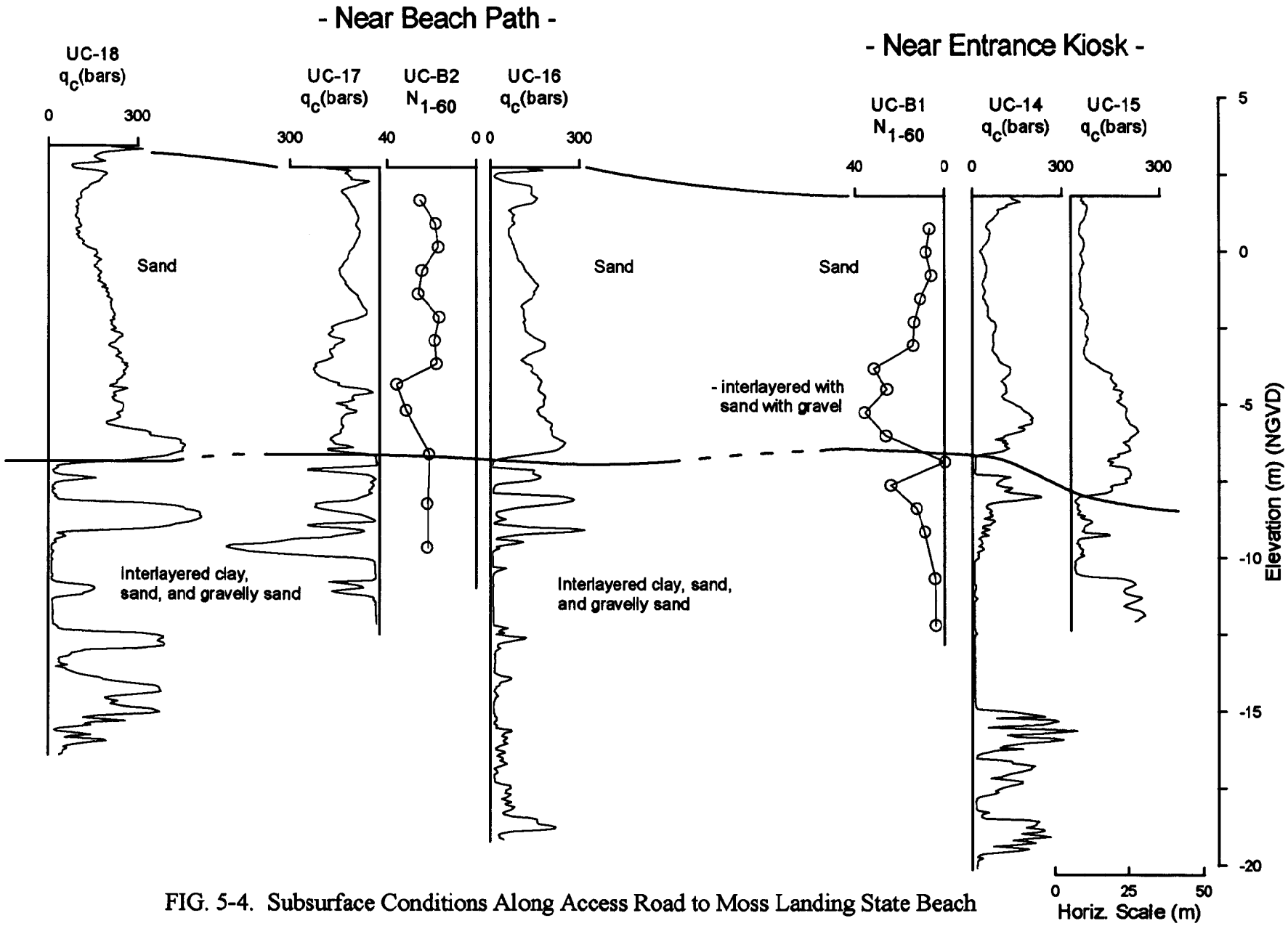


FIG. 5-4. Subsurface Conditions Along Access Road to Moss Landing State Beach

PROFILE1.GRF

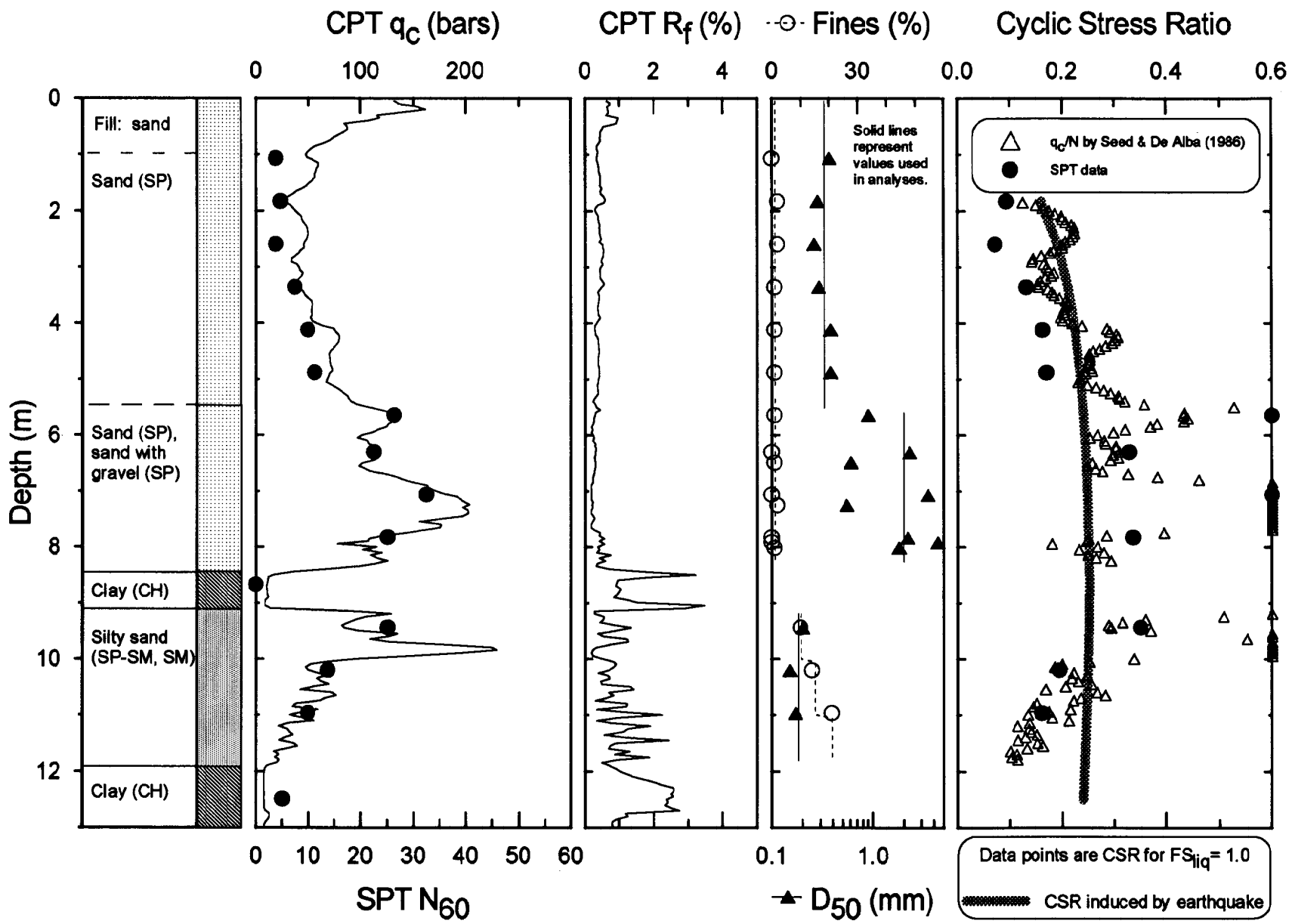


FIG. 5-5. Liquefaction Analyses of Adjacent SPT (UC-B1) and CPT (UC-14) Data Near the Entrance Kiosk at the State Beach

PAIRUCB1.GRF

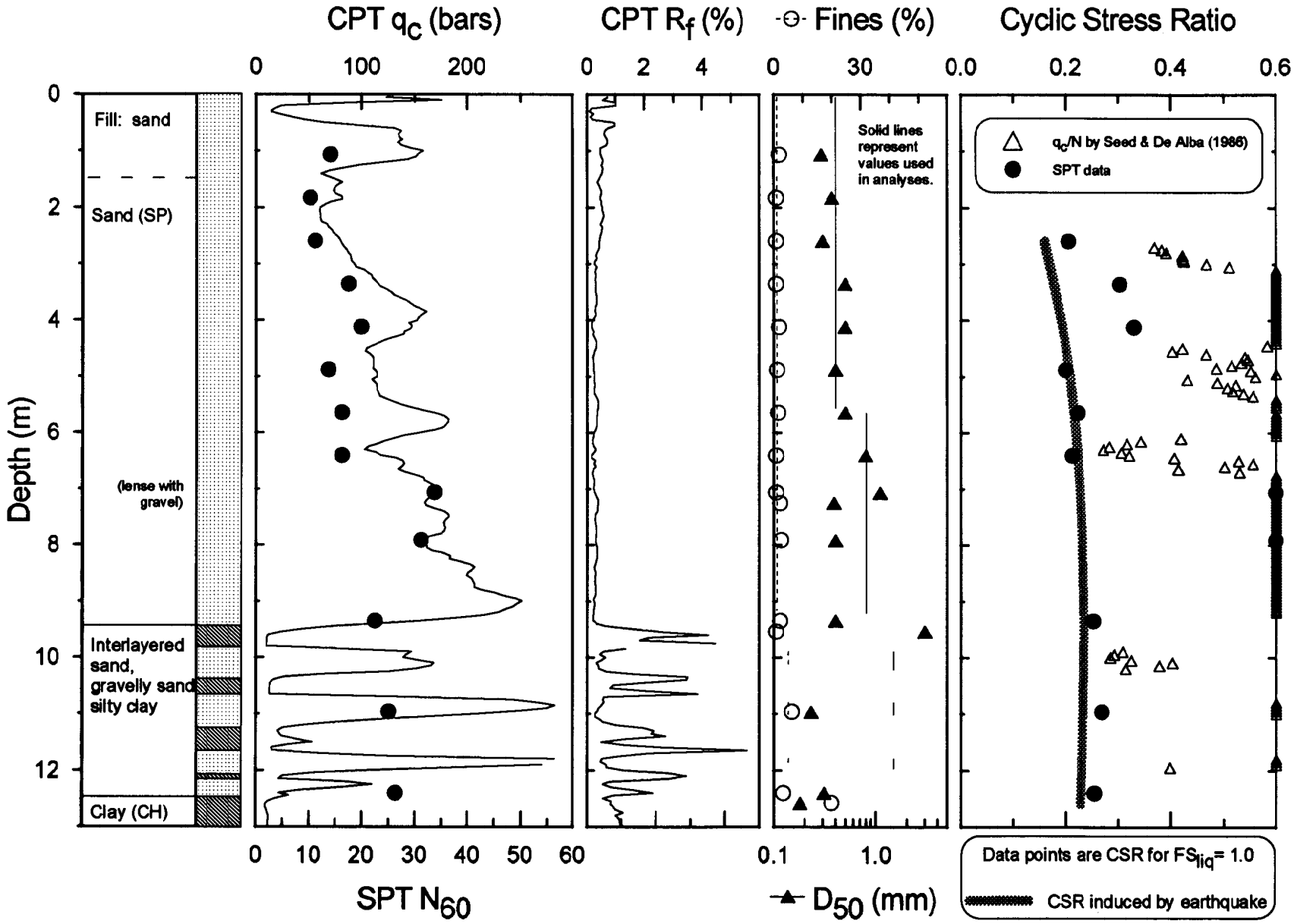


FIG. 5-6. Liquefaction Analyses of Adjacent SPT (UC-B2) and CPT (UC-16) Data Near the Beach Path at the State Beach

PAIRUCB2.GRF

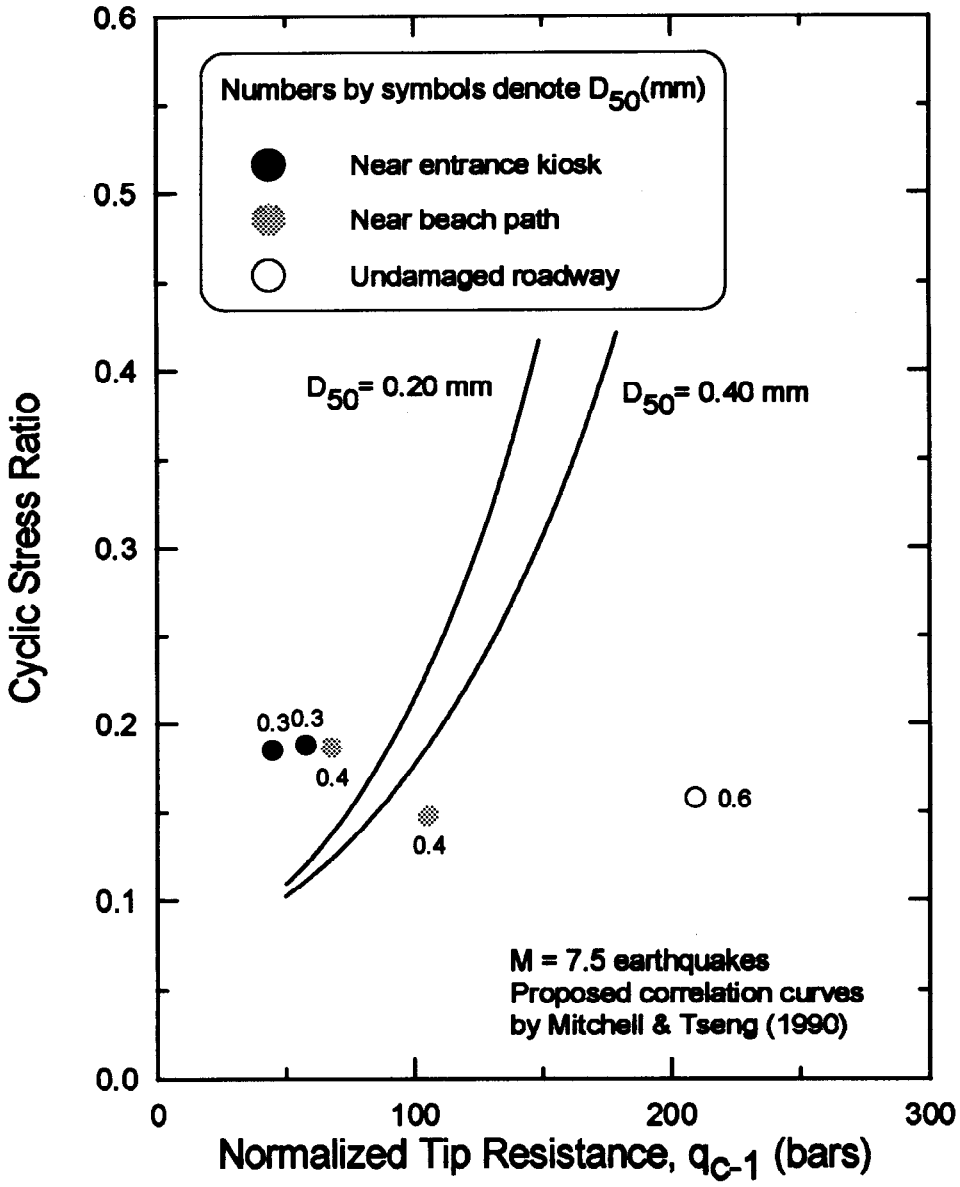


FIG. 5-7. Correlation of CPT Tip Resistance to Liquefaction Resistance at the Moss Landing State Beach

beach-1.grf

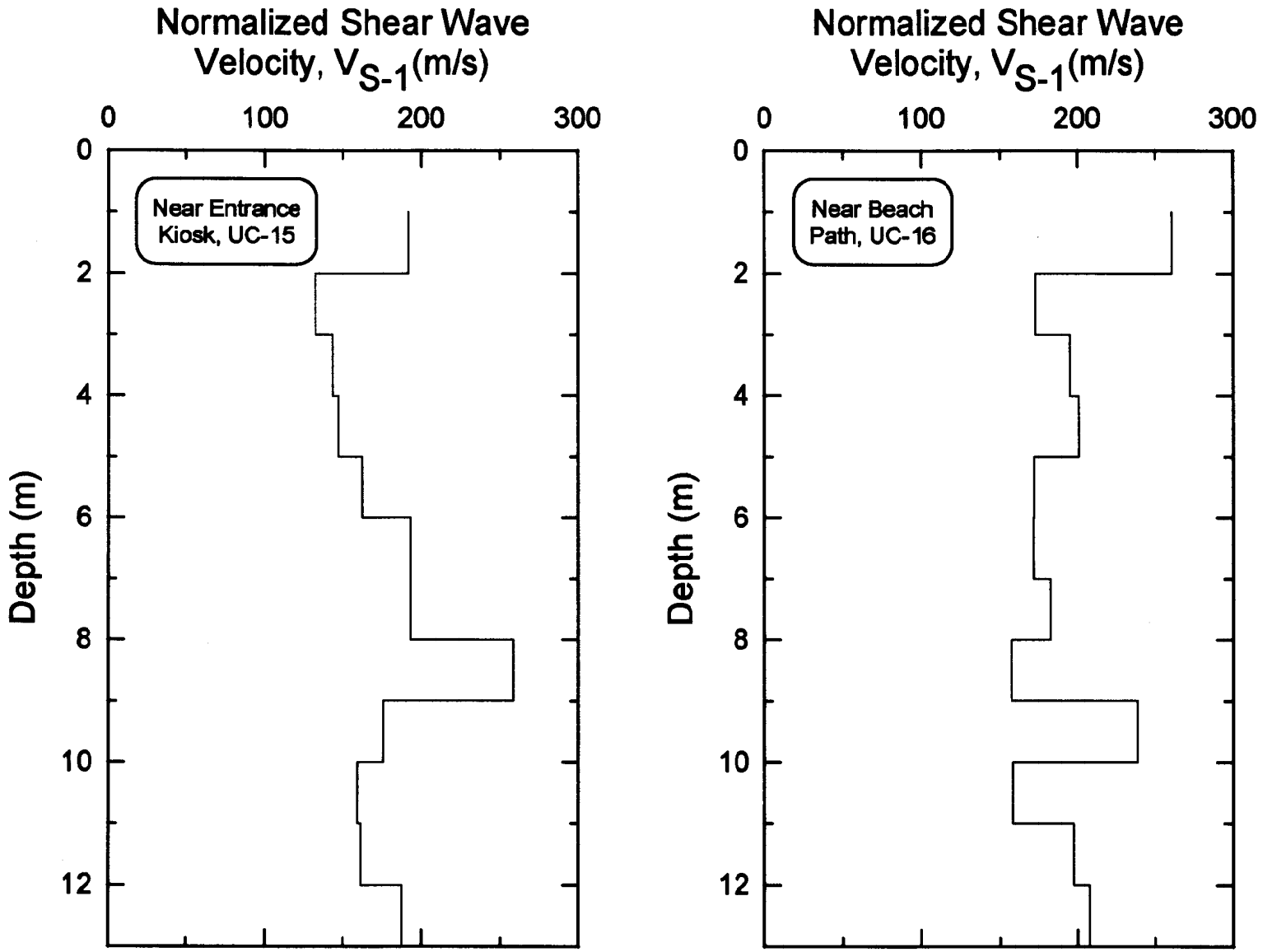


FIG. 5-8. Normalized Shear Wave Velocity Profiles at the Moss Landing State Beach

v-beach1.grf

# 6. MOSS LANDING HARBOR DISTRICT FACILITY

## 6.1 Site Description

The Moss Landing Harbor District Facility is located in the South Harbor on the spit of land separating the Moro Cojo Slough and the Old Salinas River channel. The Harbor Master's Office is located near the northern end of this spit, as shown on Figs. 1-2 and 6-1 (adapted from Creegan and D'Angelo 1991). The surface of the spit around the office is a paved parking lot that varies in elevation from about 1.9 to 3.0 m (NGVD). Several docks are accessed off this parking lot.

Design recommendations for the Harbor Master's Office called for the building foundations to consist of a thickened floor slab placed on a minimum of 10 cm of compacted, open-graded, clean rock over a minimum of 0.46 m of compacted fill (Michael David Obele & Associates 1967). The thickened floor slab was to provide an effective foundation width of 0.92-m. Architectural drawings show reinforcing steel being continuous between the thickened slab sections and the floor slabs (Waterman & Kuska Architects 1967).

## 6.2 Observations of Earthquake Effects

Considerable damage occurred to the parking lot as a result of the Loma Prieta earthquake. Fig. 6-2 shows sand boils along a 25-mm-wide crack parallel to the western edge of the parking lot along the Old Salinas River. The ejecta at this location, and other locations in the parking lot, consisted of relatively clean sands to slightly silty sands. Fig. 6-3 shows more severe cracking, with deformations of about 15 cm horizontally and 30 cm vertically, at the northern end of the parking lot next to Dock "C." A detailed map of cracks and damage to the parking lot and Harbor District Facilities was prepared by Creegan and D'Angelo (1990) as part of the plan documents for the eventual repairs. At the Harbor Master's Office, structural damage was minor and amounted to hairline cracking of the concrete floor slabs. Minor ground cracks were also observed around the perimeter of the office along the contact between its foundation and the adjacent soils. A spread of about 1 cm occurred in the pipe connecting the office and a sewer pump-out station located west of the structure (Souza 1993).

## 6.3 Field Investigations and Aerial Photos

Field investigations were performed in three general locations: near Dock "C" (Fig. 6-3), at the northwest corner of the Harbor Master's Office, and along the western edge of the parking lot along the Old Salinas River (Fig. 6-2). These three locations experienced ground displacements ranging from about 1 to 30 cm, as described above.

Five CPT soundings and two rotary wash borings were performed at the locations shown in Fig. 6-1. Three of the CPT soundings (UC-12, UC-19, UC-21) included shear wave velocity measurements. Appendix A contains the logs of the CPT soundings which were performed on August 18, 19, and 20, 1993. Appendix B contains the logs of the two rotary wash borings which were performed on January 19 and June 20, 1994. Appendix C contains the results of grain size analyses and Atterberg Limit tests. The procedures and equipment used were identical to those described in Section 4.

Aerial photos of the harbor from about 1952 (Fig. 2-3) show the section of the Moro Cojo Slough adjacent to the present parking lot to have been diked off from the harbor and then used for sedimentation or dredging disposal. Since 1952, the slough has been dredged open to allow docks to be placed within the old Moro Cojo Slough channel. These photographs also show the parking lot to be located in an area of filled ground, although the upper fill would appear to have been placed above the water level on soils already deposited by 1952. Long-time local resident "Whitey," a former employee of the Harbor District, confirmed that the fill used to raise the parking lot was placed on "mucky soil that was easy to get equipment stuck in . . . " and " . . . land that was already above the water at low tide, including all around the edges of the lot." Fig. 2-2 shows that the shoreline in 1854 included most of the present parking lot (the shoreline for the parking lot area in 1910 and 1933 was apparently omitted from Fig. 2-2). The natural shoreline fluctuations illustrated in Fig. 2-2 also indicate that the below-water-level sediments deposited around the tip of the parking lot spit are very recent deposits, possibly including some mix of natural sediments and dredging spoils.

## 6.4 Subsurface Soil Conditions

The subsurface conditions across the Harbor Master's Office and parking area are shown in Fig. 6-4. A roughly 1- to 1.5-m-thick sandy fill overlies a 2- to 2.5-m-thick layer of soft silty clay with liquid limits of 29 to 38, plasticity indices of 7 to 15, a minus 5 μm fraction of 19 to 22%, and USCS classifications of CL and ML.

Below the soft silty clay is a layer of sand, silty sand, and sandy silt that ranges in thickness from about 1 m near Dock "C" to about 2.2 m at the western edge of the lot. The sands in most of this layer have between 4 and 12% fines and a $D_{50}$ between 0.17 and 0.46 mm, while the upper portion of this layer near the office was a sandy silt with about 80% non-plastic fines. This sand layer appears to have been the source of the sand ejecta observed along the western edge of the lot (see Fig. 6-2) and elsewhere in the parking lot.

On the western edge of the parking lot and beneath the office, the layer of sand to sandy silt is underlain by a layer of silty clay with interlayers of silty sand and sand that extends to depths of at least 15 to 25 m (the depth explored). At depths less than about 12 m, the silty clay is soft to medium-stiff with liquid limits of 44 to 62, plasticity indices of 23 to 40, and USCS classifications of CL and CH. Silty sand and sand interlayers in this depth interval are generally less than about 0.5 m thick. Below depths of about 12 m, the clay is very stiff to hard, with liquid limits of about 62 to 65, plasticity indices of about 40, and a USCS classification of CH.

Near Dock "C," the stratum below the layer of sand to sandy silt differs slightly from the western side of spit as follows. Between depths of about 5 to 7 m, there is a soft to medium-stiff silty clay with thin interlayers of sand and silty sand, liquid limits of 35 to 41, plasticity indices of 15 to 20, and a USCS classification of CL. Between depths of about 7 and 11 m, there is a layer of dense sand with interlayers of sand with gravel, sand with gravel and clay, and clay. Below depths of about 11 m and extending to at least 15 m (the depth explored) is the very stiff to hard clay as also encountered at these depths on the western side of the lot and beneath the office.

## 6.5 Evaluation of Liquefaction Based on SPT and CPT Data

The potential for triggering of liquefaction in the subsurface soils was evaluated using the same procedures previously described in Section 1.3. Results of the liquefaction triggering analysis for boring UC-B3 and CPT UC-21, located 1.5 m apart, near Dock "C" are shown in Fig. 6-5. The most likely source of liquefaction would be the layer of sand and silty sand between depths of about 3.6 and 4.6 m, which appears to have been the source for the sand ejecta observed along the western edge of the lot. The analysis of the CPT data in this sand and silty sand layer (typically 10% fines, $D_{50}$ of 0.3 mm) would suggest that it experienced significant liquefaction, with an overall average factor of safety close to about 1.0. The single SPT value in this sand and silty sand layer was high compared to the CPT data, and would indicate that liquefaction was unlikely. Liquefaction may also have occurred in the sand and silty sand interlayers encountered in the silty clay between depths of about 4.6 and 8.0 m. However, these sand and silty sand interlayers are generally too thin to develop fully representative SPT blow counts or CPT tip resistances, and thus evaluating their liquefaction potential can only be done qualitatively. A 0.5-m-thick sand interlayer at a depth of about 7.1 m developed a CPT tip resistance greater than that in the sand and silty sand layer between 3.6 and 4.6 m depth. Combined with the grain size data, this sand interlayer would be expected to be more resistant to liquefaction than the sand and silty sand layer between 3.6 and 4.6 m depth. Furthermore, the other CPT sounding near Dock "C" encountered no significant sand or silty sand interlayers within this silty clay layer (depths of 5-7 m in UC-20; see Fig. 6-4) and yet similarly large surface deformations were observed at both CPT locations. In consideration of the available data and analysis results, it appears reasonable to conclude that the sand and silty sand layer between 3.6 and 4.6 m depth was the most likely source of liquefaction-induced deformations near Dock "C."

Results of liquefaction triggering analyses for boring UC-B5 and CPT UC-19, located 1.5 m apart near the northeast corner of the Harbor Master's Office, are shown in Fig. 6-6. Analysis of the sand to sandy silt layer between depths of about 4.4 and 6.8 m indicates that liquefaction would not be expected based on the SPT data and that only very limited liquefaction would be expected based on the CPT data. In the underlying silty clay layer, interlayers of sand and silty sand at depths of about 7.1 and 9.5 m exhibited relatively low penetration resistances (CPT and SPT) despite their thicknesses of roughly 0.5 m and 0.9 m, respectively. The analysis results suggest that these thin interlayers could have liquefied and thus contributed to the observed deformation of about 1 cm near the Harbor Master's Office.

Triggering analyses were also performed for CPTs UC-12 and UC-13 along the western edge of the parking area adjacent to the Old Salinas River. Within the sand and silty sand layer between depths of about 3.0 and 4.7 m, the CPT tip resistances were generally larger than measured at Dock "C" and comparable to those measured at the northeast corner of the office. Analyses of the CPT data indicate that limited liquefaction would be expected to develop near the middle of this layer (4.2 m depth) where both CPT signatures show a thin zone having relatively low tip resistances and high friction ratios (suggesting a higher fines content). Of the thin sand and silty sand interlayers in the underlying silty clay layer, some show very high tip resistances while others are too thin to develop a representative tip resistance. Consequently, analysis of the these sand and silty sand interlayers is inconclusive. Despite these difficulties, the analyses' prediction of limited liquefaction in the sand and silty sand layer between depths of about 3.0 and 4.7 m is in reasonable agreement with the observed ground cracking and sand ejecta at this location.

Critical combinations of earthquake-induced cyclic stress ratio and normalized CPT tip resistance are shown in Fig. 6-7. Critical CPT tip resistances were estimated using the guidelines previously described in Section 1.3. Cyclic stress ratios are adjusted to equivalent cyclic stress ratios for M=7.5 earthquakes based on the ratios presented by Seed and Idriss (1982). The field evidence, particularly the sand boils, indicates that liquefaction likely occurred in the sand to sandy silt layer between depths of about 3.0 to 6.8 m along the edges of the spit (Dock"C" and the western edge of the parking lot). At the northeast corner of the office, the most critical depth was taken as the thin silty sand layer at a depth of about 7.1 m. For reference purposes, Fig. 6-7 also shows the boundary between conditions of liquefaction and non-liquefaction proposed by Mitchell and Tseng (1990) for clean sands with $D_{50}$ values of 0.20 mm and 0.40 mm. The boundaries proposed by Mitchell and Tseng (1990) are consistent with the observed behavior at these two locations. In addition, the CPT tip resistances are lower near Dock "C" than near the western side of the parking lot, which is consistent with the observed deformations being larger near Dock "C;" no comparison is made with the northeast corner of the office where deformations were smallest because of the different distances to a free face.

## 6.6 Correlation With Shear Wave Velocity Measurements

Profiles of normalized shear wave velocity ($V_{S-1}$) near the western edge of the lot, the main office building, and Dock "C" are shown in Fig. 6-8. These $V_{S-1}$ profiles do not depict the detailed stratification of soils as identified from the CPT tip resistance profiles. Furthermore, the measurement intervals for shear wave velocity generally included more than one soil type, and thus the measured velocities often represent some average value over the different soil types. These data illustrate the difficulty in using shear wave velocity measurements, with measurement intervals of 1 to 2 m, to characterize thin strata.

Subsequently, the $V_{S-1}$ value of 167 m/s between depths of 3.1 and 4.1 m in CPT UC-12 is the only measurement that coincides fully with the sand-to-silty-sand layer suspected of liquefying. The induced cyclic stress ratios at this depth was estimated to be about 0.20, based on a peak ground acceleration of 0.25 g and after adjustment to an equivalent M=7.5 earthquake based on the ratios presented by Seed and Idriss (1982). This critical combination of normalized shear wave velocity and earthquake-induced cyclic stress ratio is consistent with the relationship in Fig. 1-6 proposed by Robertson et al. (1992).

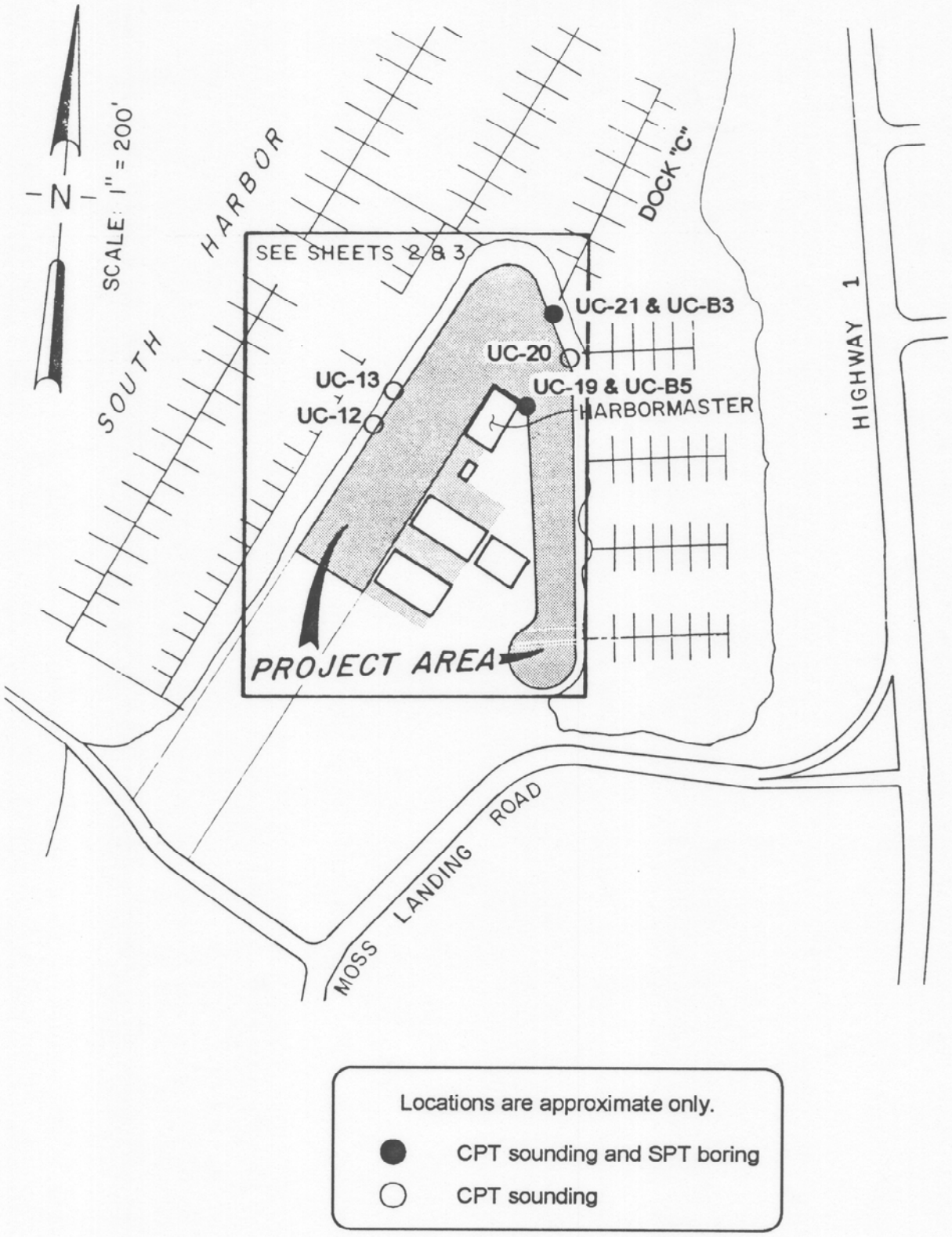


FIG. 6-1. Map of the Moss Landing Harbor District's Office

FIG. 6-2. Sand Boils Along the West Side of the Moss Landing Harbor District Parking Lot.

FIG. 6-3. Cracking at North End of Parking Lot Near Dock "C."

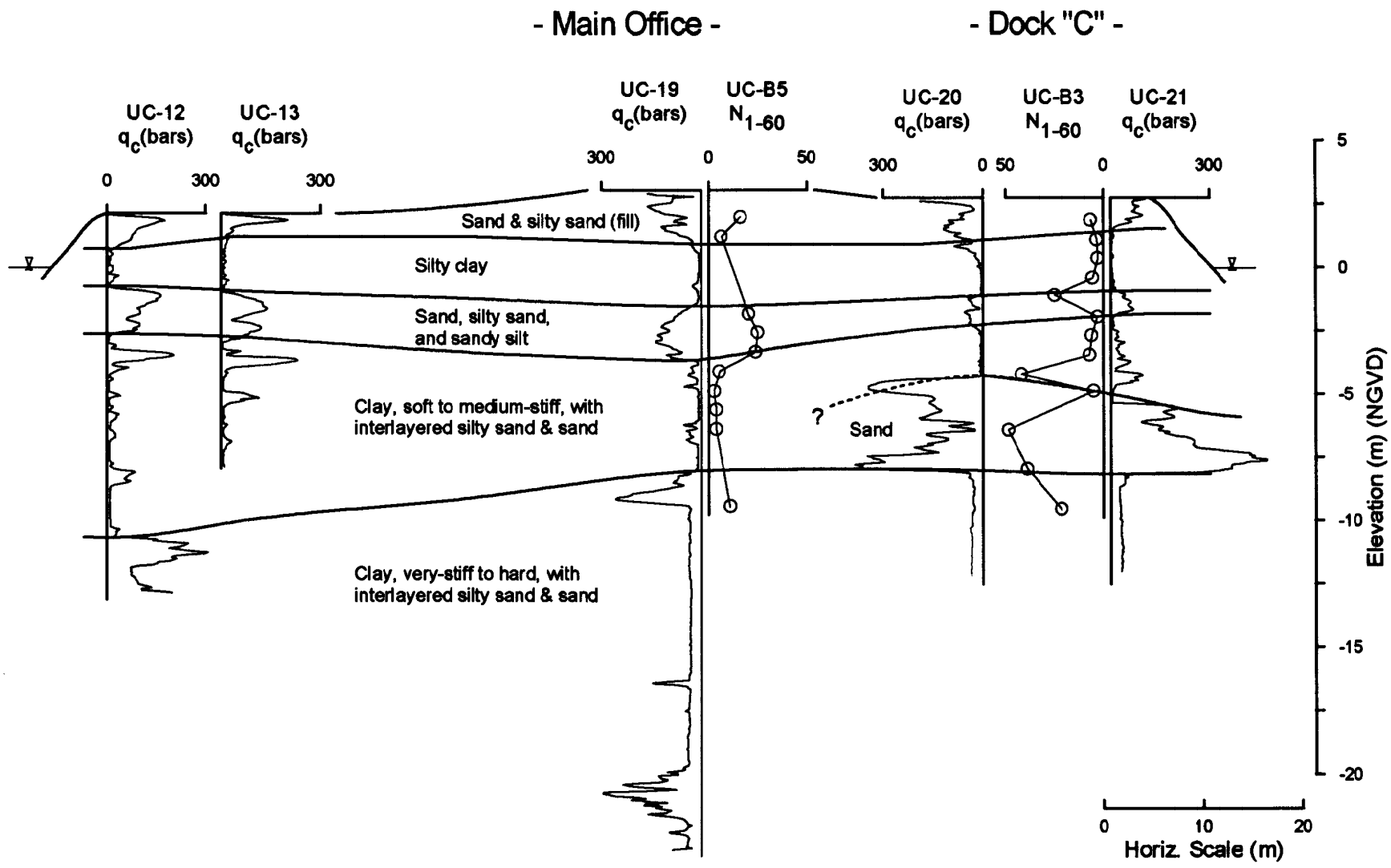


FIG. 6-4. Subsurface Conditions Across the Moss Landing Harbor Master's Office

PROHARB1.GRF

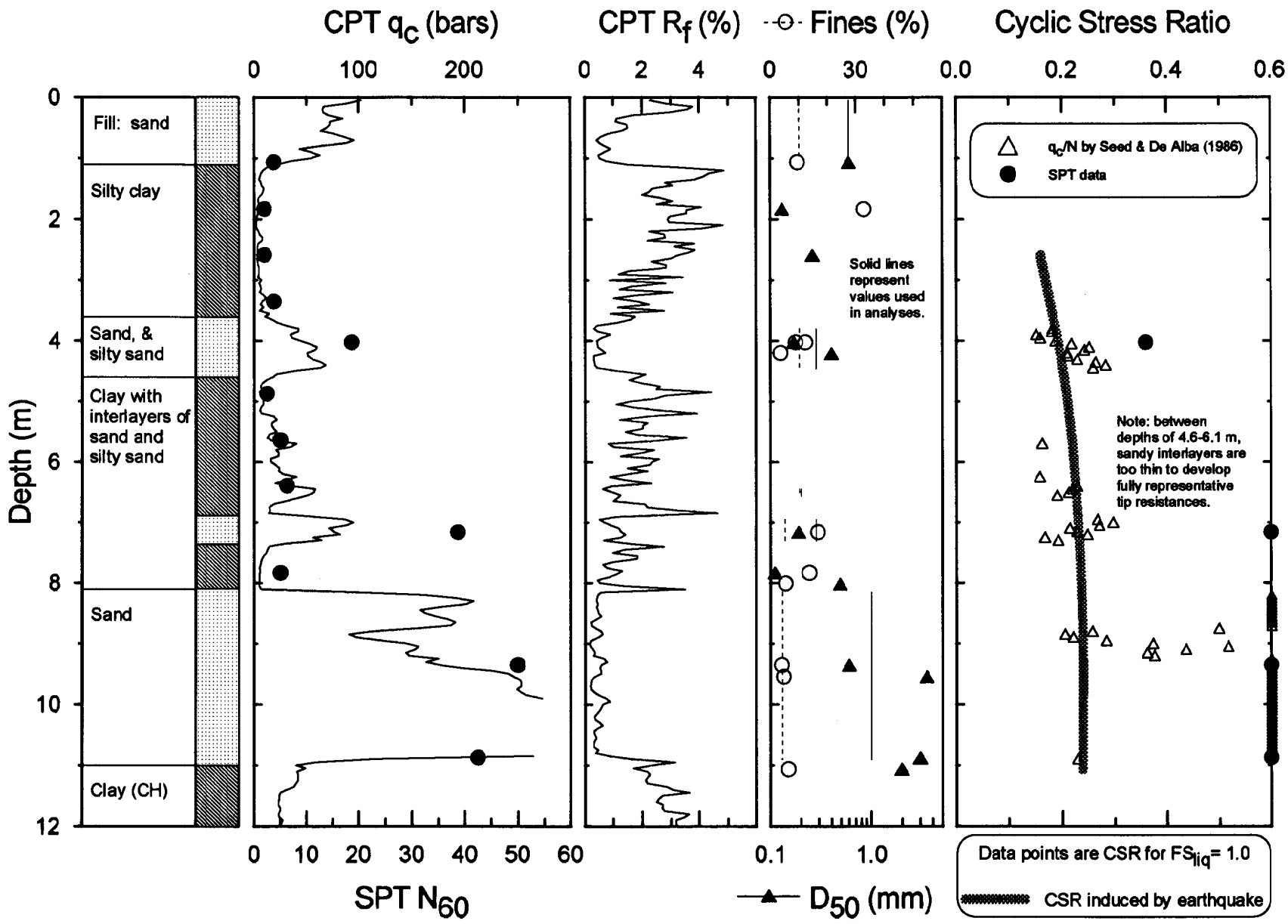


FIG. 6-5. Liquefaction Analyses of Adjacent SPT (UC-B3) and CPT (UC-21) Data Near Dock "C" of the Harbor Office

PAIRUCB3.GRF

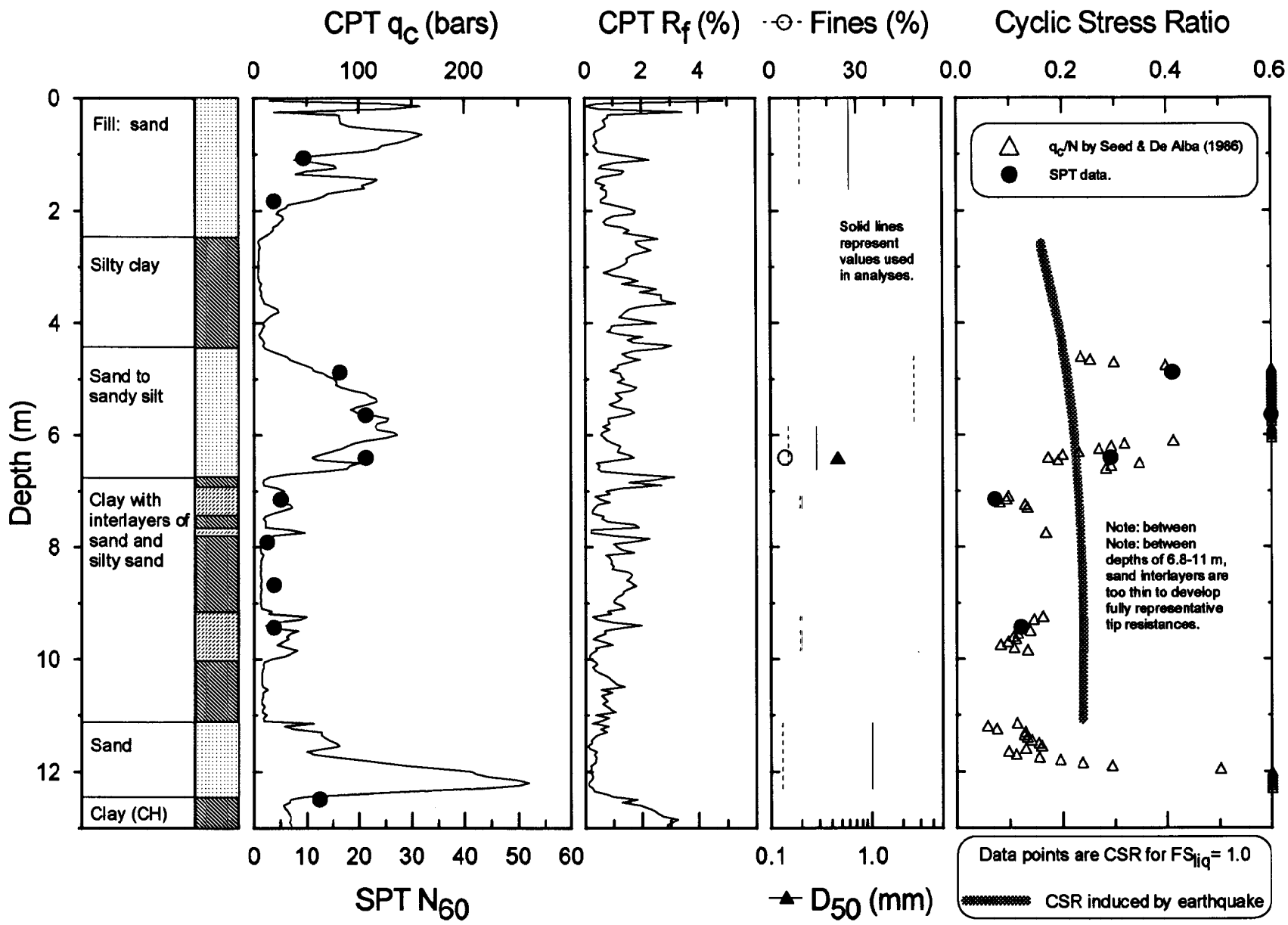


FIG. 6-6. Liquefaction Analyses of Adjacent SPT (UC-B5) and CPT (UC-19) Data Near N.E. Corner of the Harbor Office

PAIRUCB5.GRF

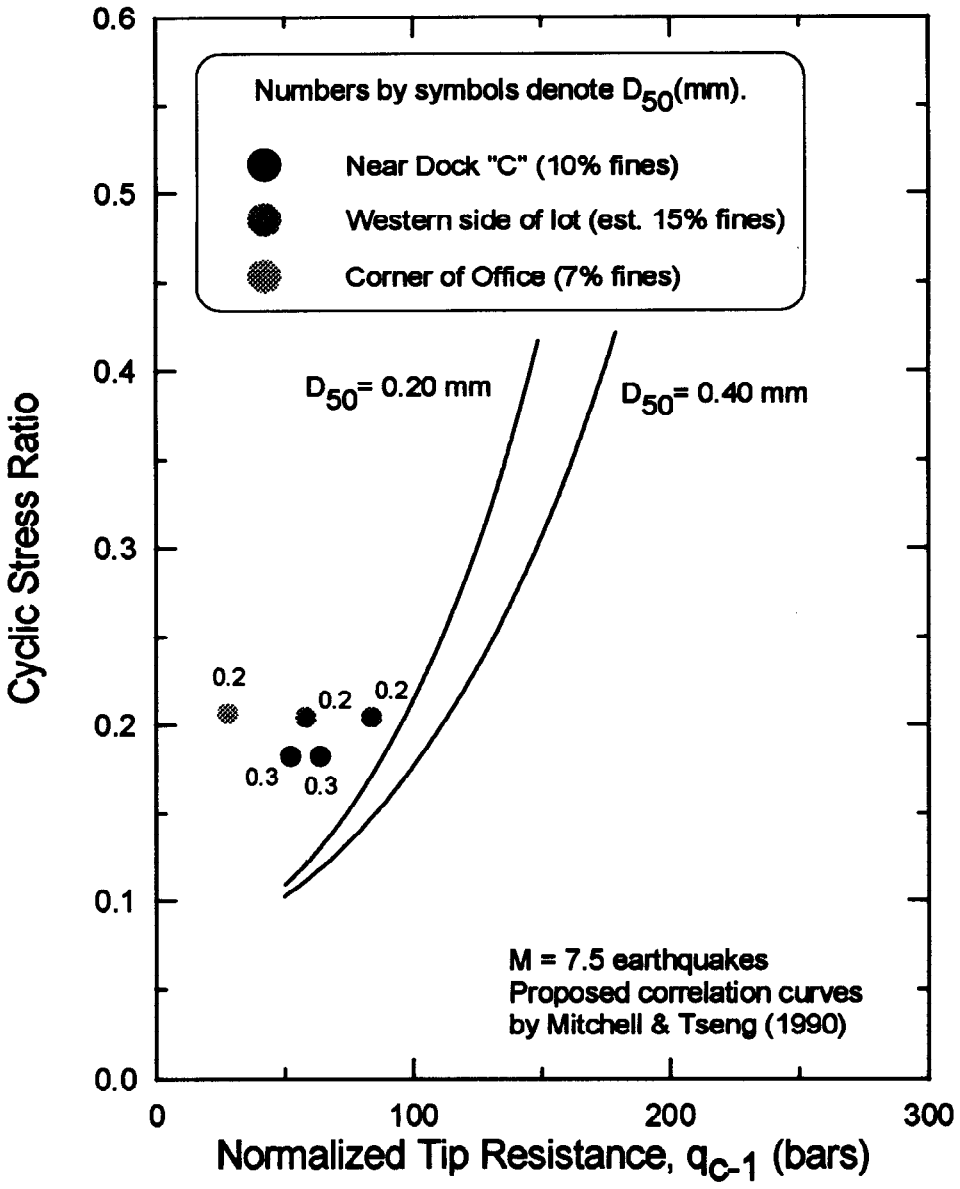


FIG. 6-7. Correlation of CPT Tip Resistance to Liquefaction Resistance at the Moss Landing Harbor Office

HARB-2.grf

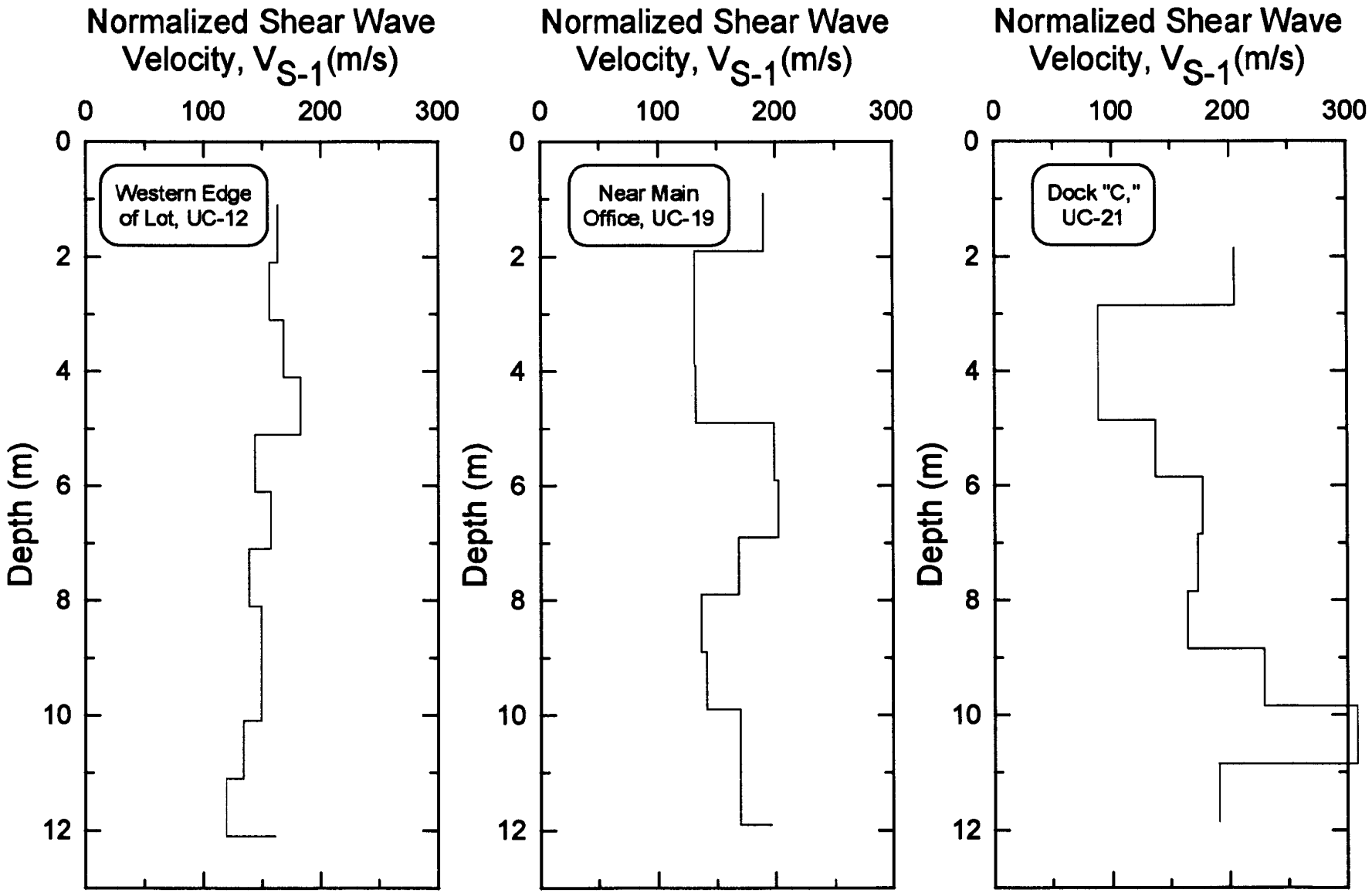


FIG. 6-8. Normalized Shear Wave Velocity Profiles at the Moss Landing Harbor Master's Office

# 7. WOODWARD MARINE

## 7.1 Site Description

Woodward Marine is located on Salmon Way off Sandholdt Road near the northern end of the Moss Landing spit and along the South Harbor, as shown on Fig. 1-2. The facilities at Woodward Marine included a boat launch ramp, a Chevron fuel service dock, and Chevron oil and gas storage tanks as shown on Fig. 7-1 (adapted from Coastland Consultants 1991). To the north of Woodward Marine is Gravelle's Boat Yard.

## 7.2 Observations of Earthquake Effects

Liquefaction-induced ground spreading was evident across much of the site. Along the shoreline, the Chevron sign and supporting pile toppled over onto the fuel dock, jetty piles were displaced horizontally, and the boat ramp and adjacent asphalt pavement experienced cracking and settlement (Fig. 7-2). A long crack, having offsets up to about 5 cm vertical and 2 cm horizontal, and located roughly 8 to 12 m back from (and parallel to) the shoreline, developed in the asphalt pavement extending from the Woodward Marine office to the boat launch ramp. The Woodward Marine office building fell of its foundation, and compression buckling was observed in the masonry brick patio surface at the building entrance. Several cracks, roughly sub-parallel to the shoreline, traversed in the asphalt pavement (Salmon Way) connecting the boat launch ramp to Sandholdt Road, with the larger cracks having horizontal displacements of up to about 5 cm. The Chevron oil and gas tanks, located on the southern side of Salmon Way at its junction with Sandholdt Road, settled and tilted between 1 and 6 degrees from vertical (Tuttle et al. 1990). Fig. 7-3 shows a view of the tilted tanks and the accumulation of vented sand around their foundations. Gray, coarse- to medium-grained sand was vented through some of the 5- to 50-mm-wide cracks near the tanks (Tuttle et al. 1990). It was also noted that the vented sand occurred mostly toward the northern side of the tanks, while little or no sand vented on the southern side of the tanks (Tuttle et al. 1990). Sand dikes were traced from the ground surface to a depth of about 0.8 m through a gravelly sand and gray, medium-grained sand to a gray, silty sand (Tuttle et al. 1990).

## 7.3 Field Investigations

Field investigations were performed near the Chevron oil and gas tanks by the USGS (as reported by Tuttle et al. 1990), and along Salmon way between the tanks and the boat ramp as part of the present study. The USGS explorations included three CPT soundings and two borings in a north-south alignment through the Chevron tanks, at the locations shown in Fig. 7-1. Logs of the USGS explorations were provided by Tinsley (1993). The explorations of the present study included three CPT soundings and one boring along Salmon Way to complete a cross-sectional profile of the site.

The procedures followed in the USGS explorations are described by Tuttle et al. (1990). CPT soundings followed ASTM D3441-79. Borings were performed using a 10 cm inside diameter, hollow stem auger. SPT tests followed the guidelines in ASTM D1586-67 with modifications for use with the hollow stem auger as described in Youd and Bennett (1983). A Mobile system (ADO sampler with sampler liners; in-hole sampling hammer; and safe-T-driver hoist) was used for which

the drop-efficiency of the hammer was reported as 68%.

For the present study, three CPT soundings and one rotary wash boring were performed at the locations shown on Fig. 7-1. One CPT sounding (UC-9) included shear wave velocity measurements. Appendix A contains the logs of the CPT soundings performed on August 18, 1993. Appendix B contains the log of the rotary wash boring performed on January 20, 1994. Appendix C contains the results of grain size analyses and Atterberg Limit tests. The procedures and equipment used were identical to those described in Section 4.

Historical shoreline locations, as shown in Fig. 2-2, suggest that the shoreline near Woodward Marine has fluctuated significantly and thus some shallower soil strata at this site may have been deposited very recently.

## 7.4 Subsurface Soil Conditions

The subsurface conditions along Salmon Way are shown by the profile in Fig. 7.4. A roughly 1-m-thick layer of sandy fill appears to blanket the site. To the eastern end of Salmon way (toward the shoreline), the fill is underlain by a roughly 2.2-m-thick layer of sand and silty sand. The upper half of this layer is typically a silty sand with about 15% fines and a $D_{50}$ of about 0.2 mm, while the lower half is typically a sand with about 3% fines and a $D_{50}$ of about 0.6 mm. To the western end of Salmon Way, the fill is underlain by a 1- to 2-m-thick layer of soft silty sand, sandy silt, and silt. Within this layer, the silty sands and sandy silts had 26 to 51% fines, $D_{50}$ values of 0.07 to 0.36 mm, and USCS classifications of SM and ML. Also within this layer were thin clayey silt lenses, for which one sample had 93% fines and a USCS classification of MH and another sample had 88% fines and a USCS classification of CL. This soft layer of silty sand to silt is underlain by a thin zone of sand to depths of about 3.5 m, which appears similar to the sand encountered at similar depths along the eastern end of Salmon Way.

Along the full length of Salmon way, between depths of about 3.5 to 5.5 m there is a layer of sand having less than about 3% fines and $D_{50}$ values of 0.4 to 0.9 mm. Extending to depths of about 14 m below this sand layer, there is a layer of high plasticity clay with interlayers of silty sand and sand. Dense sand with clay interlayers was encountered from about 14 m depth to the depth explored (which was less than about 16 m in all soundings).

Subsurface conditions parallel to Sandholdt Road and passing through the Chevron oil and gas tank enclosure are shown by the profile in Fig. 7-5 (based on the data by Tuttle et al. 1990; Tinsley 1993). As described by Tuttle et al. (1990), there is a change in the stratification between the north and south sides of the tank: the soft silty sand to sandy silt layer at depths of 0.7 to 2.7 m on the north side is not encountered on the south side. Interestingly, venting of soils was much greater toward the northern side and the vented material was apparently coarse- to medium-grained sand. This would suggest that liquefaction must have occurred in the sands underlying the soft sandy silt layer towards the northern side of the tanks, and that the presence of the lower permeability sandy silt layer somehow facilitated the venting process (Tuttle et al. 1990).

## 7.5 Evaluation of Liquefaction Based on SPT and CPT Data

The potential for triggering of liquefaction was evaluated using the same procedures previously described in Section 1.3. The results of the liquefaction triggering analysis for boring UC-B4 and CPT UC-11, located 1.5 m apart near the boat ramp, are shown in Fig. 7-6. The analysis of the CPT data indicates that liquefaction would be expected to have developed within the silty sand and sand between depths of about 1.7 and 3.4 m. Referring to the subsurface profile in Fig. 7-4, this zone of expected liquefaction was also encountered in CPT UC-10, which is located roughly half-way along Salmon Way.

Liquefaction triggering analyses were also performed for the data obtained near the Chevron fuel tank enclosure, including boring USGS-15A and CPT soundings USGS-14A, USGS-15A, and UC-9. The low SPT blow counts and CPT tip resistances in the soft sandy silt layer between depths of about 0.7 and 2.7 m would suggest that this layer may be suspected of having liquefied during the Loma Prieta earthquake, but the data on the plasticity characteristics of this silt are too limited to properly evaluate its likely behavior. Regardless of how the silt layer behaved, the venting of clean sands to the ground surface in this area would suggest that liquefaction must also have occurred in the underlying sands.

Critical combinations of earthquake-induced cyclic stress ratio and normalized CPT tip resistance for each of the CPT soundings are shown in Fig. 7-7. Critical CPT tip resistances were estimated using the guidelines previously described in Section 1.3. Cyclic stress ratios are adjusted to equivalent cyclic stress ratios for M=7.5 earthquakes based on the ratios presented by Seed and Idriss (1982). Along the eastern end of Salmon Way (CPTs UC-10 and UC-11), the critical depths were taken in the silty sand and sand layer between depths of about 1.7 and 3.4 m. This sand layer was also considered critical near the Chevron fuel tank enclosure, as evidenced by the sand ejecta within the fuel tank enclosure. On the south side of the fuel tanks (USGS-14A, Fig. 7-5), the critical sand layer extended from the surface fill down to the underlying dense sands and the critical normalized CPT tip resistance was 110 bars at a depth of 3.6 m. On the north side of the fuel tanks (UC-9 and USGS-15A; Figs. 7-4 and 7-5), characterization of the critical sand layer is difficult because the layer becomes relatively thin and is sandwiched between the overlying soft sandy silt and the underlying dense sands. In both UC-9 and USGS-15A, the normalized CPT tip resistance in the critical sand layer increased gradually from about 5 bars at the contact with the soft sandy silt to about 140-150 bars at 0.4 m below the contact, and then stayed relatively constant over the next 0.4 m. The gradual transition in CPT tip resistances is thought to reflect a real transition in soil characteristics because the transition interval is relatively thick and similar gradual transitions in CPT tip resistance are seen elsewhere at Woodward Marine where the soft sandy silt layer is not encountered. Subsequently, the critical normalized CPT tip resistances for CPTs UC-9 and USGS-15A were taken over a 0.3 m interval beginning 0.15 m below the contact with the soft sandy silt, resulting in values of about 105 and 81 bars, respectively. While these values are quite sensitive to the interval thickness over which the tip resistance is averaged, the 0.3 m interval used herein resulted in values reasonably close to the critical value of 116 bars obtained from USGS-14A. Given the subjectiveness of the critical tip resistances for CPTs UC-9 and USGS-15A, these data points are labelled as "medium-confidence" in Fig. 7-7. For reference, Fig. 7-7 also shows the boundary between conditions of liquefaction and non-liquefaction proposed by Mitchell and Tseng (1990) for clean sands with $D_{50}$ values of 0.20 mm and 0.40 mm. The boundaries proposed by Mitchell and

Tseng (1990) are generally consistent with the observations of widespread ground deformations and liquefaction-induced sand boils in this area.

## 7.6 Correlation With Shear Wave Velocity Measurements

A profile of normalized shear wave velocity ($V_{S-1}$) west of the Chevron fuel tanks is shown in Fig. 7-8. The $V_{S-1}$ profile follows the general details of stratification identified by the CPT tip resistance profile, but the measurement intervals were too coarse to isolate the thin zone of sand suspected of liquefying (2.5 to 3.0 m depth). The $V_{S-1}$ value of 138 m/s between 2.05 and 3.05 m depth is likely a low estimate for the sand suspected of liquefying because the upper half of this interval is a soft sandy silt. Consequently, these data are not compared to the relationships proposed by Robertson et al. (1992) in Fig. 1-6 because of their questionable representativeness for these thin strata. These data illustrate the difficulty in using shear wave velocity measurements, with measurement intervals of 1 to 2 m, to characterize thin strata.

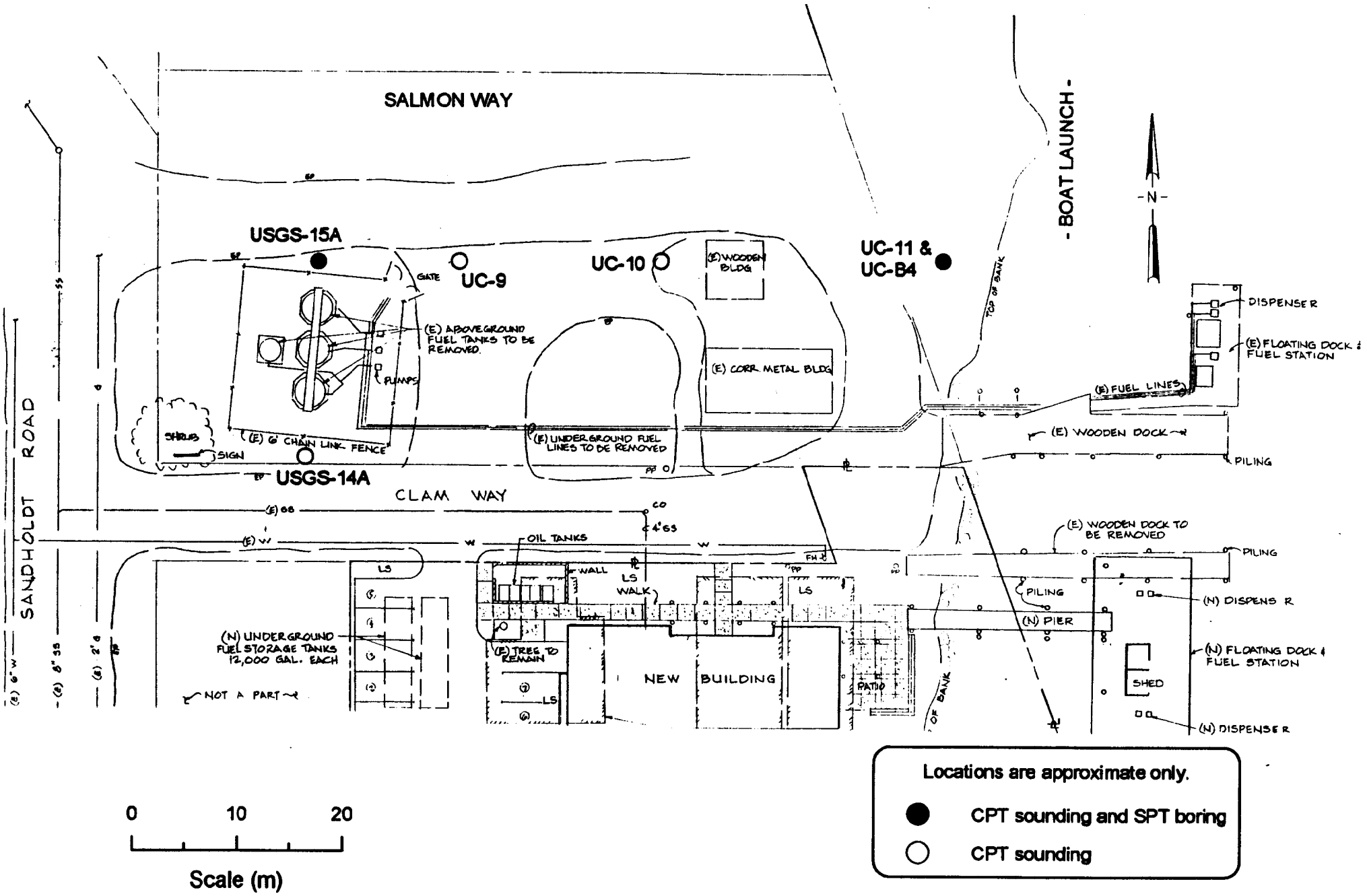


FIG. 7-1. Map of the Woodward Marine Site

FIG. 7-2. Cracking and Settlement of the Boat Launch at Woodward Marine.

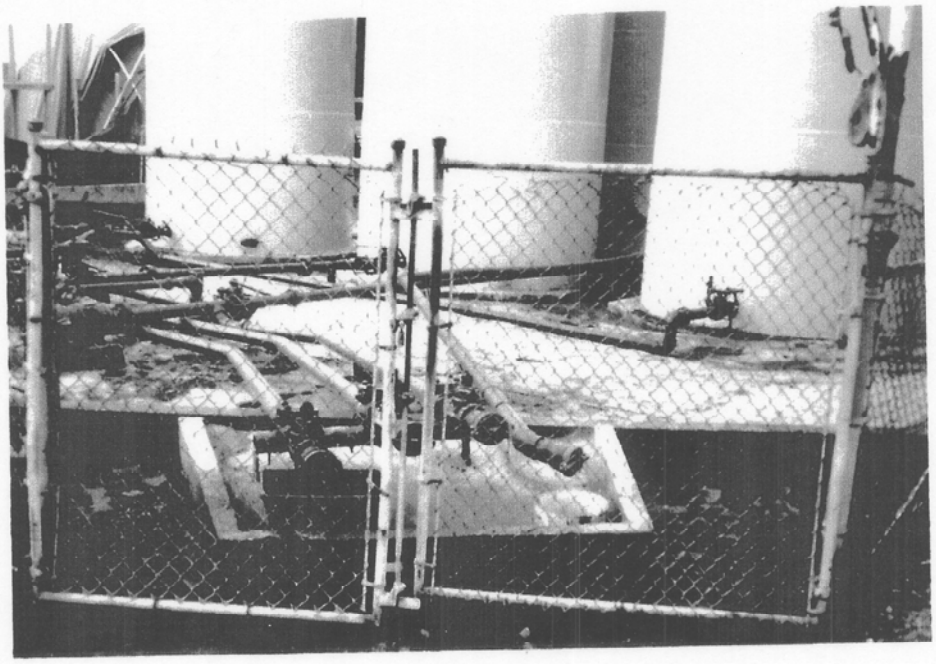

FIG. 7-3. Sand Boils and Differential Settlement at the Chevron Fuel Tank Enclosure at Woodward Marine.

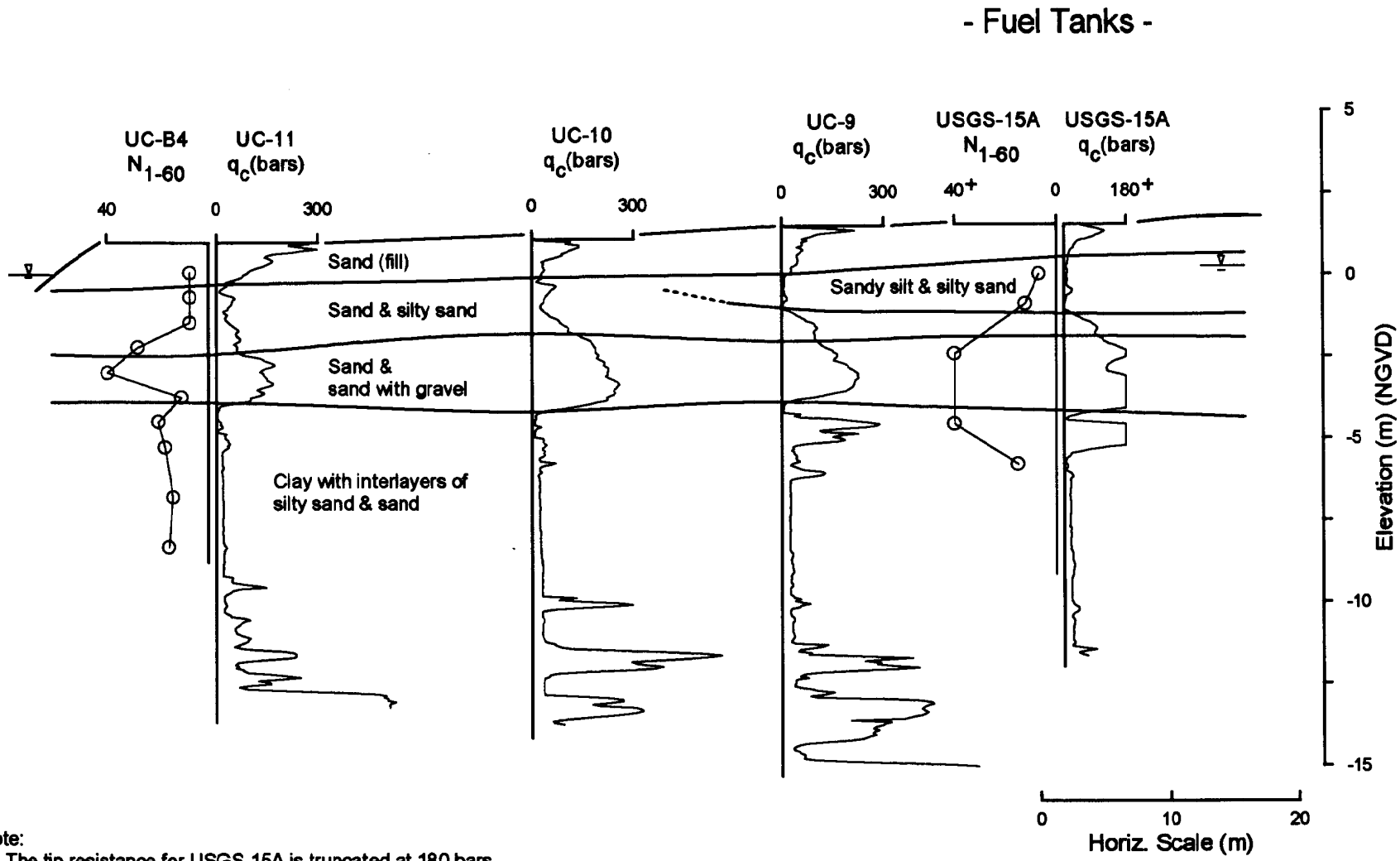


Note:
1. The tip resistance for USGS-15A is truncated at 180 bars.

FIG. 7-4. Subsurface Conditions Along Salmon Way at Woodward Marine

PROWOOD1.GRF

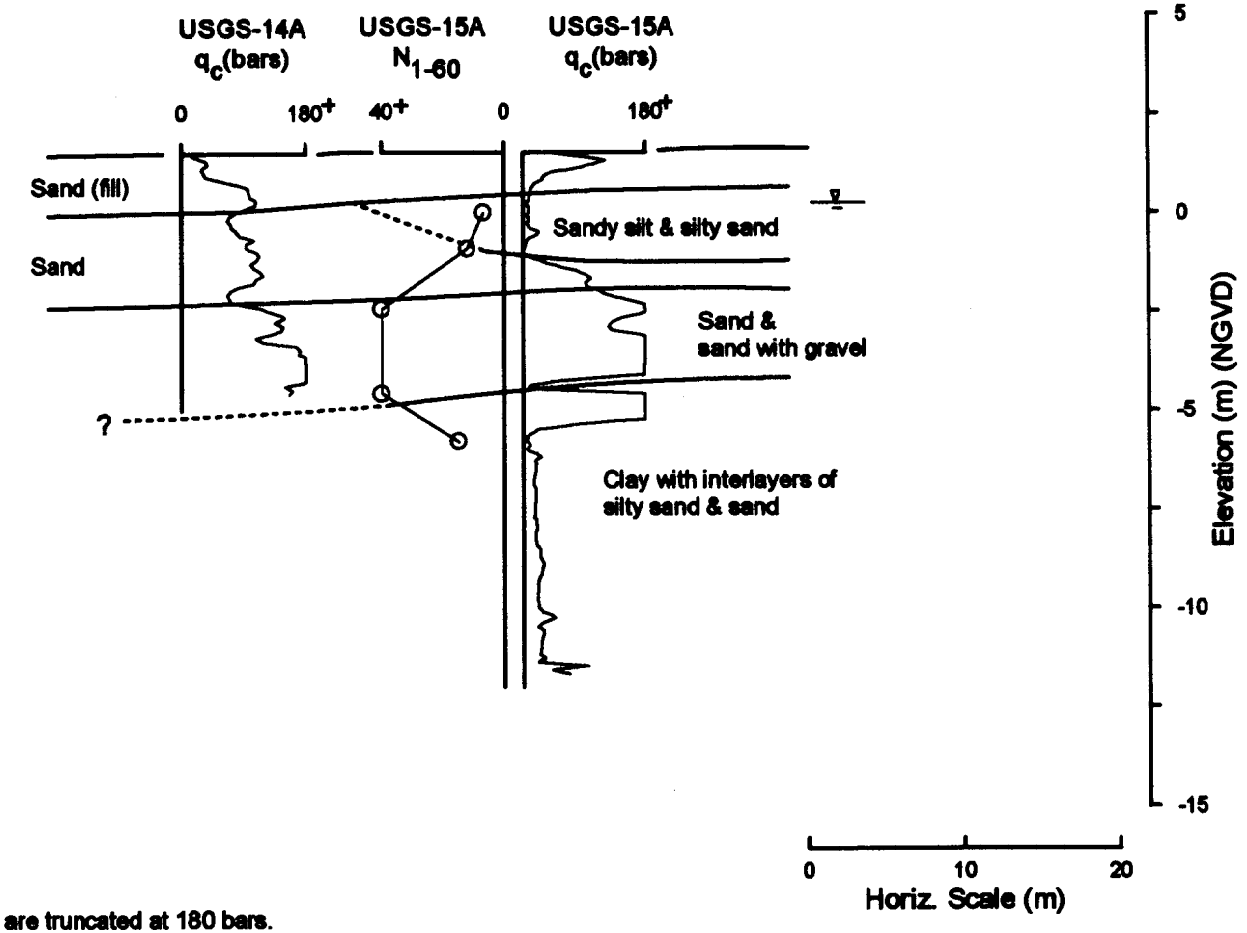


Note:
1. The tip resistances for USGS-14A and 15A are truncated at 180 bars.

FIG. 7-5. Subsurface Conditions Across Fuel Tank Enclosure - Parallel to Sandholdt Road

PROWOOD2.GRF

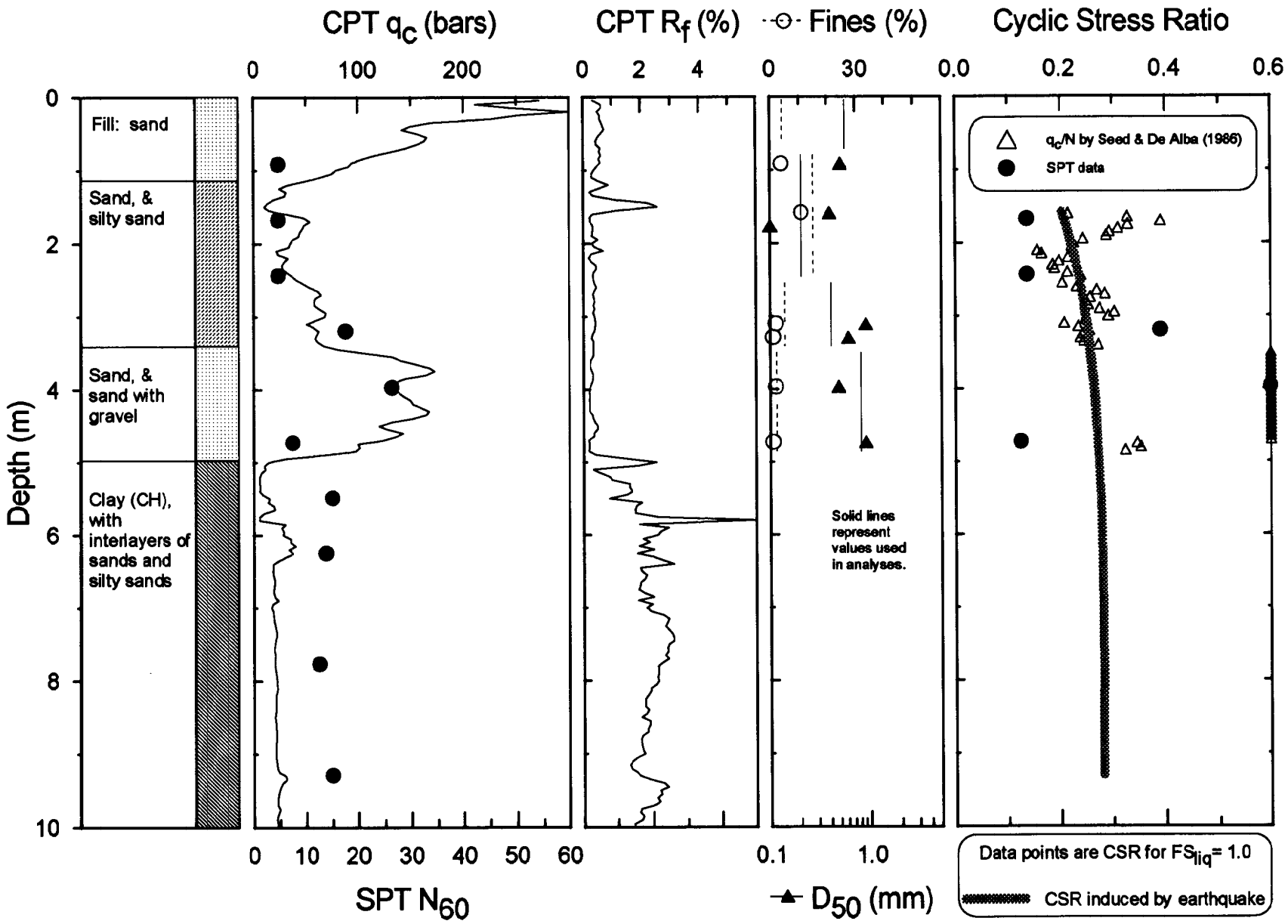


FIG. 7-6. Liquefaction Analyses of Adjacent SPT (UC-B4) and CPT (UC-11) Data Near Woodward Marine's Boat Ramp

PAIRUCB4.GRF

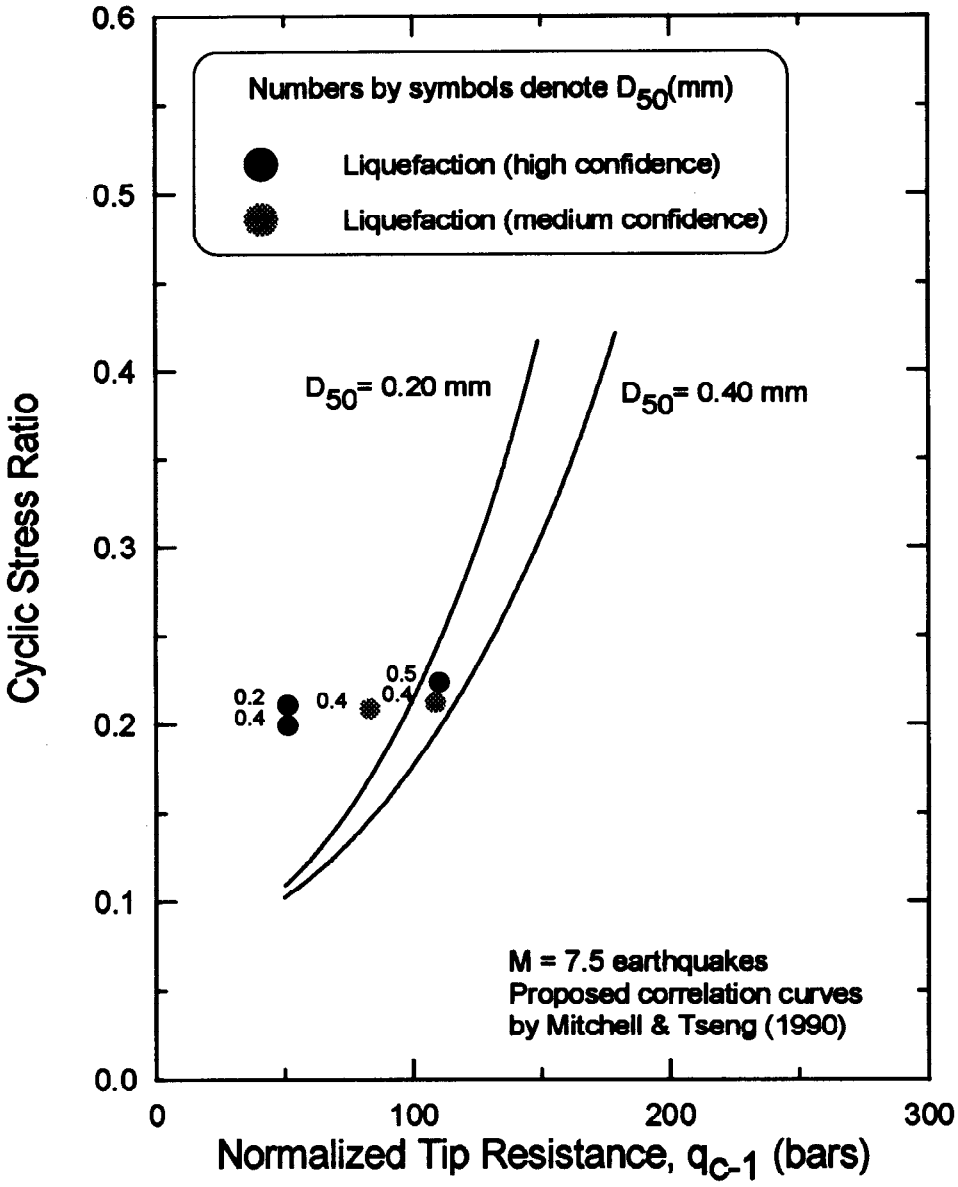


FIG. 7-7. Correlation of CPT Tip Resistance to Liquefaction Resistance at Woodward Marine

wood-2.grf

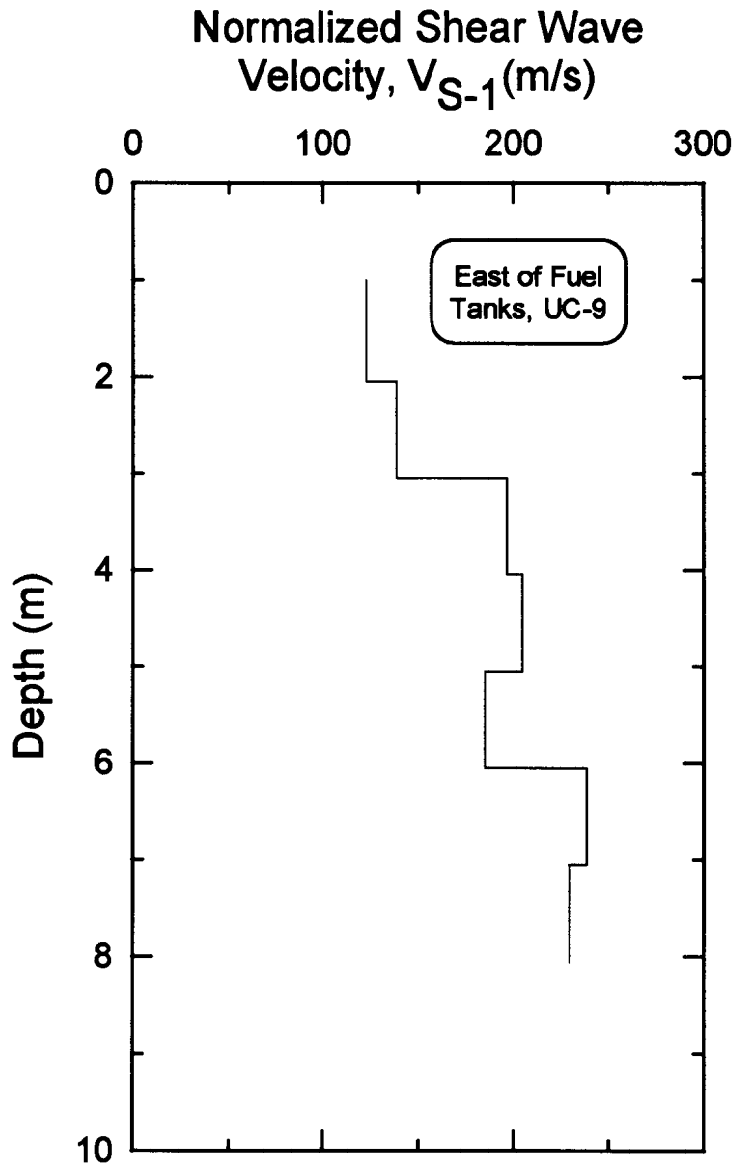


FIG. 7-8. Normalized Shear Wave Velocity Profile at Woodward Marine

# 8. MBARI FACILITIES AND SANDHOLDT ROAD

## 8.1 Site Description

The Monterey Bay Aquarium Research Institute (MBARI) facilities include three main buildings and a pier located along Sandholdt Road on the Moss Landing spit. These facilities are located between about 100 and 300 m north from the western approach to the timber bridge crossing the Old Salinas River (Fig. 1-2). A site plan of the facilities is shown in Fig. 8-1. At the time of the Loma Prieta earthquake, the MBARI Technology Building and the Concrete Pier were nearing completion. Construction of Buildings No. 3 and No. 4 began in 1994. The site of Building No. 3 was previously an unpaved parking lot located to the north of the Technology Building. Between the Technology Building and Building No. 3 is an existing one-story wood building, the front portion of which is occupied by Phil's Fish Market. The site of Building No. 4 is located between the old site of the General Fish Company (which has been torn down since the Loma Prieta earthquake) and the Technology Building.

The Technology Building is a concrete tilt-up structure founded on structurally interconnected spread footings embedded about 1 m below grade. The building floor is a concrete slab-on-grade that rests on a 0.3-m-thick compacted gravel sub-base (Rutherford and Chekene 1988). The Concrete Pier consists of a reinforced concrete deck supported on 0.5-m-diameter, driven prestressed concrete piles with maximum production pile lengths of about 24 m (Rutherford and Chekene 1993). Phil's Fish Market is located in a one-story wood building founded on (non-connected) spread footings, with the floor appearing to be an unreinforced slab on grade. The General Fish Company buildings were constructed of wood, but details of the foundation or construction are not known.

## 8.2 Observations of Earthquake Effects

The Technology Building was undamaged by the shaking and there was no evidence of damage or settlement to the foundation or concrete floor. A couple of cracks less than about 1 cm wide were observed in the asphalt pavement to the front (eastern side) and north side of the building. There was no evidence of sand boils in the immediate area of the building. Based on topographical surveys, Rutherford and Chekene (1993) concluded that "neither the (Technology) building nor the (Concrete) pier had settled much as a result of the earthquake."

The Concrete Pier was essentially undamaged by the shaking and there was no evidence of settlement or lateral movement of the pier itself (based on survey data by Rutherford and Chekene 1993). Minor concrete spalling was observed at the joints between some piles and the deck. Lateral movements were observed in the soils around the pier, however. The adjacent edge of Sandholdt Road settled and displaced laterally towards the harbor by about 8 cm and 25 cm just south and north of the pier, respectively. Fig. 8-2(a) shows settlements of Sandholdt Road around a deep sewer well just to the north of the Concrete Pier. Beneath the pier deck, the rip-rap was estimated to have settled about 15 cm relative to the deck.

In the unpaved parking area that now is the location of Building No. 3, several hairline cracks formed subparallel to the harbor with the crack frequency being greatest near Sandholdt Road and

decreasing to the western end of the lot. No evidence of sand boils was observed in the parking area.

The front of the wood building that houses Phil's Fish Market is estimated to have experienced settlements of about 5 to 8 cm and lateral spreading movements of about the same amount. Door and window frames skewed and the concrete floor was severely cracked and tilted in spots. The concrete floor in the rear portion of this building was reported to have experienced widening of cracks that existed before the earthquake.

The site of the General Fish Company appears to have experience minor lateral movements. Barminski (1993) observed ground cracks at a few spots toward the eastern side of the site and moderate cracks in the buildings (up to 8 cm). In particular, a significant ground crack was observed along the northern side of the "Existing Metal Building" at the location of boring EB-5 shown on Fig. 8-1. Lateral spreading movements for this entire site were estimated at 5 to 7.5 cm by Barminski (1993), but this estimate is considered qualitative since there is little other supporting documentation of how ground cracking was distributed across the site (i.e., localized or widespread). Barminski (1993) also estimated lateral spreading deformations of 2.5 cm at the MBARI Technology Building, which in comparison with the conclusions of Rutherford and Chekene (1993) suggests that Barminski may have been more conservative in his interpretation of field behavior.

Extensive ground deformations were observed all along Sandholdt Road, including the portion paralleling the waterfront alongside the MBARI facilities. Fig. 8-2(b) shows a view (looking north) of Sandholdt Road about midway between the timber bridge and the Concrete Pier, three days after the earthquake. Cracks in the asphalt pavement occurred parallel to the waterfront, with the zone of significant cracking generally being limited to between the road centerline and the shoreline edge of the road. Three slope inclinometers located along the shoreline edge of the road indicated lateral deformations of about 30, 8, and 25 cm, respectively.

## 8.3 Field Investigations

Field investigations in the area were performed by Rutherford and Chekene (1987, 1988, 1993), Harding Lawson and Associates (1988), and under the present study. Locations of exploratory borings and CPT soundings are shown on the site plan in Fig. 8-1.

Rotary wash borings (with bentonite slurry) were performed for Rutherford and Chekene (1988, 1993) by Taber Consultants using a Concore rig. A fish tail bit was used for drilling. SPT tests were performed using a safety hammer, a cathead and rope system with 2 wraps of the rope around the cathead, and a 5-cm-outside diameter split spoon sampler with room for liners. A few samples were obtained using a California split spoon sampler (6.3-cm outside-diameter). Energy measurements for this rig and these procedures while drilling at shallow depths in soft clay on another project indicated an average energy ratio of about 65% (Taber 1994). Given the differences in energy ratios that may arise from different operators and soil conditions, it seems reasonable to conclude that the blow counts reported by Rutherford and Chekene can be essentially taken as $N_{60}$ values. CPT soundings performed by Rutherford and Chekene (1988, 1993) and under the present study were both completed by VBI In-Situ Testing, using the equipment and procedures previously described in Section 4.

The borings by Harding Lawson (1988) were performed using both auger and rotary wash drilling methods. SPT tests were performed using both a standard 5 cm outside diameter split spoon and an 8.6-cm outside-diameter Sprague and Henwood split barrel sampler. The recorded blow counts using the larger sampler were converted to equivalent standard SPT blow counts using an unspecified method before presentation on the boring logs. The purpose of these borings was to investigate stability of the waterfront slope during dredging of the harbor, not liquefaction. Consequently, the procedural details were not reported, and the procedures generally recommended for liquefaction assessments may not have been strictly followed. Keeping this limitation in mind, the blow counts reported on the boring logs were taken as equivalent to $N_{60}$ values.

For the present study, CPT soundings and a rotary wash boring were performed using the procedures previously described in Section 4. Two CPT soundings (UC-4, UC-6) included shear wave velocity measurements. Logs and laboratory data are presented in Appendices A, B and C.

Historical shoreline locations, as shown in Fig. 2-2, suggest that the shoreline along the harbor side of Sandholdt Road in the vicinity of the MBARI facilities has fluctuated significantly and thus some shallower soil strata along this portion of Sandholdt Road may have been deposited very recently. Furthermore, the shoreline along this portion of Sandholdt Road was recently modified as part of slope modifications and harbor dredging operations (Harding Lawson 1988).

## 8.4 Subsurface Soil Conditions

Subsurface conditions are illustrated by the three cross-sectional profiles shown in Figs. 8-3, 8-4, and 8-5. As shown on the site plan in Fig. 8-1, the cross-sections cut across the spit, perpendicular to the shoreline, at the locations of the three slope inclinometers installed by Harding Lawson and Associates (1988). In general, similar subsurface conditions exist at these three locations.

The site is underlain by a 8- to 12-m-thick layer of poorly graded sand with interlayers of gravelly sand and sandy gravel in its lower portion. This layer averages less than 5% fines (ranges from 1% to 8%) with measured $D_{50}$ values ranging from 0.2 to 2.1 mm. Occasional thin lenses of clayey silt are encountered throughout the layer. At cross-sections A-A' and B-B', layers of clayey silt up to 1.5 to 2.5 m thick intrude laterally into the sand layer from the harbor side. These clayey silt layers are generally soft to medium-stiff and of low-plasticity (classifications of ML and CL). Hydrometer tests on samples from boring UC-B10 at depths of 3.7 and 5.3 m showed minus 5 μm fractions of 18% and 14%, respectively.

Underlying the sand layer is a 1.5- to 6-m-thick layer of silty clay that varies in thickness at the three different profiles, being thickest at the Technology Building and thinnest at the site of Building No. 4. This clay layer is generally soft to medium-stiff, with liquid limits of 50 to 77, plasticity indices of 25 to 43, and primarily classifying as CH/MH by the USCS. Thin interlayers of sands are encountered, with the concentration being greatest toward the western side of the spit.

Underlying the first silty clay layer is another layer of silty clay with interlayered sands that extends to depths of roughly 23 m. This silty clay is generally stiff to very-stiff, with liquid limits of 55 to 70, plasticity indices of 23 to 34, and predominant USCS classifications of MH/CH. Atterberg

Limits for this silty clay layer are very similar to those for the overlying soft- to medium-stiff silty clay layer, as shown by the data in Fig. 8-6. The sand interlayers are generally very dense.

From a depth of about 23 m to the depths explored, very dense clayey and silty sands were encountered.

## 8.5 Evaluation of Liquefaction Based on SPT Data

The potential for triggering of liquefaction in the foundation soils was evaluated using the same procedures previously described in Section 1.3. The results of the analyses using the available SPT data are summarized in groups corresponding to local areas as follows:

(i) the old site of the General Fish Company, on Fig. 8-7;
(ii) the site of the new Building No. 4, on Fig. 8-8;
(iii) the site of the MBARI Technology Building, on Fig. 8-9;
(iv) the site of the new Building No. 3, on Fig. 8-10; and
(v) along Sandholdt Road, on Fig. 8-11.

In the following presentations of the SPT data, blow counts are not shown if the recovered sample was considered nonsusceptible to liquefaction (i.e., the high plasticity clay and silt layers).

At the old site of the General Fish Company, the analysis results shown in Fig. 8-7 suggest that liquefaction would be expected in limited zones. At elevation 0 m, the one blow count that clearly indicates liquefaction comes from boring EB-5 (Rutherford and Chekene 1993) which was located next to a mapped surface crack. Near elevation -4.5 m, there are three blow counts that would suggest liquefaction occurred. One of these comes from boring EB-5, which was adjacent to a CPT sounding. The log of boring EB-5 and the adjacent CPT sounding, as shown in Fig. 8-12, clearly suggest that the low blow counts at elevation -3.0 and -4.5 m were influenced by interlayered clay seams although the SPT samples did not penetrate the clay interlayers. Thus, the CPT sounding suggests that liquefaction would not be expected at this elevation near boring EB-5. Since the other borings at this site were not adjacent to CPT soundings, it is not possible to evaluate to what extent clay or silt interlayers may have adversely affected SPT blow counts. Nonetheless, two of the other blow counts indicating liquefaction at about elevation -4.5 and -7.5 m were taken above and below a soft clay layer in boring EB-1, as shown on the profile in Fig. 8-3. These data illustrate the utility of performing adjacent CPT soundings and SPT borings. Overall, the SPT data suggests that liquefaction may have occurred in zones of limited extent, which is consistent with the absence of significant lateral spreading deformations.

At the site of Building No. 4, the analysis results shown in Fig. 8-8 suggest that liquefaction would not be expected other than at a single point at elevation -8. 5 m. It should be noted that four other blow counts would have indicated liquefaction near this elevation if interpreted strictly from the boring log data, but the data were discarded because: (1) comparison of boring EB-3 with the adjacent CPT sounding indicated that a blow count in this zone was unrepresentatively low due to nearby soft interlayers; and (2) it appears that three samples from boring B-5 described as sandy silt should have coincided with the high plasticity clay layer encountered at these depths in other borings, as illustrated in the cross-sectional profiles in Figs. 8-3 to 8-5, and are suspected of being misclassified in the field. The results of the liquefaction analyses are consistent with the absence of any reported ground deformations in this area.

At the Technology Building, the analysis results are shown in Fig. 8-9 for the one available boring. One blow count at elevation -1 m indicates liquefaction, while blow counts at other elevations indicate liquefaction was unlikely. If a thin zone of sand did liquefy then it must have either resulted in settlements small enough not to affect the building or have been of limited enough extent such that the overlying soils and foundation effectively limited its surface expression.

At the site of Building No. 3, the analysis results shown in Fig. 8-10 suggest that isolated pockets of sand may have generated high excess pore pressures during the earthquake (i.e., low factors of safety against liquefaction), but that extensive liquefaction would not be expected. Of the seven blow counts in sands (less than 12% fines) indicating factors of safety against liquefaction less than about 1.6 between elevation 1 m and elevation -6 m, five of them were from boring EB-5 (Rutherford and Chekene 1988). Of the three borings located in this area, Boring EB-5 is the closest to the harbor side of the lot where hairline ground cracking was more concentrated. It should be noted that the lowest three SPT blow counts in boring EB-7 (Rutherford and Chekene 1988) were discarded as it is believed they were adversely influenced by the presence of the high plasticity clay layer, as illustrated on the profile in Fig. 8-4. The samples for these three SPT tests were visually classified as sandy silts on the logs, with one sample containing an "elastic" (i.e., high plasticity) silt lens. As shown of Fig. 8-6, the cumulative data of all studies show the soils in this layer to be of high plasticity (CH or MH) and would thus be expected to have a high resistance to liquefaction. Overall, the analysis results in Fig. 8-10 agree with the general absence of significant ground deformations in this area.

Along Sandholdt Road, the analysis results shown in Fig. 8-11 suggest that extensive liquefaction would be expected between about elevation 0 m and -3 m, while liquefaction would not be expected at greater depths. Of the nine blow counts indicating liquefaction above elevation -3 m, five were from borings by Harding Lawson and Associates (1988). As previously mentioned, there is some uncertainty regarding the procedures and conversions used in the Harding Lawson study. Nonetheless, their data is consistent with the data obtained by Rutherford and Chekene (1988) and in this study along Sandholdt Road. Overall, the analysis results in Fig. 8-11 are in agreement with the observations of large lateral spreading deformations and settlements along Sandholdt Road.

## 8.6 Evaluation of Inclinometer Data Along Sandholdt Road

Three slope inclinometers were positioned along the shoreline edge of Sandholdt Road to monitor possible movements of the shoreline slope during dredging operations in the harbor. The inclinometers were installed by Harding Lawson and Associates (1988) before the Loma Prieta earthquake. Readings before the earthquake were taken in slope inclinometer SI-5 on April 11, 1989 and in slope inclinometers SI-2 and SI-4 on June 14-16, 1989. Readings after the earthquake were taken in all three slope inclinometers on November 30, 1989 (Tillis 1990). The three inclinometers showed lateral displacements of the ground surface toward the harbor of about 30, 8, and 25 cm, which can be attributed to the effects of the earthquake since prior measurements and observations show the shoreline slope was not deforming measurably.

Slope inclinometer SI-2 was positioned near a loading dock across from the location of Building No. 4 as shown on the site plan in Fig. 8-1 and the profile in Fig. 8-3. A CPT sounding (UC-4) and a boring (UC-B10) were performed 1.5 m and 3.0 m away from the inclinometer,

respectively. The results of liquefaction analyses of the SPT and CPT data are shown in Fig. 8-13 along with the slope inclinometer measurements; the clayey silt was considered nonliquefiable for the analyses shown in Fig. 8-13. The inclinometer measurements show that the edge of the road displaced laterally about 28 cm toward the harbor and about 10 cm south roughly parallel to the shoreline. Lateral deformations of the road were accompanied by settlements of 5 to 8 cm and cracking of the road surface approximately 4.5 to 6.0 m landward of the slope crest. The slope inclinometer data indicate that liquefaction was limited to between depths of about 2.0 and 4.5 m, over which the deformations correspond to an approximate uniform shear strain of about 12%. Near the bottom of this depth interval of lateral deformations, there is a 0.6-m-thick soft clayey silt layer sandwiched between poorly graded sand above and below. A sample of this clayey silt from boring UC-B10 had a liquid limit of 32, a plasticity index of 7, a USCS classification of ML, and 18% finer than 5 μm. Just below the zone of lateral deformations, there is a 1.4-m thick layer of clayey silt having similar characteristics; the upper portion was classified as CL (agrees with a liquid limit of 46 and plasticity index of 21 obtained at this depth by Harding Lawson 1988) and the lower portion was classified as ML. A hydrometer test on the (ML) sample from a depth of 5.3 m showed a minus 5 μm fraction of 14%. The above index data and the CPT signature indicate that the 0.6-m-thick clayey silt layer that deformed is very similar to the underlying 1.4-m-thick clayey silt layer that did not deform. This would support a hypothesis that the 0.6-m-thick clayey silt layer did not significantly strain itself but rather the slope inclinometer deformations were due to lateral loads imposed on the casing by liquefied sands above and below it. On the other hand, the low-plasticity characteristics of the clayey silt suggest that it could be susceptible to significant earthquake-induced excess pore pressures and softening. Softening of the 0.6-m-thick clayey silt layer could be associated with significant strains within itself, or have reduced its ability to restrain the inclinometer casing from deforming laterally under lateral loads from above or below.

Another interesting aspect of the slope inclinometer SI-2 data is that liquefaction-induced shear strains appear relatively uniform across the sand layer between depths of about 2.1 and 3.6 m despite the CPT tip resistance varying from about 75 bars over the upper half to about 160 bars over the lower half (with correspondingly large differences in the calculated factors of safety against liquefaction). The corresponding SPT data does not show as large a variation in penetration resistance across this sand layer as does the CPT data, but this may be simply attributable to the larger effective zone of influence around a SPT sampler than around a CPT tip. It is also noted that the mean grain size is relatively similar across the full thickness of this sand layer and thus the differences in CPT tip resistance do not appear to be a grain size effect. One possibility that may warrant further investigation is how the denser portion may be affected by pore pressure redistribution from the adjoining looser layer as it liquefies. Another possibility is that the deformations are not controlled exclusively by the soils encountered in CPT UC-4 and boring UC-B10, but rather by the entire mass of soil involved in the lateral spread whose stratification and other characteristics may be somewhat different from those encountered in UC-4 and UC-B10.

Slope inclinometer SI-4 was positioned along the shoreline edge of Sandholdt Road across from the Technology Building as shown on the site plan in Fig. 8-1 and the profile in Fig. 8-4. A CPT sounding (RC-1 by Rutherford and Chekene 1988) was located nearby as shown on the site plan. The results of a liquefaction analysis of the CPT data are shown in Fig. 8-14 along with the slope inclinometer measurements. The inclinometer measurements show that the edge of the road displaced laterally about 7.4 cm toward the harbor and negligibly along the shoreline direction. These data

show lateral displacements developing over three depth intervals. Roughly 4.0 cm of displacement developed in the poorly graded sand between the ground surface and a depth of about 2.5 m. This zone of displacement includes a roughly 0.5-m-thick zone of sand having very low tip resistances (roughly 30 bars) compared to the deeper sands. The tide level at the time of the earthquake corresponds to a depth of about 2.8 m, but these shallower soils may still be saturated due to a time lag between ground water levels and the tide level and by capillary effects. Roughly 2.0 cm of displacement developed between depths of about 4.0 and 7.0 m corresponding to an approximate uniform shear strain of about 0.7%. Soils in this depth interval appear to be poorly graded sand in the upper 0.6 m and clayey silt over the remainder. Note that this clayey silt stratum was largely interupted by dense sand at CPT RC-2 located east and slightly north of slope inclinometer SI-4, as shown in Figs. 8-1 and 8-4. No deformations developed between depths of about 7.0 and 9.0 m in slope inclinometer SI-4, within which there were a couple of dense sand interlayers. Roughly 1.2 cm of displacement developed across the high plasticity silty clay layer between depths of about 9.0 and 12.5 m, corresponding to an approximate uniform shear strain of about 0.3%.

Slope inclinometer SI-5 was positioned along the shoreline edge of Sandholdt Road just north of the Concrete Pier as shown on the site plan in Fig. 8-1 and the profile in Fig. 8-5. A CPT sounding (RC-4 by Rutherford and Chekene 1988) was located nearby as shown on the site plan. The results of a liquefaction analysis of the CPT data are shown in Fig. 8-15 along with the slope inclinometer measurements. The inclinometer measurements show that the edge of the road displaced about 25 cm laterally toward the harbor and negligibly parallel to the shoreline. Roughly 16 cm of the displacement developed in the poorly graded sand between depths of about 4.0 and 6.0 m, corresponding to an approximate uniform shear strain of about 8%. Roughly 1.3 cm of lateral displacement developed across the high plasticity clay and silt between depths of about 8.2 and 12.4 m, corresponding to an approximate uniform shear strain of 0.3%.

The deformation profiles obtained from the slope inclinometer data described above all suggest that deformations developed as relatively uniform shear strains over different strata, and not as displacements concentrated along individual shear planes. These data suggest that for these conditions the prediction of lateral displacements based on rigid block behavior coupled with a Newmark-type displacement analysis (e.g., Dobry and Baziar 1992) may not be a physically correct representation of behavior, although it may be a reasonable approximation for engineering purposes. Despite this limitation, the "apparent residual shear strength" of the liquefied soils at the slope inclinometer locations were back-calculated by assuming that the roadway's surface cracking represents the lateral extent of deformations at depth, that liquefaction occurred early in the shaking, and that a Newmark-type approach (Newmark 1965; Makdisi and Seed 1978) was applicable. The back-calculated apparent residual shear strengths were about 5 kPa at SI-2 and 8 kPa at SI-5. At these two inclinometers, the normalized tip resistances for the most critical depths were about 123 and 110 bars, respectively. By proposed correlations to residual shear strength (e.g., Ishihara 1993), these CPT tip resistances would normally indicate much greater residual shear strengths than were back-calculated. However, many case histories used to develop such empirical correlations involved much greater strains and deformations than observed at these inclinometers. Thus, these data suggest that shear strains and deformations significantly larger than observed at the slope inclinometers may be required to mobilize the full residual shear strength of the subsurface soils. Consequently, when liquefaction-induced deformations are being predicted using a Newmark-type approach with residual shear strengths estimated from empirical correlations such as by Seed (1987), Seed and Harder

(1990), or Ishihara (1993), a prediction of small displacements may be unconservative because it is incompatible with the deformation required to mobilize the full residual shear strength of a liquefied soil.

## 8.7 Correlation With Shear Wave Velocity Measurements

Profiles of normalized shear wave velocity obtained by seismic CPT measurements adjacent to slope inclinometer SI-2 and across the road from SI-5 are shown in Fig. 8-16. Down-hole shear wave velocity measurements were also performed within the casings of slope inclinometers SI-2, SI-4 and SI-5 after the earthquake (Mejia 1992; Barminski 1993). In slope inclinometer SI-2, down-hole shear wave velocities were reported to be 146 m/s from 0.0-4.6 m depth, 186 m/s from 4.6-12.2 m depth, and 284 m/s from 12.2-18.3 m depth. In slope inclinometer SI-4, down-hole shear wave velocities were reported to be 146 m/s from 0.0-6.1 m depth, 178 m/s from 6.1-15.2 m depth, and 264 m/s from 15.2-18.3 m depth. In slope inclinometer SI-5, down-hole shear wave velocities were reported to be 174 m/s from 3.0-9.1 m depth. The seismic CPT profiles shown in Fig. 8-16 are consistent with the stratification identified by the CPT signatures. The down-hole shear wave velocity measurements were presented as averages and thus do not follow the detailed stratification. Nonetheless, the seismic CPT and down-hole measurements are generally consistent.

Adjacent to slope inclinometer SI-2, the $V_{s-1}$ value of 115 m/s between 2.0 and 3.0 m depth in CPT UC-4 coincides roughly with the loose sand that liquefied, although the measurement interval includes small portions of soft clay at the top and dense sand at the bottom. The $V_{s-1}$ value of 204 m/s between 8.0 and 9.0 m depth coincides with the dense sand that did not liquefy. The induced cyclic stress ratios at these two depths are estimated to be about 0.17 and 0.23, respectively. These cyclic stress ratios are based on a peak ground acceleration of 0.25 g, and are adjusted to an equivalent M=7.5 earthquake based on the ratios presented by Seed and Idriss (1982). The above combinations of normalized shear wave velocity and earthquake-induced cyclic stress ratio are consistent with the relationship in Fig. 1-6 proposed by Robertson et al. (1992).

Across the road from slope inclinometer SI-5, the $V_{s-1}$ value of 169 m/s between 5.95 and 6.95 m depth in CPT UC-6 coincides with the zone of sand having the lowest CPT tip resistance. No visible deformations were observed at the location of UC-6 (west side of Sandholdt Road), while significant deformations were visible east of Sandholdt Road's centerline and 25 cm of lateral deformation were measured in slope inclinometer SI-5. This difference in observed ground deformations is consistent with the CPT tip resistances being significant larger at UC-6 than at RC-4 (beside SI-5). The induced cyclic stress ratio at a depth of 6.45 m at UC-6 is estimated at 0.23. This combination of normalized shear wave velocity and earthquake-induced cyclic stress ratio would plot just on the liquefiable side of the relationship in Fig. 1-6 proposed by Robertson et al. (1992).

The down-hole $V_{s-1}$ value of 189 m/s between 3.0 and 9.0 m depth in the casing of slope inclinometer SI-5 cannot be taken as representative of the deformed interval (4-6 m depth) because of the large measurement interval used.

## 8.8 Correlations With CPT Data

Critical combinations of normalized CPT tip resistance ($q_{c-1}$) and earthquake-induced cyclic

stress ratio ($CSR_{eq}$) obtained near the slope inclinometers along Sandholdt Road are summarized in Fig. 8-17. Critical CPT tip resistances were estimated using the guidelines previously described in Section 1.3. Cyclic stress ratios are adjusted to equivalent cyclic stress ratios for M=7.5 earthquakes based on the ratios presented by Seed and Idriss (1982). The three slope inclinometers provided seven critical combinations of $q_{c-1}$ and $CSR_{eq}$ plotted on Fig. 8-17; 3 "Liquefaction" and 4 "Nonliquefaction." The three points on Fig. 8-17 labelled "No liquefaction evident" correspond to CPTs UC-2, UC-3, and UC-6 which were located across Sandholdt Road from slope inclinometers SI-4, SI-2, and SI-5, respectively. These three CPT locations were to the west of where ground deformations and cracking along Sandholdt Road were visibly evident, but there were no structural features or survey data to rule out the possibility of some small movement having occurred. For reference purposes, Fig. 8-17 also shows the boundaries between conditions of liquefaction and non-liquefaction proposed by Mitchell and Tseng (1990) for clean sands with $D_{50}$ values of 0.20 mm and 0.40 mm. The boundaries proposed by Mitchell and Tseng (1990) are generally consistent with the data near the slope inclinometers.

Recall that for slope inclinometer SI-2 (see Section 8.6), liquefaction-induced shear strains occurred across a sand layer having CPT tip resistances that ranged from about 75 bar to about 160 bar. For this clean sand layer ($D_{50}$ = 0.4 mm), the critical combination plots just outside the proposed boundary for clean sands with $D_{50}$ of 0.40 mm (note, $q_c$=75 bar becomes $q_{c-1}$=120 bar). The data point for the tip resistance of 160 bar would plot far outside the proposed boundaries, but it is not clear whether this apparently denser portion would behave independently of the adjoining looser portion (e.g., possible pore pressure redistribution effects) and thus is not plotted.

Fig. 8-18 summarizes critical combinations of normalized CPT tip resistance and earthquake-induced cyclic stress ratio obtained near the MBARI Facilities other than along Sandholdt Road. Again, critical CPT tip resistances were estimated using the guidelines previously described in Section 1.3. Cyclic stress ratios are adjusted to equivalent cyclic stress ratios for M=7.5 earthquakes based on the ratios presented by Seed and Idriss (1982). Visual classifications on the borehole logs along with the limited available grain size analysis data indicate that the critical combinations correspond to relatively clean sands (less than 5% fines) with typical $D_{50}$ values estimated at 0.4 to 0.7 mm (full range from 0.2 to 2.0 mm). The only data point for "Liquefaction" is from CPT-5 (near boring EB-5 on Fig. 8-1), which was located alongside a documented significant ground crack. All remaining data are labelled as "No liquefaction evident," because the interpretation of some data is hampered by incomplete observations of earthquake effects. For example, isolated ground cracks were observed at some locations near the MBARI Facilities, but these may have been the consequence of only localized pockets of liquefaction such as encountered at the location of CPT-5 and boring EB-5 on Fig. 8-1. However, the reported earthquake effects at the locations of the other available CPTs were generally insignificant which suggests that either liquefaction did not occur or its surface manifestation was limited. Subsequently, the term "No liquefaction evident" is a reasonable label to describe these data according to the more global behavior of their respective sites.

## 8.9 Pre- and Post-Earthquake CPT Soundings

As part of the present study, three post-earthquake CPT soundings were performed adjacent to three pre-earthquake CPT soundings at the site of the new Building No. 3 at the locations shown on Fig. 8-1. The post-earthquake CPT soundings were positioned 1.6 m away from the pre-

earthquake CPT soundings in directions chosen to avoid encountering nearby test-pit and boring locations. Coordinate positions of the pre-earthquake CPT soundings and borings were provided by Rutherford and Chekene (Khasali 1993). These positions were subsequently located in the field by survey using pre-earthquake coordinates of existing building corners. Consequently, there is an estimated error in the re-established CPT locations of about 0.3 m, primarily because of earthquake-induced ground deformations. Both pre- and post-earthquake CPT soundings were performed by VBI In-Situ Testing, Inc.

Fig. 8-19 shows the pre- and post-earthquake CPT tip resistance profiles at the three locations. The observed differences in tip resistances between the CPT pairs are generally of an amount that is consistent with natural variability (even within a 1.6 m distance) for this depositional environment. It does, however, appear that the post-earthquake tip resistances are slightly greater than the pre-earthquake tip resistances between depths of about 4.0 to 7.0 m at all three locations. Also shown on Fig. 8-19 are the profiles of "critical" tip resistance that would correspond to a factor of safety against liquefaction of 1.0 based on Seed et al. (1985) SPT-based correlation and a $q_c/N_{60}$ ratio of about 8.0. The "critical" tip resistance profiles serve to indicate that the lowest factors of safety against liquefaction probably occurred between depths of about 3.0 to 7.0 m, which roughly corresponds to the depth interval which may appear to have experienced some earthquake-induced increase in tip resistance. Any earthquake-induced increase in tip resistance was, however, relatively small (less than 15%), which might have been expected since surface evidence of liquefaction (e.g., significant ground deformations or sand boils) was not observed at these locations.

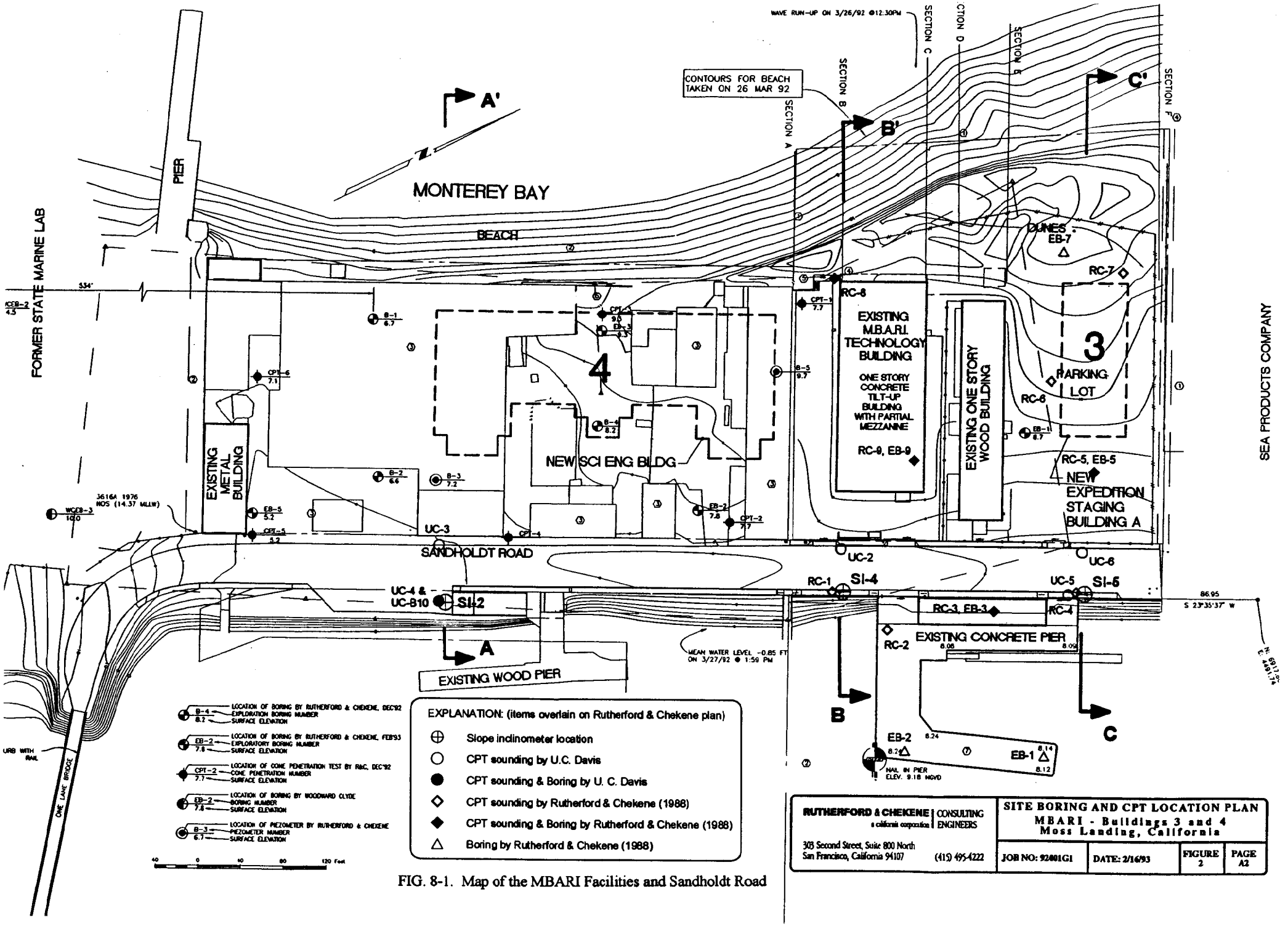


FIG. 8-1. Map of the MBARI Facilities and Sandholdt Road

FIG. 8-2(a). Differential Settlement at a Sewer Well on Sandholdt Road, Just to the North of the MBARI Pier (looking north).

FIG. 8-2(b). Cracking Along Sandholdt Road Just to the South of the MBARI Pier (looking north).

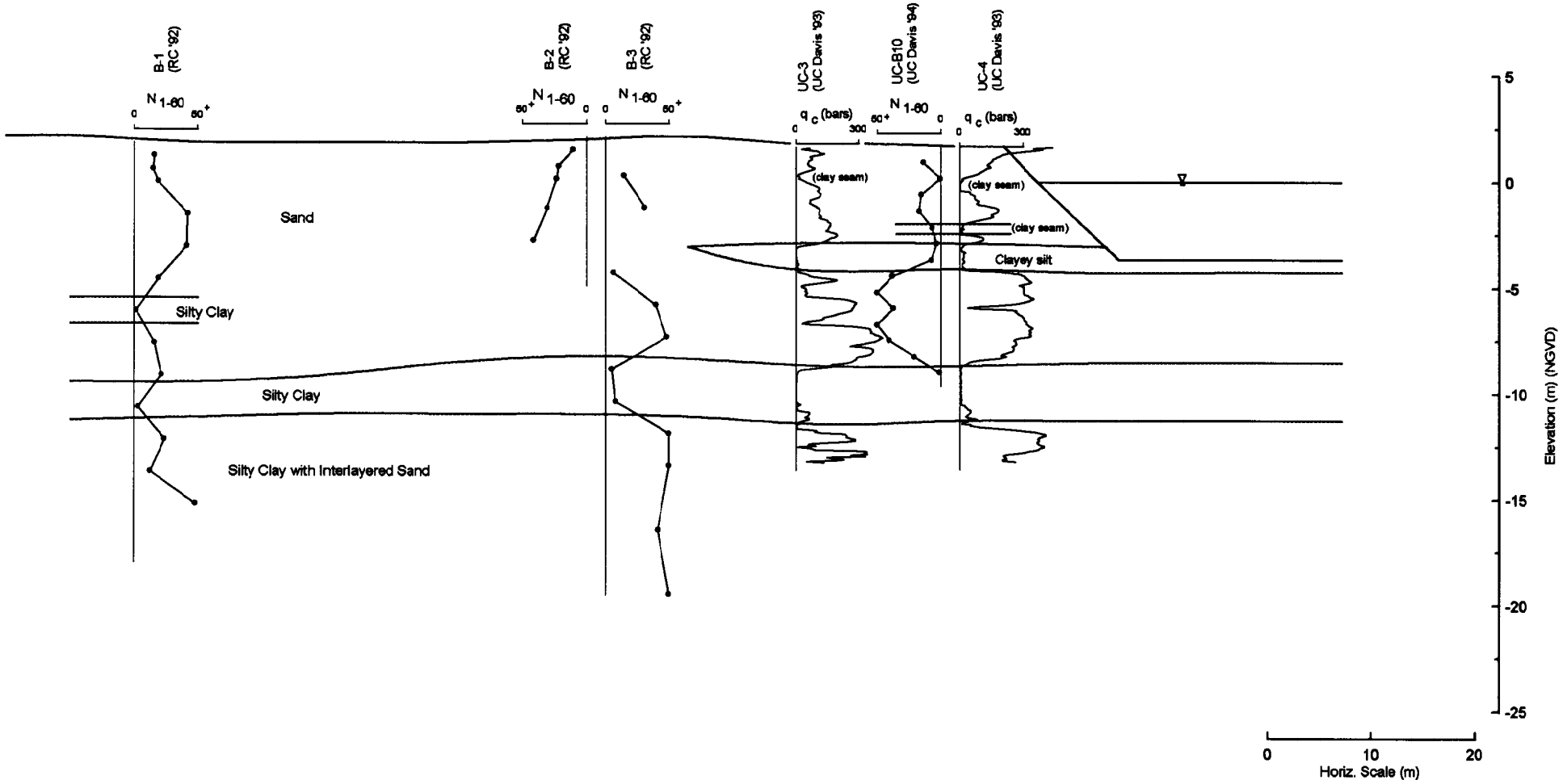


FIG. 8-3. Subsurface Conditions at Cross-Section A-A' Across MBARI Building No. 4

XSECT-A1.GRF

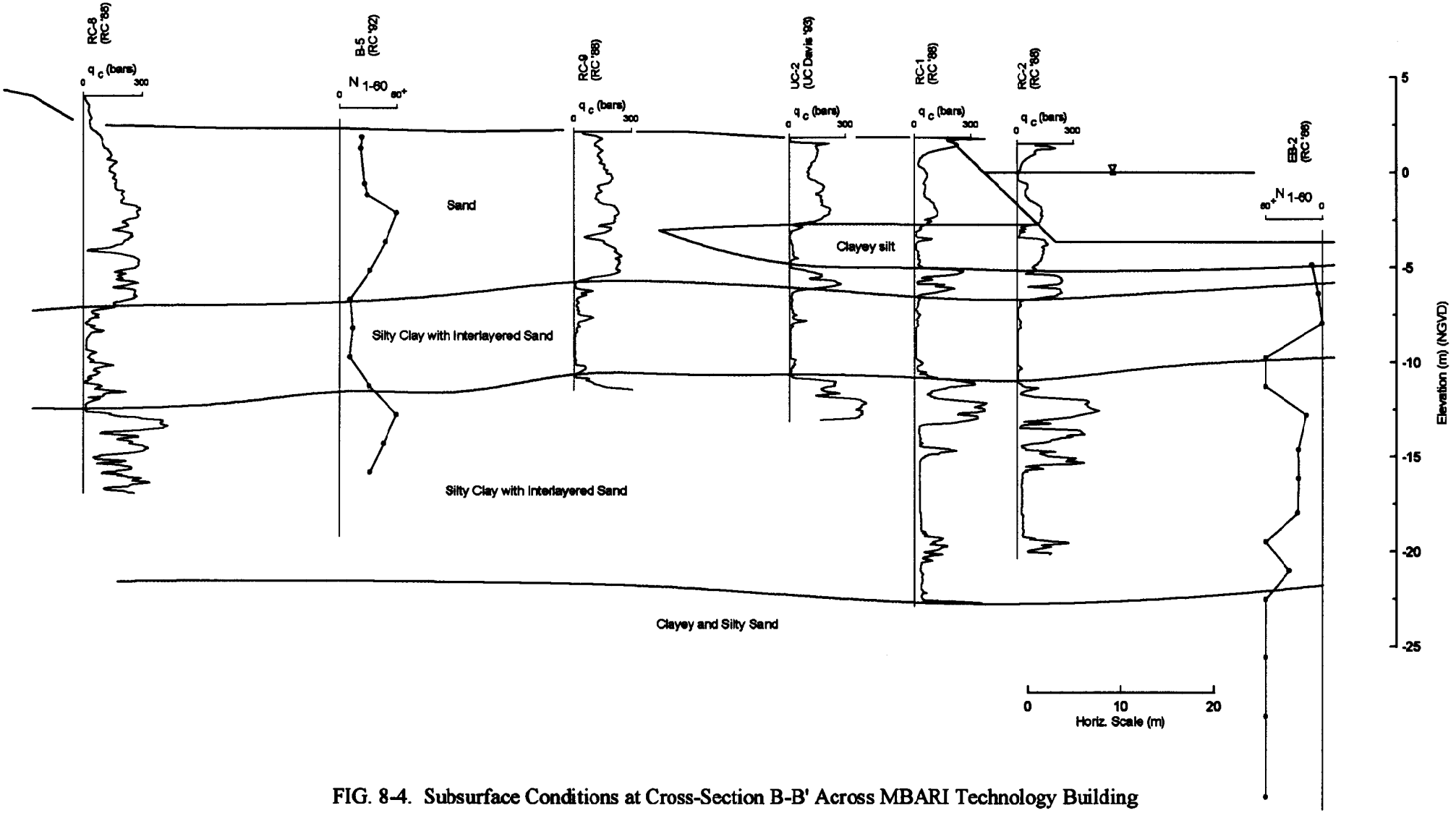


FIG. 8-4. Subsurface Conditions at Cross-Section B-B' Across MBARI Technology Building

XSECT-B1.GRF

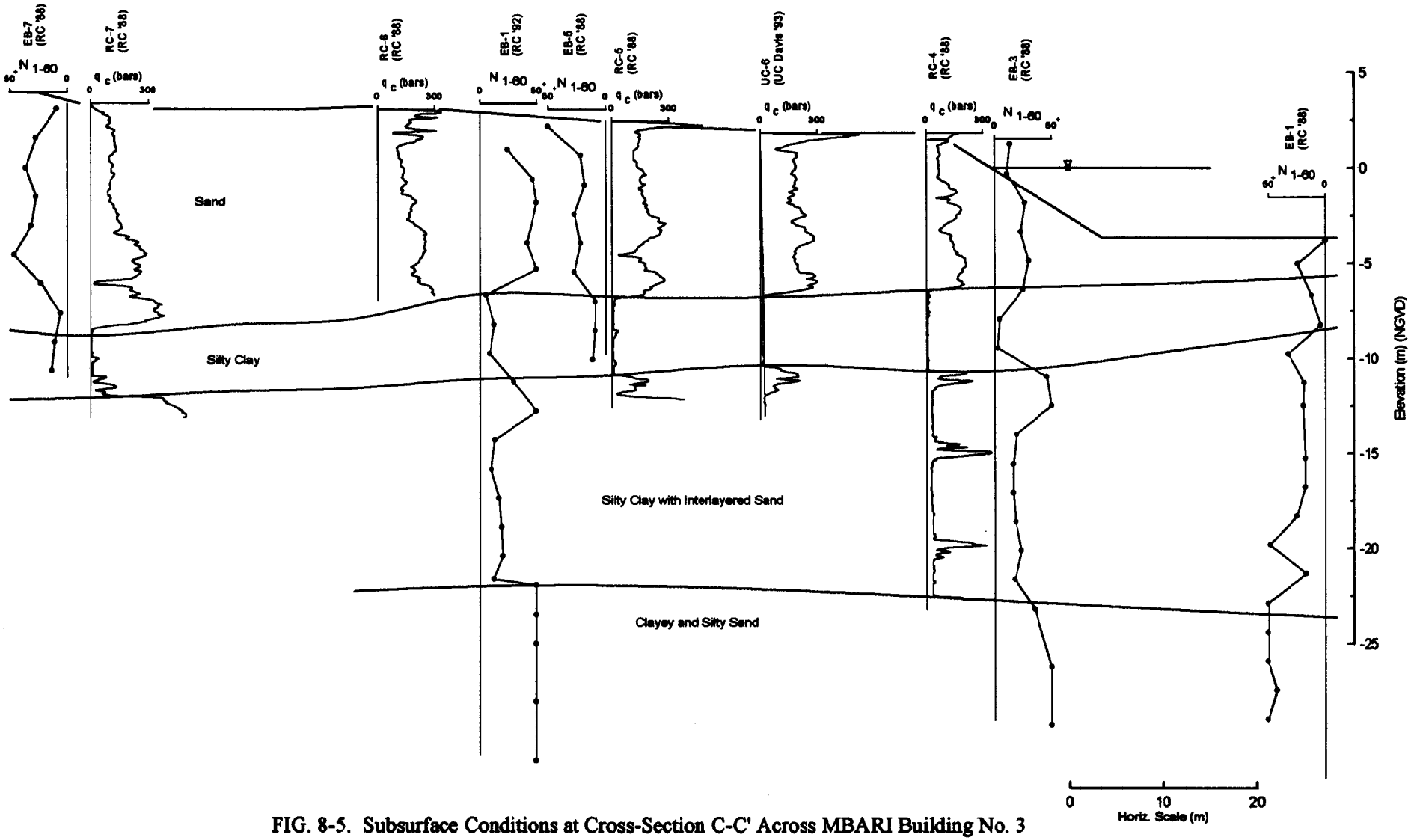


FIG. 8-5. Subsurface Conditions at Cross-Section C-C' Across MBARI Building No. 3

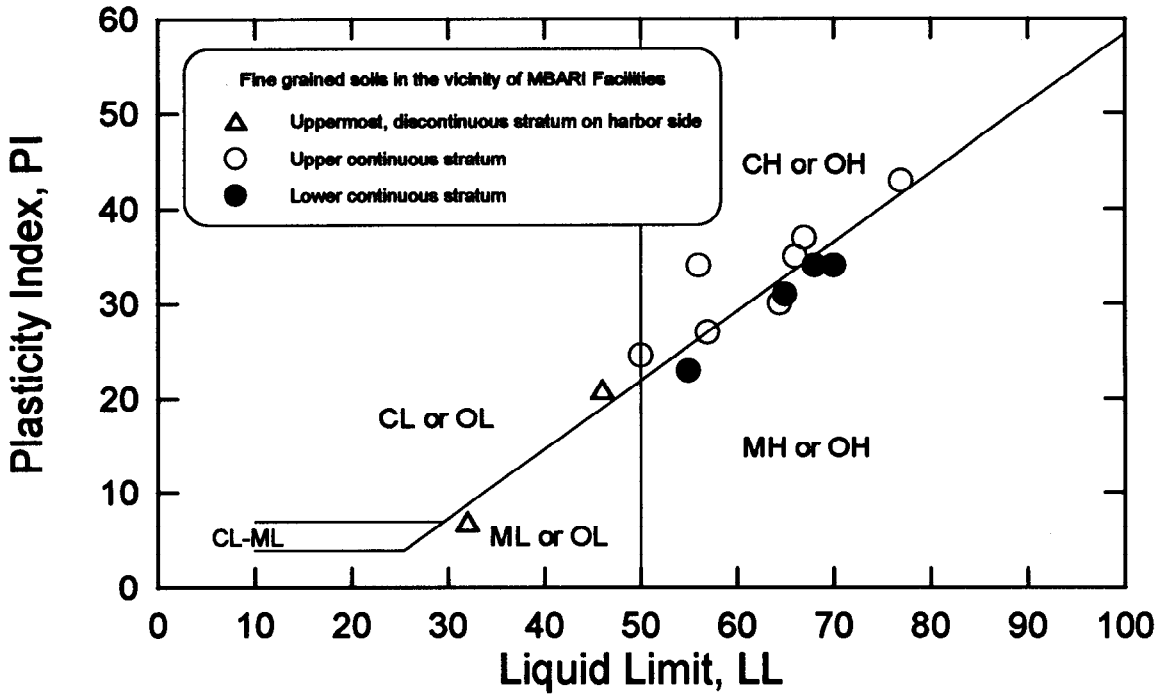


Data are from the following borings:
EB-1, EB-3 by Rutherford & Chekene (RC '88)
EB-1, EB-5 by Rutherford & Chekene (RC '93)
B-2, B-4, E-2 by Harding Lawson Associates (HLA '88)
UCD-B10 by U. C. Davis (UCD '94)

FIG. 8-6. Atterberg Limits of Fine Grained Soils in the Vicinity of the MBARI Facilities

ABERG-MB.GRF

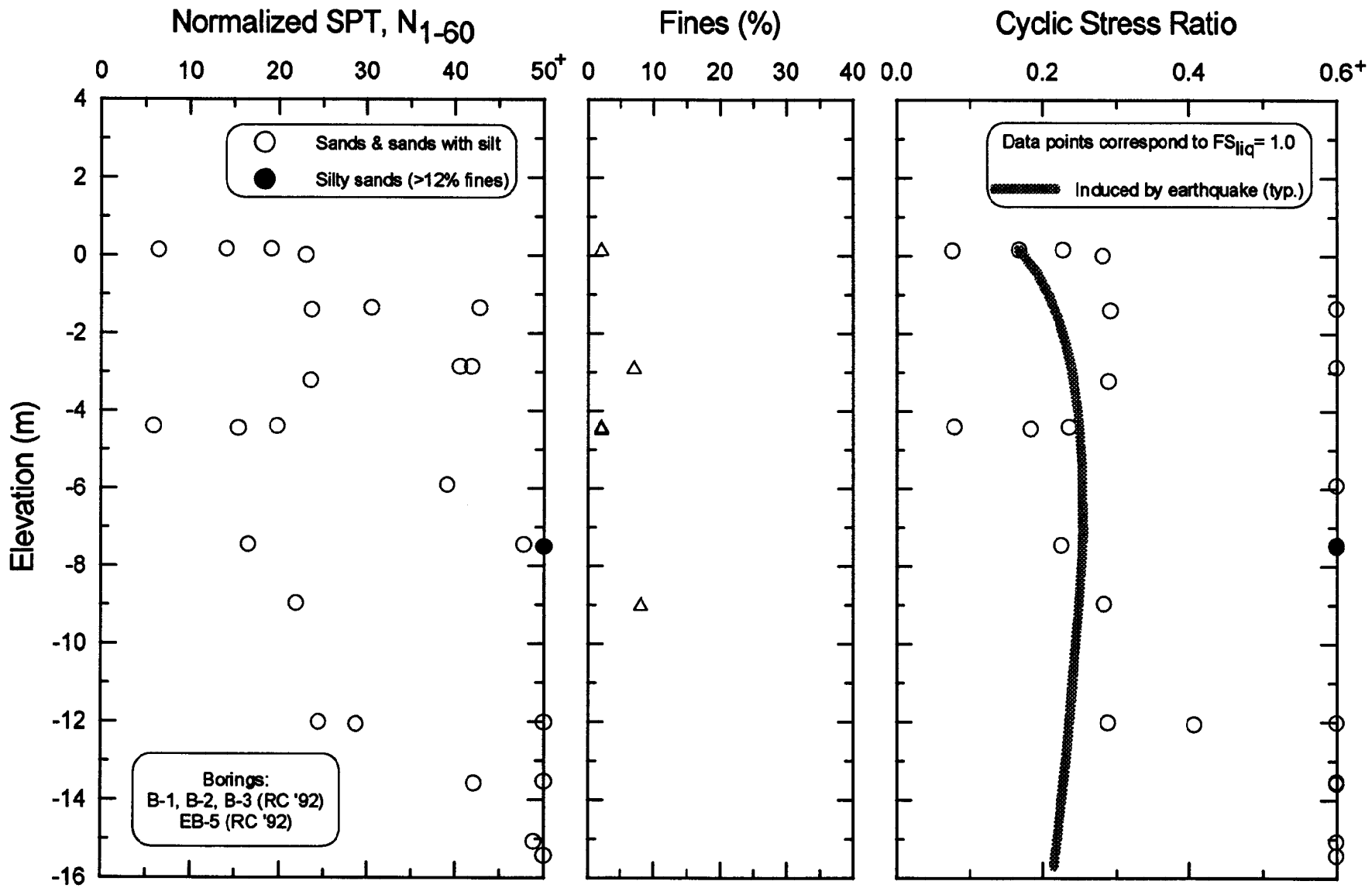


FIG. 8-7. Liquefaction Analysis of SPT Data at the Old Site of the General Fish Company

SPT-G1-A.grf

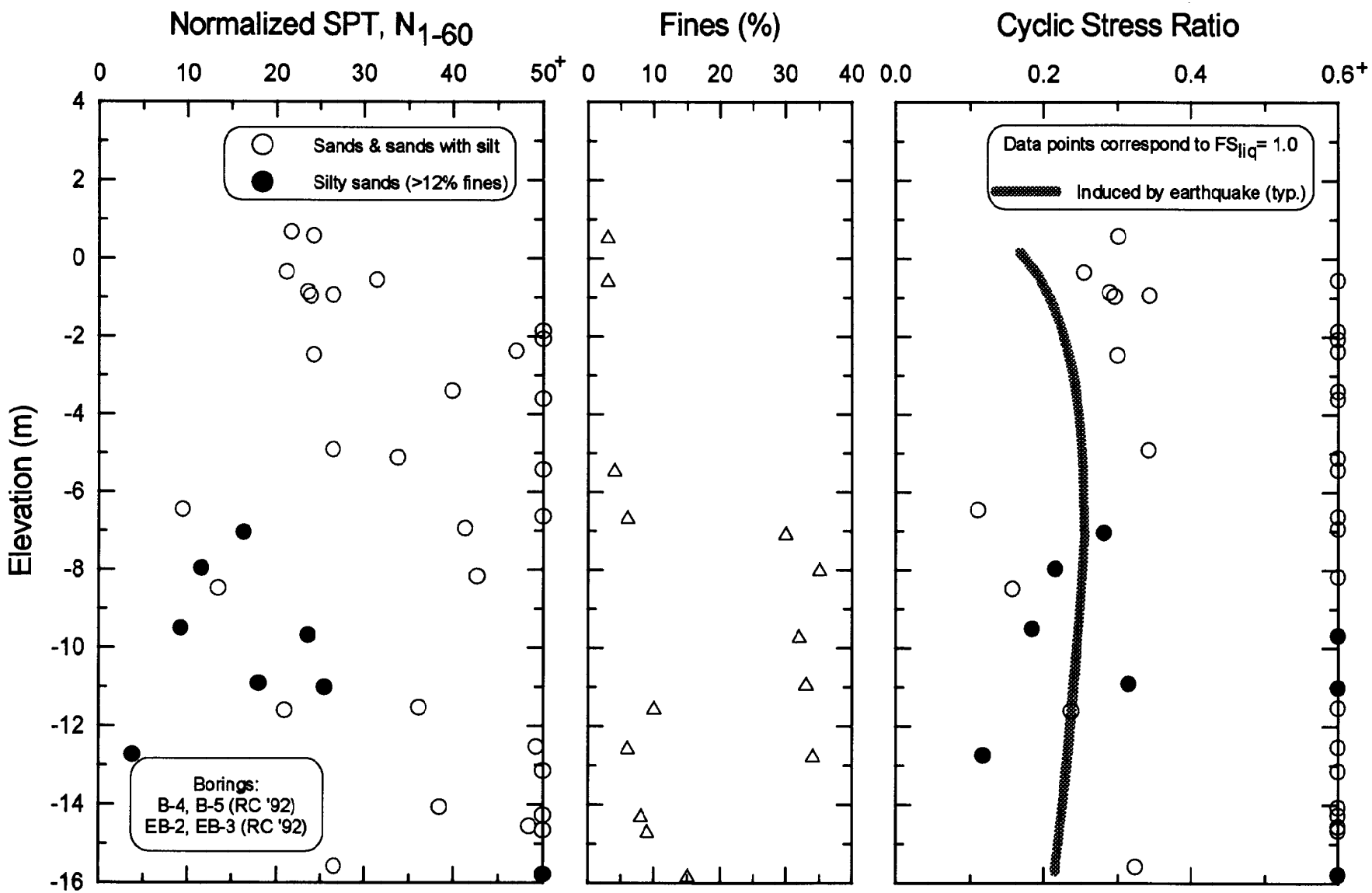


FIG. 8-8. Liquefaction Analysis of SPT Data at the MBARI Building No. 4

SPT-G2-A.grf

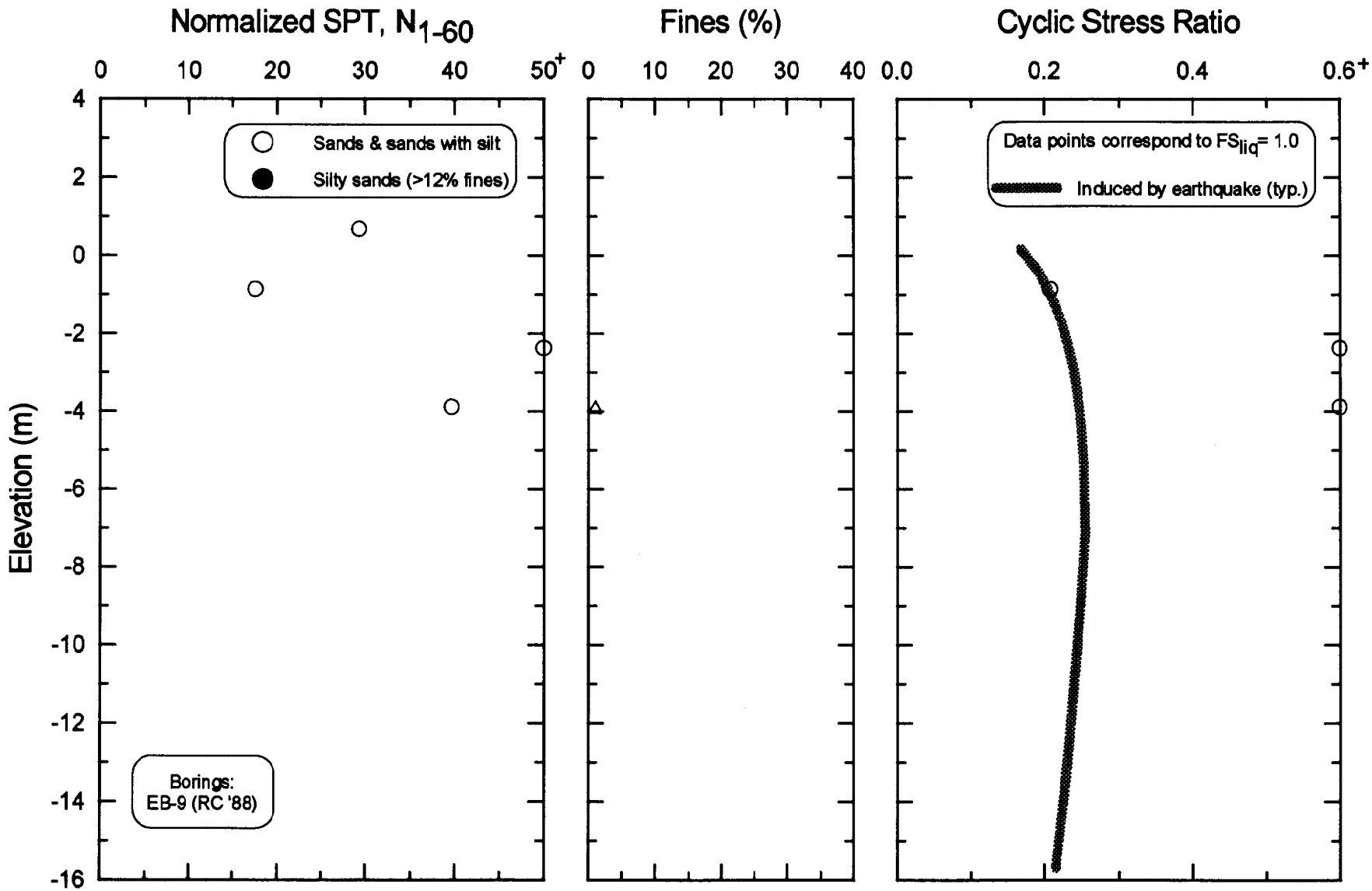


FIG. 8-9. Liquefaction Analysis of SPT Data at the MBARI Technology Building

SPT-G3-A.grf

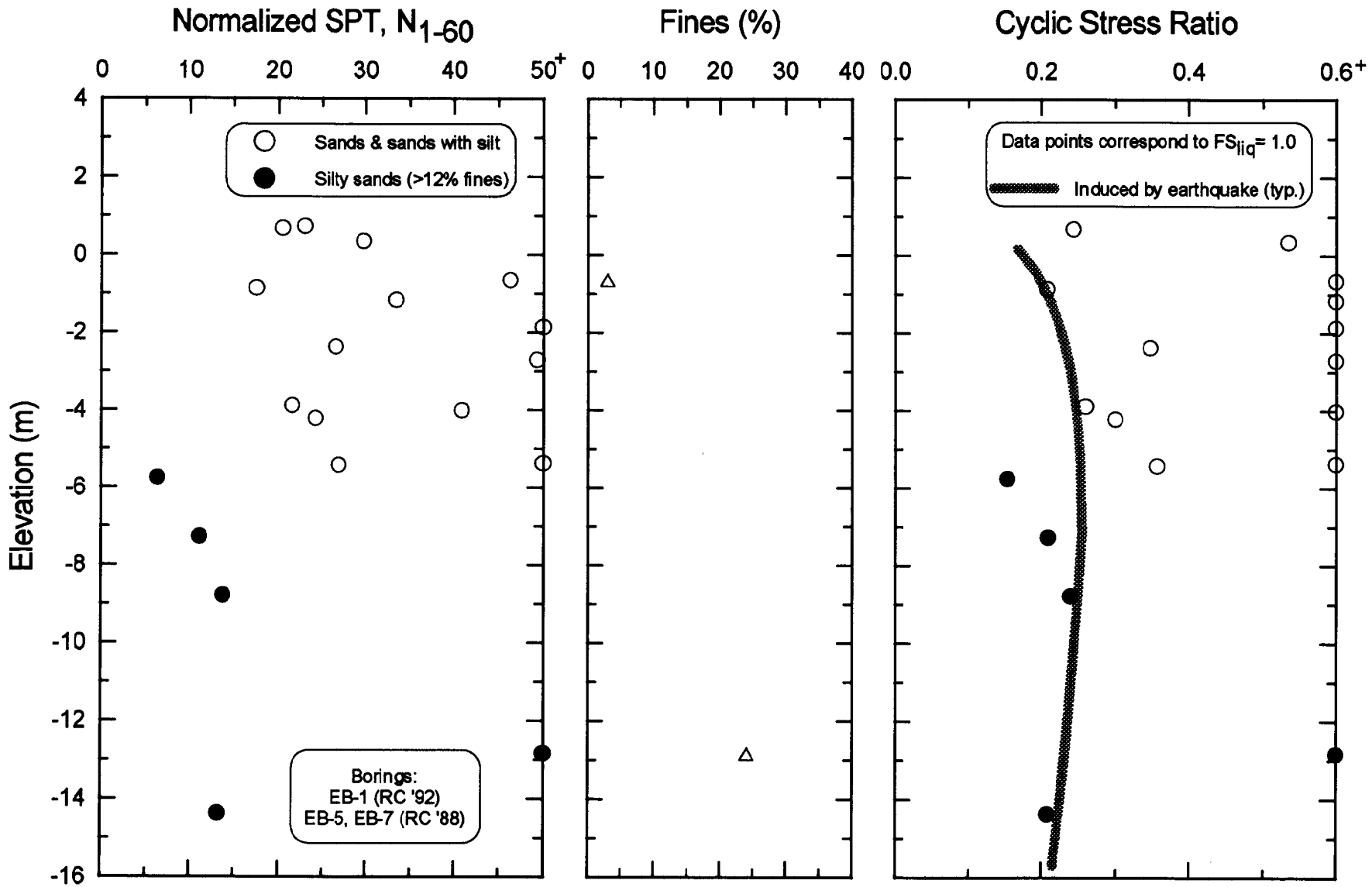


FIG. 8-10. Liquefaction Analysis of SPT Data at the MBARI Building No. 3

SPT-G4-A.grf

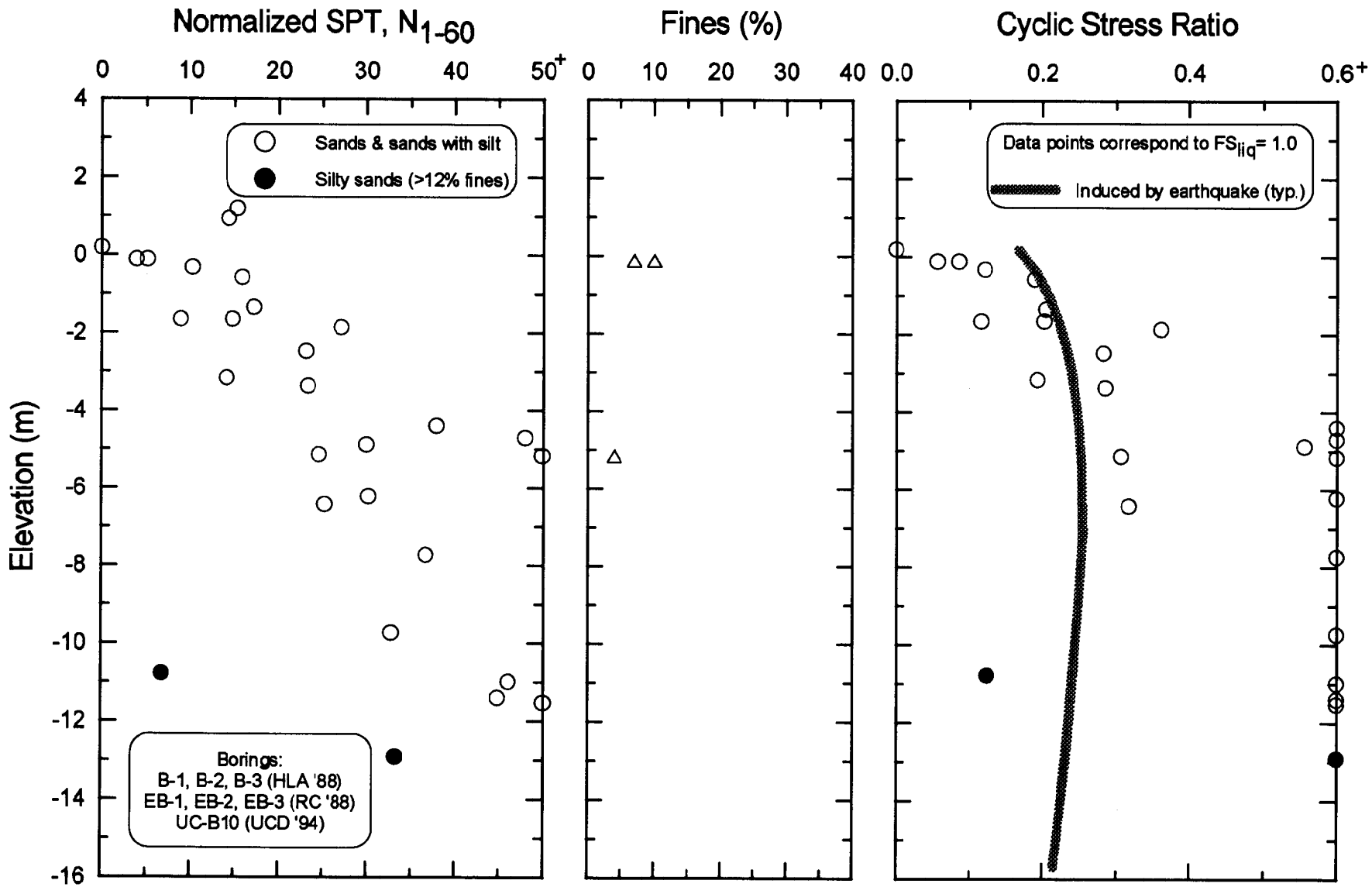


FIG. 8-11. Liquefaction Analysis of SPT Data Along Sandholdt Road Between the Timber Bridge and MBARI Building No. 3

SPT-G56A.grf

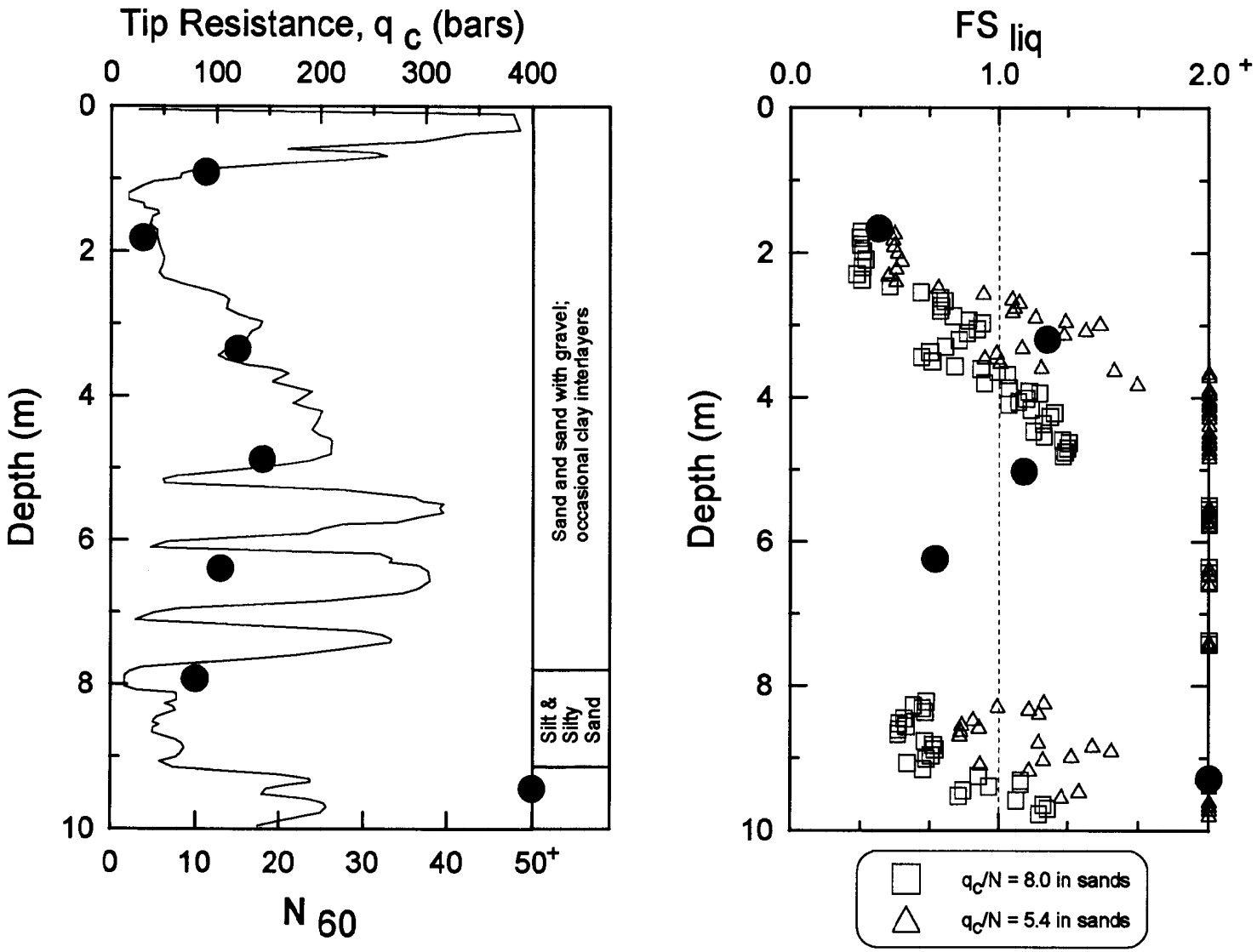


FIG. 8-12. Liquefaction Analysis of Adjacent SPT and CPT Soundings: CPT-5 and EB-5 by Rutherford & Chekene (1992)

PAIR5-93.GRF

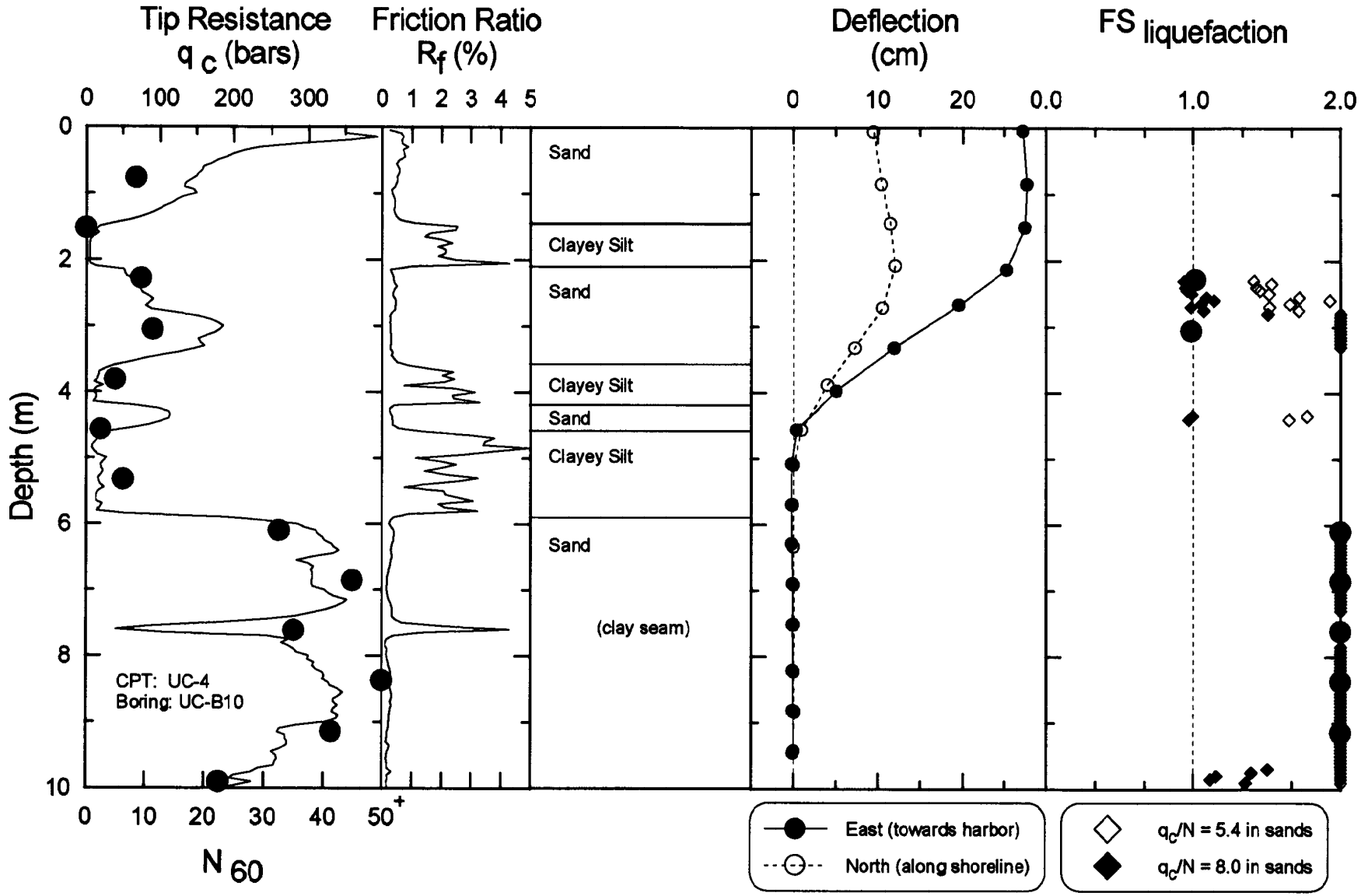


FIG. 8-13. Liquefaction Analysis of SPT and CPT Data Adjacent to Slope Inclinometer SI-2

SINC-2A.GRF

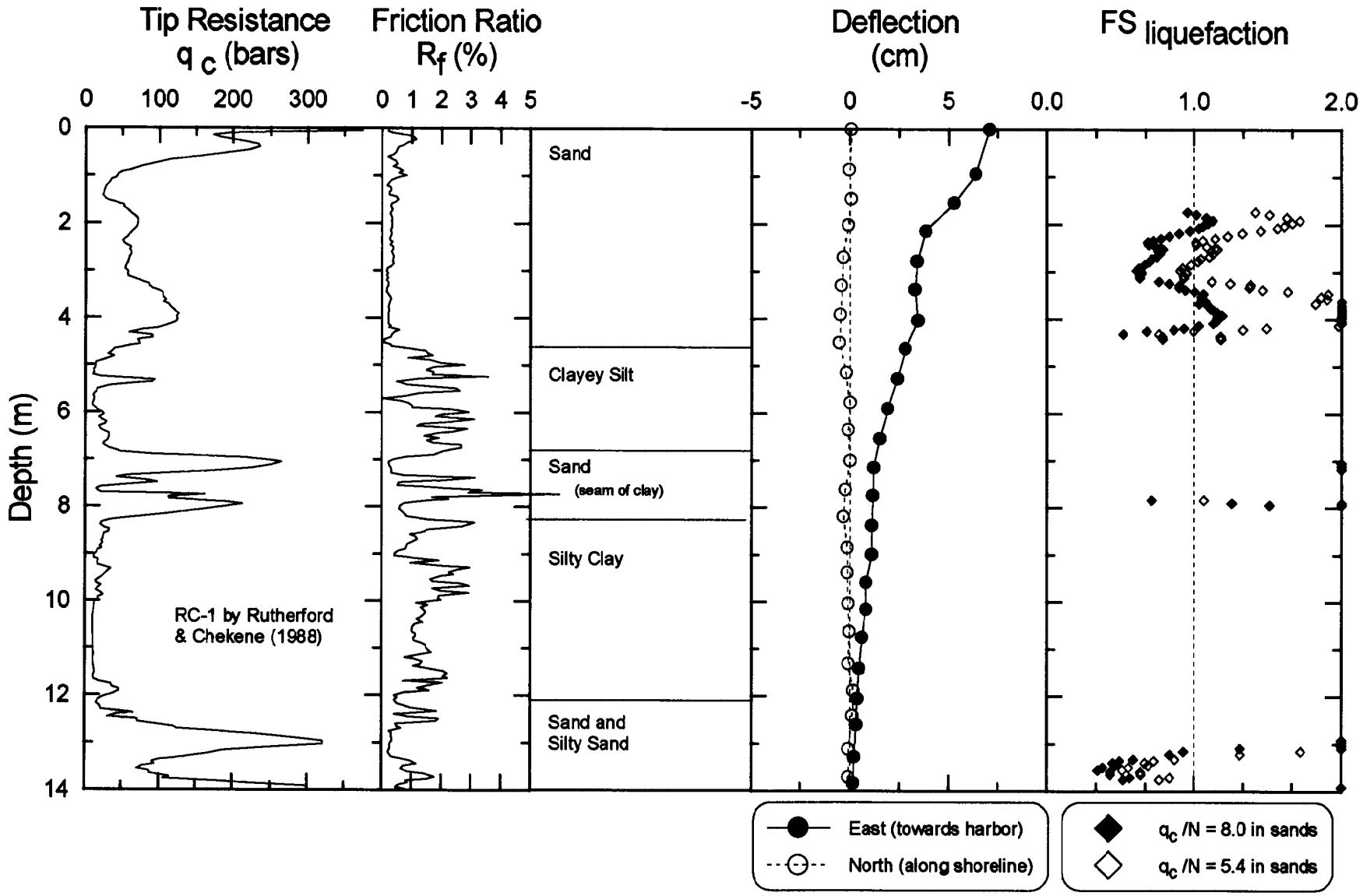


FIG. 8-14. Liquefaction Analysis of CPT Sounding Adjacent to Slope Inclinometer SI-4

SING-4A.GRF

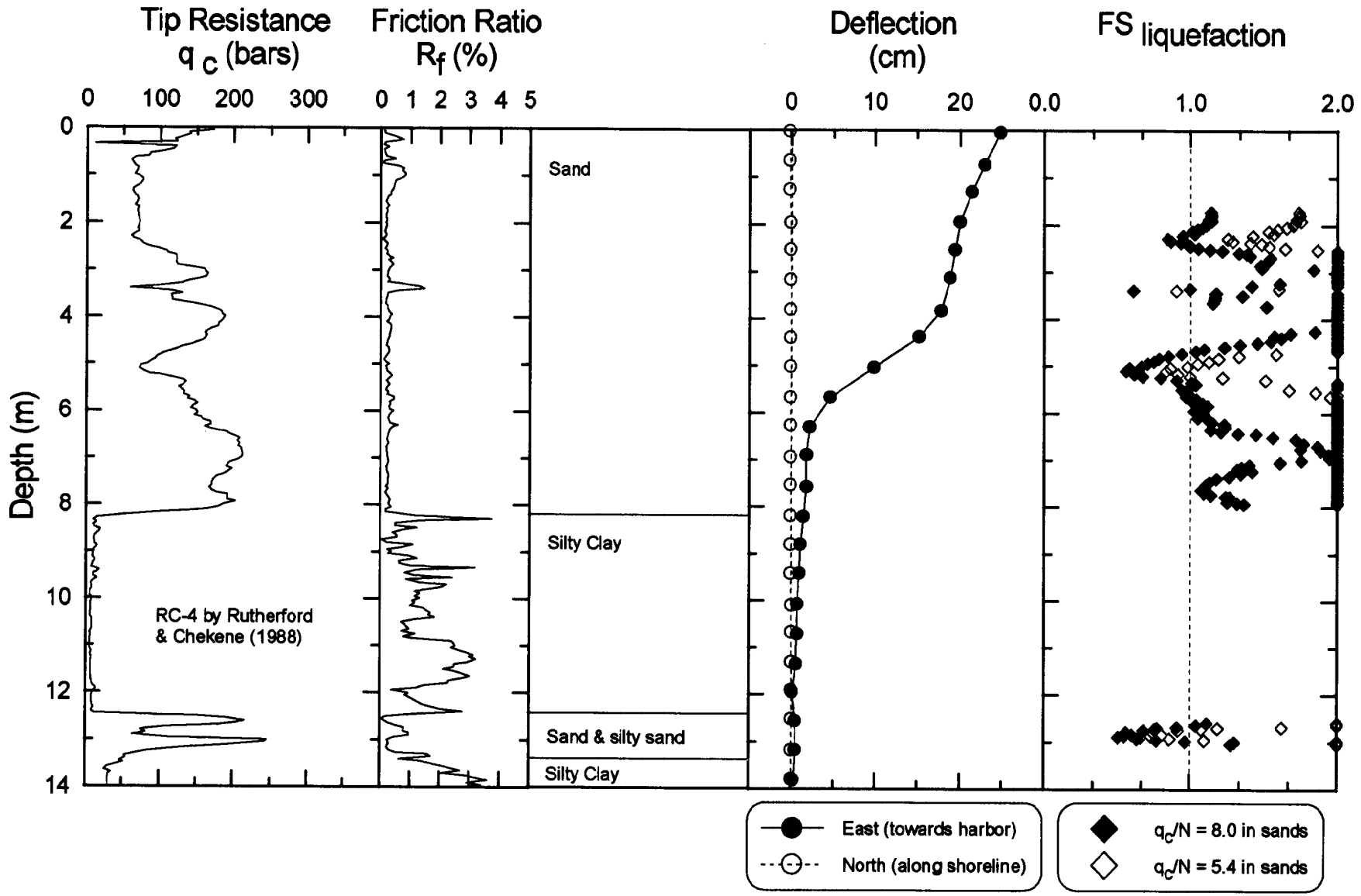


FIG. 8-15. Liquefaction Analysis of CPT Sounding Adjacent to Slope Inclinometer SI-5

SING-5A.GRF

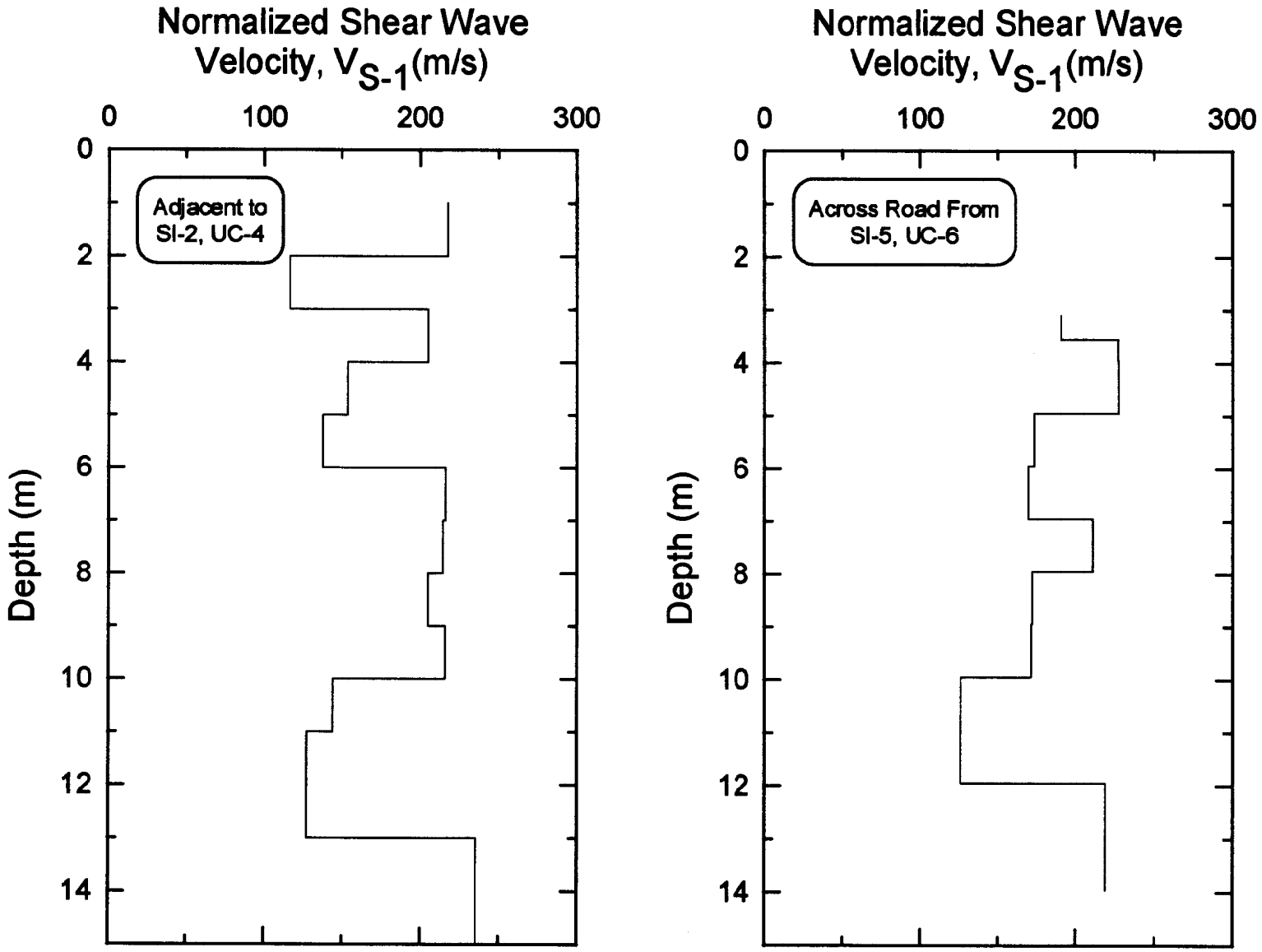


FIG. 8-16. Normalized Shear Wave Velocity Profiles along Sandholdt Road

v-sroad1.grf

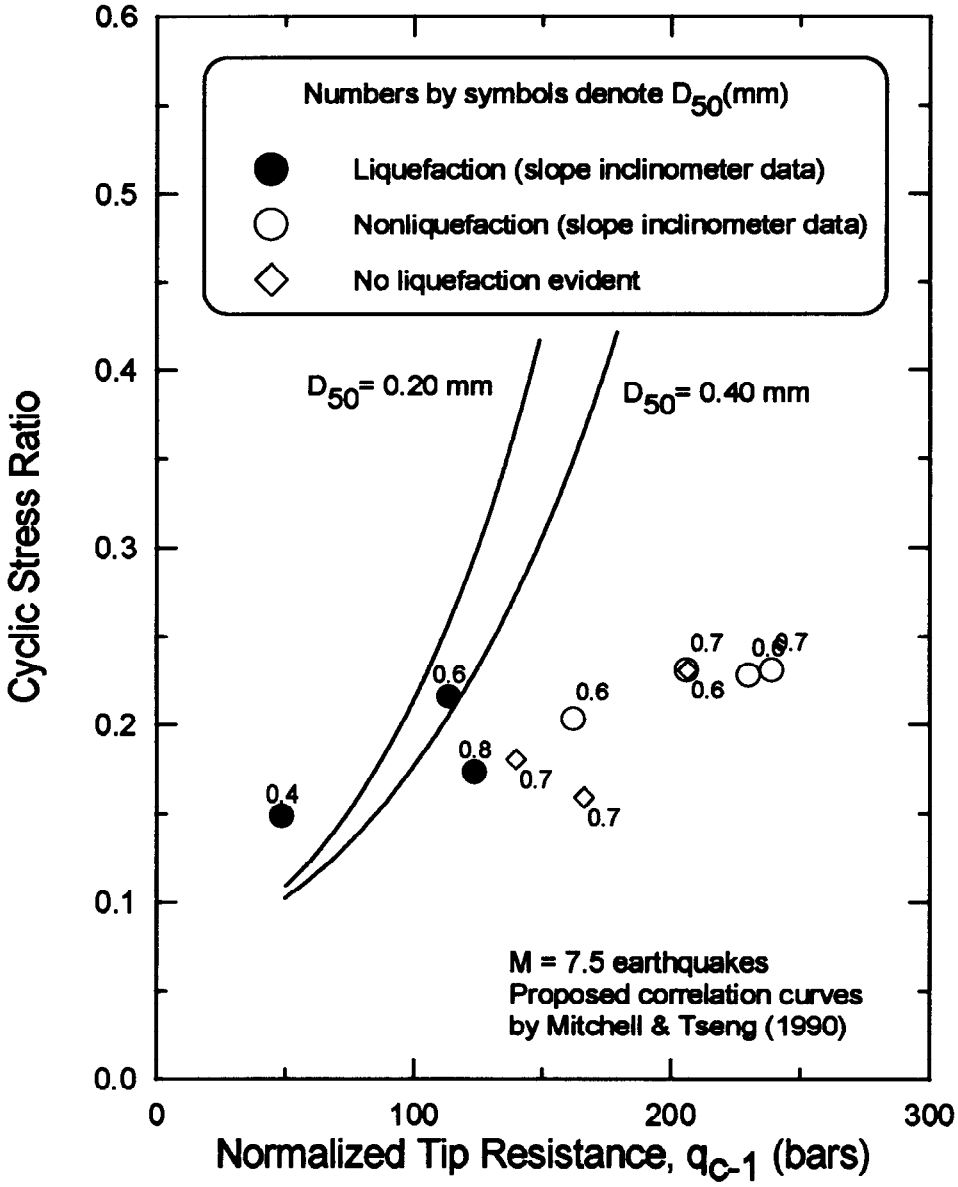


FIG. 8-17. Correlation of CPT Tip Resistance to Liquefaction Resistance along Sandholdt Road

sandrd-2.grf

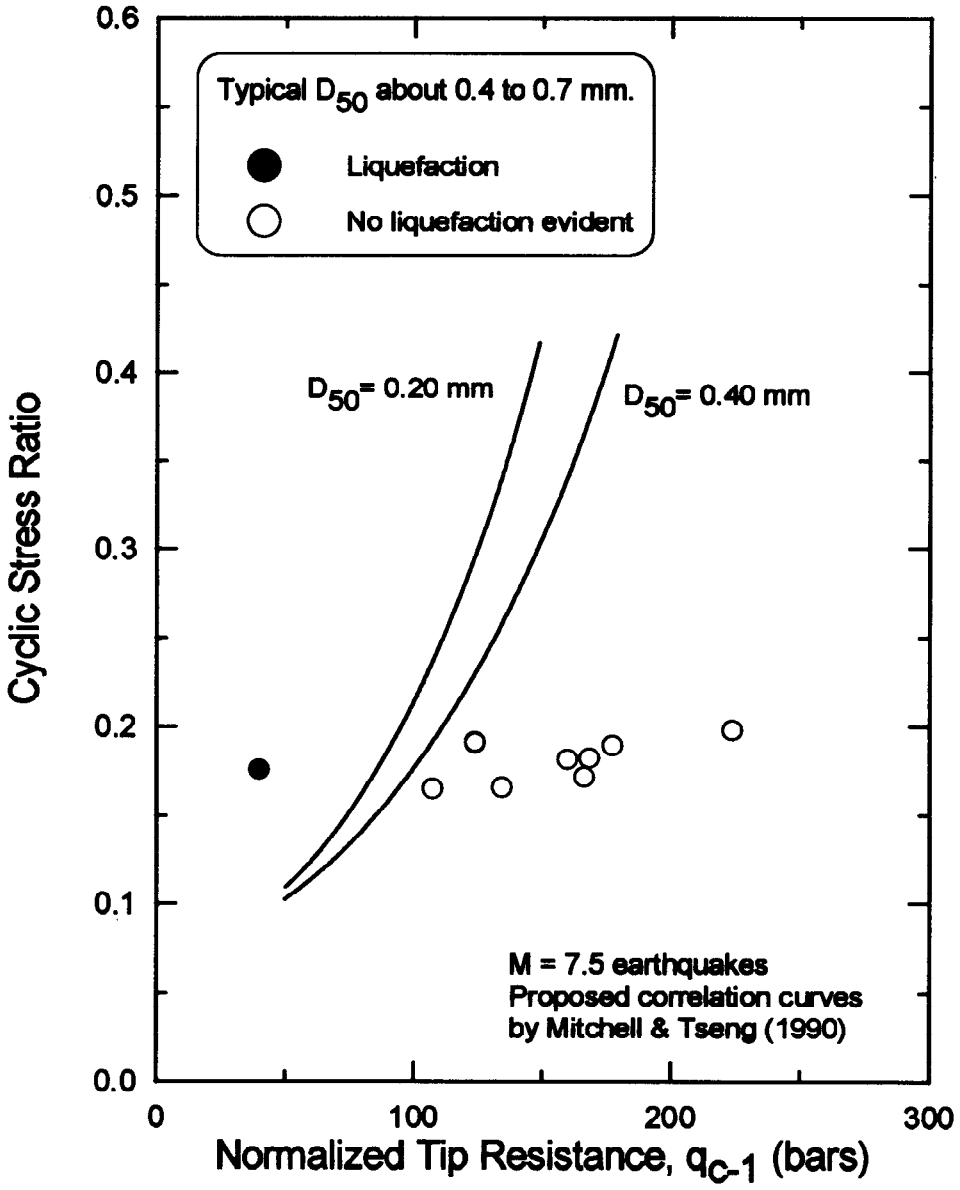


FIG. 8-18. Correlation of CPT Tip Resistance to Liquefaction Resistance in Vicinity of MBARI Facilities (excluding Sandholdt Road)

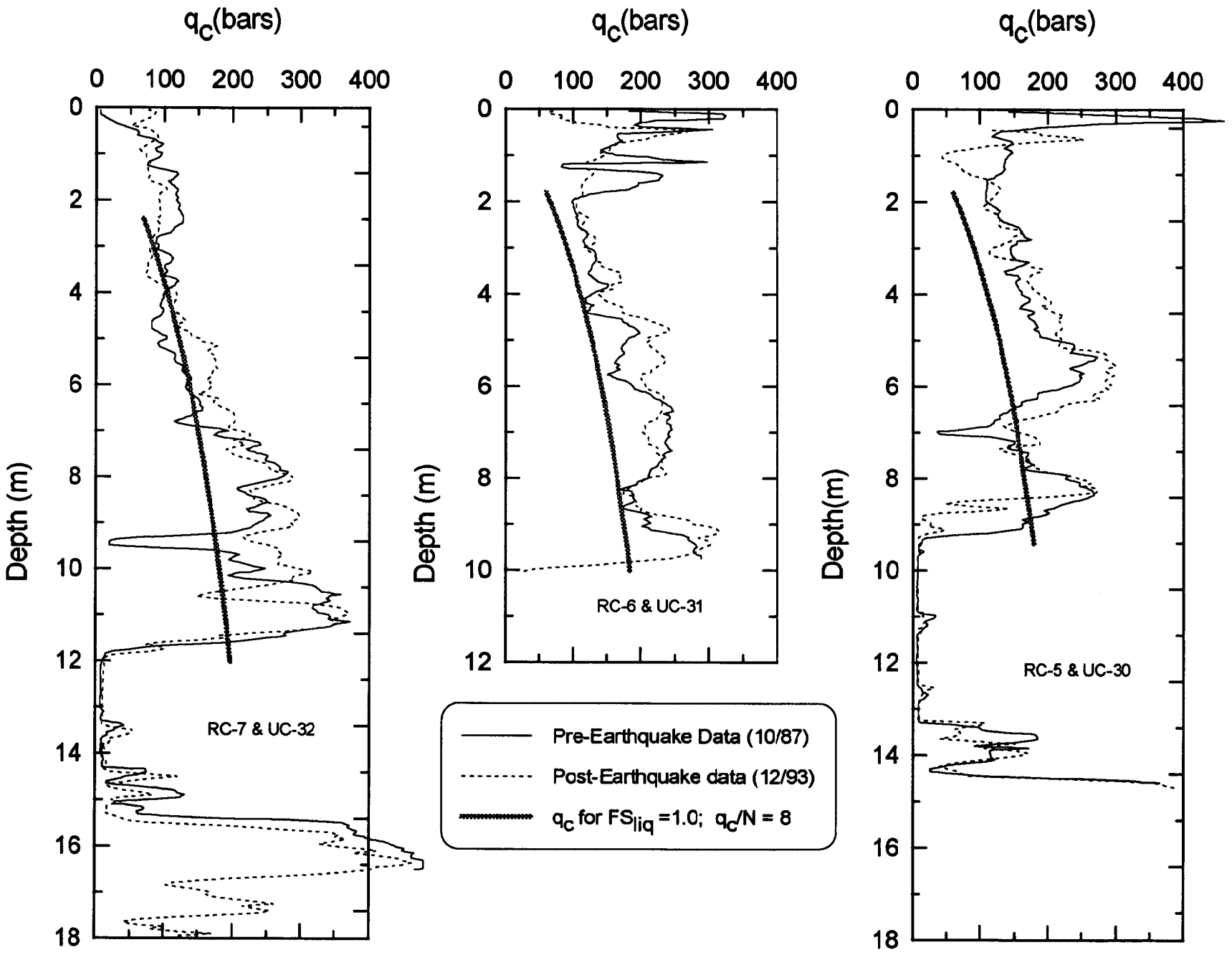


FIG. 8-19. Pre- and Post-Earthquake CPT Soundings at MBARI Building No. 3

FISH2.GRF
(chk rwb 8/94)

# 9. MOSS LANDING MARINE LABORATORY

## 9.1 Site Description

The Moss Landing Marine Laboratory (MLML) operated by the California State University was located on the Moss Landing spit, just south of the timber bridge as shown on Fig. 1-2. These facilities consisted of two main buildings and a west wing surrounding a courtyard, as shown on Fig. 9-1. The northern building was a one- and two-story wood-frame structure founded on spread footings and with a raised wood floor. The southern building and the west wing were one-story wood-frame-and-shear-wall structures with concrete slab-on-grade floors. The eastern half of the southern building was founded on 0.40-m-diameter cast-in-place concrete piers up to 5.5 m deep. The western half and the west wing were founded on shallow strip footings.

The MLML facility also included several concrete fish tanks and planters within the courtyard, and a 10.7-m-high, 4.6-m-diameter concrete sea-water storage tank on the eastern end of the courtyard. The fish tanks and planters were founded on grade. The sea water tank was supported on a 0.6-m-thick concrete mat founded 0.6 m below the ground surface. A 4.5-m-high concrete sea-wall founded at about elevation 0 m protected the facility from wave action in Monterey Bay.

## 9.2 Observations of Earthquake Effects

The MLML facilities were damaged beyond repair by liquefaction-induced lateral spreading and differential settlement of the site. Although the structures were practically torn apart at the foundation, the structures did not collapse and no severe injuries occurred to the approximately 50 people reportedly occupying the building at the time. The level of damage sustained is illustrated in Figs. 9-2(a) and 9-2(b), which show racking of the southeast and southwest corners of the laboratory, respectively.

Measurements of ground deformations from a post-earthquake survey by Brian Kangas Foulk (1989) and the approximate locations of major ground cracks are summarized on the site plan in Fig. 9-1. Additional information and estimates of ground deformations are available in Raggett and Associates (1989). The survey data shows that the buildings spread 1 to 1.3 m at the ground surface in the east-west direction, while displacements in the north-south direction were small. Along the Monterey Bay (west) side of these structures, ground deformations are estimated to be about 0.7 m laterally toward the Bay and about 0.35 m vertically (settlement). Along the Old Salinas River (east) side of these structures, ground deformations are estimated to be about 0.45 m laterally toward the river and about 0.3 m vertically (settlement). Along the eastern side of Sandholdt Road near the river shoreline, measured lateral displacements were 0.8 to 1.4 m towards the river. Overall, the total extension of the spit from lateral spreading of this site appears to have ranged from about 1.4 m on the north side to about 2.1 m on the south side.

Severe cracking in the foundation and slab floor occurred in the southern building, as illustrated in Fig. 9-3. Cracks up to 15 cm wide developed in the slab and separations of up to 25 cm occurred between building floors and walls. The northern building also suffered severe cracking at the roof and foundation levels with separations more than 45 cm at some locations.

At the volleyball court south of the laboratory, soil boils geysering up to 1 m flowed for 30 to 45 minutes after the earthquake (Greene et al. 1991). Fig. 9-4 shows a view of the ejecta that consisted of predominantly fine-grained clayey silt at some boils and medium-grained sand at other boils. A sample of the clayey silt ejecta at the ground surface had a liquid limit of 38, a plasticity index of 17, a fines content of 78%, and a minus 5 μm fraction of 24%. Raggett & Associates, Inc. (1989) reported that sand boils erupted at a couple of points around the eastern end of the southern building; it should be noted, however, that this report described the soil ejecta at the volleyball courts as also being sand, and thus no distinction may have been attempted between sand boils and silt boils. Significant quantities of water containing fine-grained, dark gray, suspended sediment upwelled through cracks in the corporation yard pavement several times after the earthquake (Larry Jones 1989).

## 9.3 Field Investigations

Field investigations at this site were performed by Woodward-Clyde Consultants (1990) and U.C. Davis (present study). Additional data in the area of the corporation yard area were obtained from Fugro (1980) who performed a test grid of eight borings and eight CPTs as part of a USGS research grant. Limited data was available from a foundation design consultant's report as well, but it is not included herein due to uncertainties regarding the procedures and equipment used.

The procedures followed in the Woodward-Clyde explorations are described by Woodward-Clyde (1990). CPT soundings were performed using the same equipment and procedures used by U.C. Davis under the present study. Borings were performed using a rotary-wash drill rig with a 124-mm ($4\ ^7/_8$ in) tricone bit and bentonite slurry. SPT tests were performed using a CME automatic trip hammer and a safety hammer operated with a cathead and rope system with two turns of the rope. The sampler was a standard 5-cm-outside diameter split spoon with room for liners. Samples were obtained with the liners omitted, and thus the blow counts were corrected based on the data presented by Seed et al. (1985) as follows: blow counts less than 10 were not corrected, blow counts between 10 and 20 were increased by 10%, and blow counts greater than 20 were increased by 20%. Energy ratios were estimated to be about 63% and 75% for the safety hammer and automatic trip hammer systems, respectively.

The borings by Fugro (1980) were performed using a rotary wash drill rig. SPT tests were performed using both safety and automatic trip hammers.

Under the present study, three CPT soundings and six borings were performed using the procedures described in Section 4. One CPT sounding (UC-1) included shear wave velocity measurements. The CPT soundings, boring logs, and laboratory test data are presented in Appendices A, B, and C, respectively.

## 9.4 Subsurface Soil Conditions

Subsurface conditions are shown in the east-west cross-sections across the northern and southern sides of the laboratory in Figs. 9-5 and 9-6, respectively. The central portion of the spit at this site is blanketed by 1.5 to 2.5 m of loose to medium dense fine-to-medium-grained dune sand, having generally less than 4% fines and a $D_{50}$ of about 0.2 to 0.3 mm. A 3- to 6-m thick deposit of

medium-grained beach sand underlies the dune sand on the west side of the spit. The beach sand is generally loose to medium-dense, has abundant sea shell and calcareous particles, about 3 to 5% fines, and a $D_{50}$ of about 0.35 to 0.50 mm.

On the east side of the spit, a 1.5- to 3-m-thick marshland deposit of gray, clayey silt and clay is interbedded between the dune and the beach sands. This marshland deposit contains fine-grained soils ranging from low to high plasticity, occasional thin sand lenses, and significant organics. The fine-grained soils have liquid limits ranging from 31 to 58, plasticity indices ranging from 6 to 28, and a percent finer than 5 μm ranging from 18 to 49%.

On the north side of the site, the beach sand is underlain by 1.5 m of interlayered sand and clay in turn underlain by 1.5 m of dense medium-to-coarse-grained gravelly sand. On the south side, the gravelly sand directly underlies the beach sand. The gravelly sand has a $D_{50}$ of about 0.6 to 1.2 mm and 5 to 8% fines.

The gravelly sand is underlain by a layer of loose to medium dense silty sand to a depth of about 12 m, except at the location of CPT C-1. This silty sand is fine-grained with a $D_{50}$ of about 0.15 mm and about 27 to 34% fines.

Below about 12 m, a layer of soft to medium stiff clay 1.5 to 2.5 m thick is encountered. This layer is underlain by interlayered gravelly sands and silty sands with occasional silts and clays, and clayey sands. A deposit of medium stiff, highly plastic clay was encountered at a depth of 23 to 26 m in CPT C-3 and boring B-2, respectively. This deposit extends to at least 37 m (the limits of exploration).

## 9.5 Evaluation of Liquefaction Based on SPT and CPT Data

The potential for triggering of liquefaction in the subsurface soils was evaluated using the same procedures previously described in Section 1.3. The groups of borings by Fugro (1980) and under this study are analyzed separately to avoid bias due to the bulk of the data being from very localized spots.

The grid of eight borings by Fugro (1980), which consisted of four borings using a safety hammer and four borings using a trip hammer, were located in the corporation yard area near boring B-4 on Fig. 9-1 (the Fugro borings were omitted from this Fig. for clarity). A comparison of the measured SPT blow counts (N) and the corrected SPT blow counts ($N_{60}$) assuming energy ratios of 60% and 75% for the safety and trip hammers, respectively, is shown in Fig. 9-7. The corrected blow counts are in reasonable agreement, whereas the measured blow counts show significant differences over the full depth of exploration. A liquefaction analysis of the corrected SPT data, as presented in Fig. 9-8, suggests that: (1) only limited liquefaction would be expected to have occurred within the sands (less than 12% fines) between elevations of about -2.0 and -6.0 m; (2) liquefaction would be expected to have occurred within the sands and silty sands between elevations of about -6.0 and -8.0 m; and (3) limited liquefaction would be expected to have developed in the silty sands between elevations of about -12.0 and -15.0 m. Note that for the analyses shown in Fig. 9-8, the encountered clay layers (similar to as shown in the cross-sections in Fig. 9-5 and 9-6) were considered non-liquefiable.

Three borings (B-1, B-2 and B-3) were performed by Woodward-Clyde Consultants (1990) at different positions around the site, as shown on Fig. 9-1. A liquefaction analysis of the SPT data, as presented in Fig. 9-9, indicates that: (1) liquefaction would be expected to have occurred within a significant portion of the sands between elevations of about 0.5 and -2.5 m; (2) liquefaction would not be expected to have developed in the sands between elevations of about -2.5 and -6.0 m; and (3) liquefaction would be expected to have developed within a significant portion of the silty sands between elevations of about -6.0 and -9.0 m.

Six borings were performed near the volleyball court in a grid surrounding CPT C-3 on Fig. 9-1 as part of this study (locations of these borings were omitted from Fig. 9-1 for clarity). The purpose of these borings was to obtain Osterberg tube samples from the soft fine-grained soil between elevations of about -0.5 and -2.0 m and to perform SPT tests in the underlying sands and silty sands. A liquefaction analysis of the SPT data, as presented in Fig. 9-10, indicates that liquefaction would be expected to have occurred within the sands between elevations of about -2.0 and -5.5 m and within the silty sands between elevations of about -5.5 and -8.0 m.

The soft clayey silt stratum between elevations of about -0.5 and -2.0 m was also suspected of liquefying by Mejia (1992) because: (1) fine-grained clayey silt ejecta was observed at this location; and (2) a test pit within the volleyball court encountered dikes of clayey silt sediment that travelled up through the surface sand stratum to the ground surface. These observations were the incentive for obtaining Osterberg tube samples of the soft clayey silt stratum at this location for the purpose of cyclic testing in the laboratory. Such a testing program has been completed and will be reported in a separate document by Meyers (1995). The tube samples showed that this "clayey silt" stratum was comprised of finely interlayered, high and low plasticity clays and silts with a significant organics content and occasional silty sand lenses. Low plasticity samples of the clayey silt had liquid limits of 31-49, plasticity indices of 6-24, minus 5 μm fractions of 18-24%, and classifications of ML, CL, or OL. High plasticity samples had liquid limits of 56 to 58, plasticity indices of 22 to 28, minus 5 μm fractions of 47-49%, and classifications of MH, CH, or OH. A silty sand lens had 40% nonplastic fines and a minus 5 μm fraction of 13%. Cyclic triaxial tests indicate that these "clayey silts" are susceptible to developing significant strains and high residual excess pore pressures at the level of shaking experienced during the Loma Prieta earthquake (Meyers 1995). Although strains within the clayey silt stratum likely contributed to ground deformations along the east side of the site, the sand boil observed at the volley ball court indicates that liquefaction must also have occurred in the underlying sand or silty sand strata. Furthermore, the large ground deformations to the west of the clayey silt stratum indicate that the sand or silty sand strata in those areas must also have liquefied.

Interpreting the critical combinations of earthquake-induced cyclic stress ratio and normalized CPT tip resistance for the data at the MLML facility is hampered by the difficulty in deciding which subsurface soils liquefied. The beach sand is known to have liquefied on the southern side of the MLML facility, as evidenced by the sand boils in this area. The deeper silty sand stratum (between elevations of about -5.5 and -9.0 m in Figs. 9-5 and 9-6) is also a suspected source of liquefaction because it has CPT tip resistances that are significantly smaller than those in the beach sand. On the other hand, the silty sand stratum is below the bottom of the adjacent Old Salinas River channel which would seem to reduce its potential to cause large lateral spreading deformations. Subsequently, the critical strata were taken as the beach sand for CPT soundings C-3 and C-4 (near sand boils on the south side) and as the deeper silty sand for CPT soundings UC-1, UC-7, UC-8, and C-2. The

remaining CPT sounding C-1, located at the north-west corner of the site, did not encounter the deeper silty sand layer and thus the beach sand would appear to be its critical layer. The corresponding critical normalized tip resistance of 178 bars for CPT C-1 is quite high, however, and the degree to which it is representative of the soils directly beneath the MLML buildings is subject to debate.

The resulting critical combinations of earthquake-induced cyclic stress ratio and normalized CPT tip resistance at each of the CPT soundings, excluding CPT C-1, are summarized in Fig. 9-11. Critical CPT tip resistances were estimated using the guidelines previously described in Section 1.3. Cyclic stress ratios are adjusted to equivalent cyclic stress ratios for M=7.5 earthquakes based on the ratios presented by Seed and Idriss (1982). For reference, Fig. 9-11 also shows the boundary between conditions of liquefaction and non-liquefaction proposed by Mitchell and Tseng (1990) for clean sands with $D_{50}$ values of 0.20 mm and 0.40 mm. The boundaries proposed by Mitchell and Tseng (1990) are generally consistent with the observations of widespread ground deformations at the MLML site.

## 9.6 Correlation With Shear Wave Velocity Measurements

The profile of normalized shear wave velocity obtained on the northern side of the Marine Laboratory is shown in Fig. 9-12. A $V_{s-1}$ value of 171 m/s between depths of 10.0 and 12.0 m coincides with the layer of silty sand and sand suspected of having liquefied at this location. However, the lower third of this measurement interval includes a dense sand layer, and thus the actual $V_{s-1}$ value in the silty sand may be somewhat smaller than 171 m/s. Consequently, these data are not compared to the relationship proposed by Robertson et al. (1992) in Fig. 1-6. These data illustrate the difficulty in using shear wave velocity measurements, with measurement intervals of 1 to 2 m, to characterize thin strata.

## 9.7 Effect of Sample Rod Size on SPT Blow Counts

The effect of sampling rod size on SPT blow counts was evaluated during the drilling of the six boreholes near the volleyball court. An evaluation of this effect was undertaken in response to dynamic analyses of SPT systems by Abou-matar and Goble (1995) which suggested that sampling rod size could have a significant effect on the measured blow count. Consequently, SPT tests within the clean sand layer between depths of about 4.9 to 6.5 m were performed using identical procedures with the exception that 4 of the borings used AW insert-wall rods and two of the borings used NW insert-wall rods. The borings were arranged in a grid pattern, with the two borings that used NW rods staggered across the other borings. All borings were performed by the same personnel over a 2-day working period. Measured SPT blow counts in the sand layer for the 6 borings are presented in Fig. 9-13. These data show no measurable difference between SPT blow counts obtained using either AW or NW rods under these conditions.

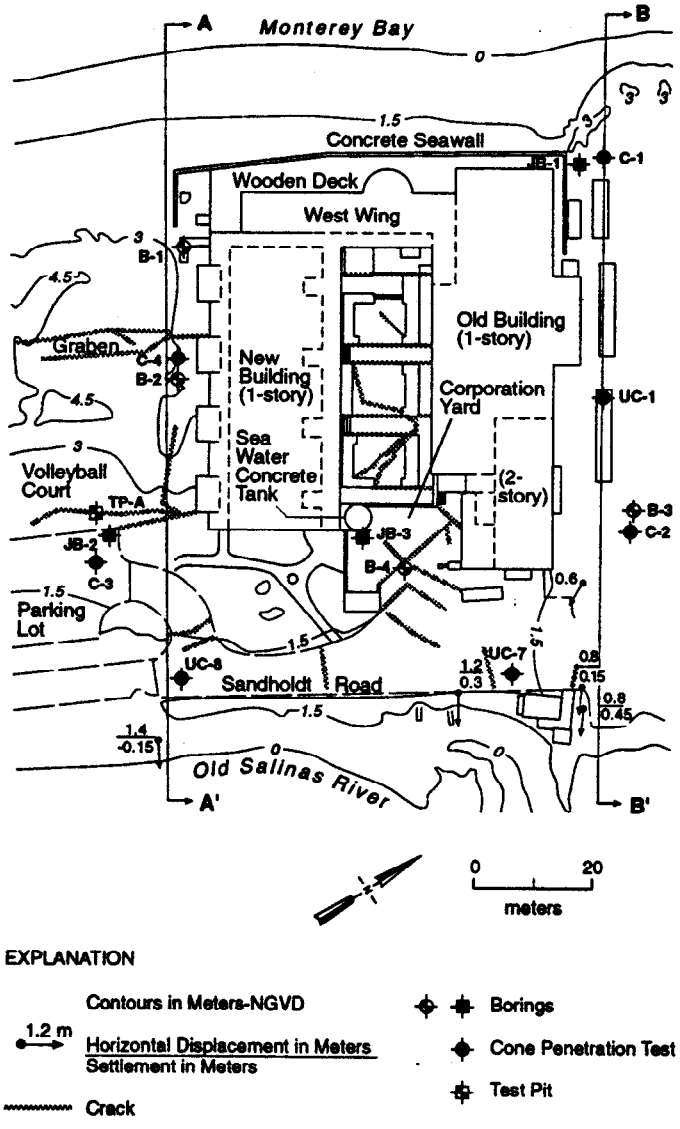


FIG. 9-1. Map of the Moss Landing Marine Laboratory (MLML) Site

FIG. 9-2(a). Racking of Director's Office at Southwest Corner of MLML.

FIG. 9-2(b). Racking of Southern Building at Southeast Corner of MLML.

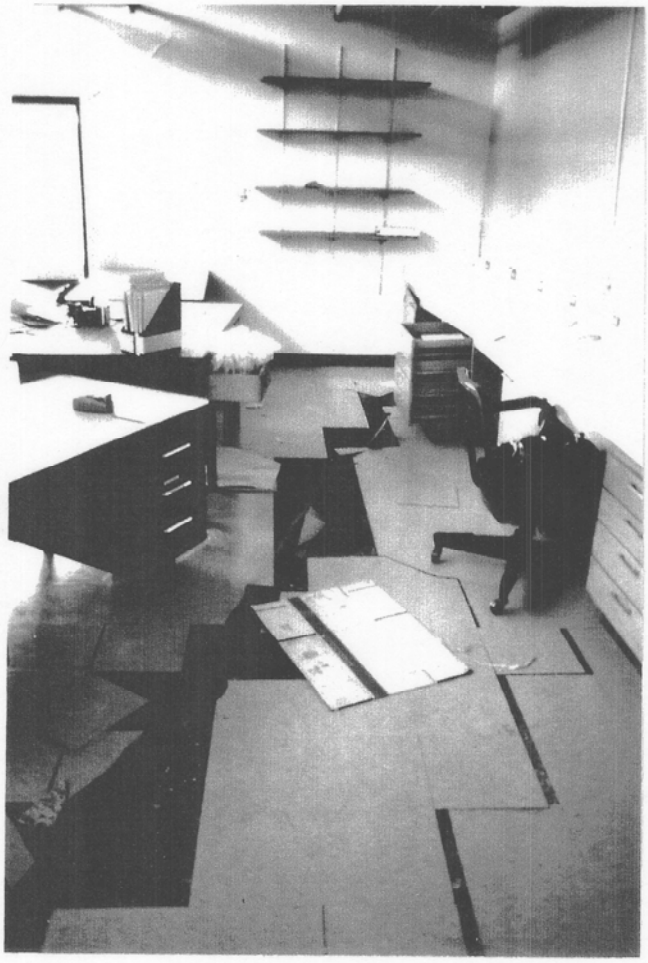

FIG. 9-3. Cracking of Concrete Floor in MLML Southern Building.

FIG. 9-4. Soil Boil Ejecta in Volley Ball Court.

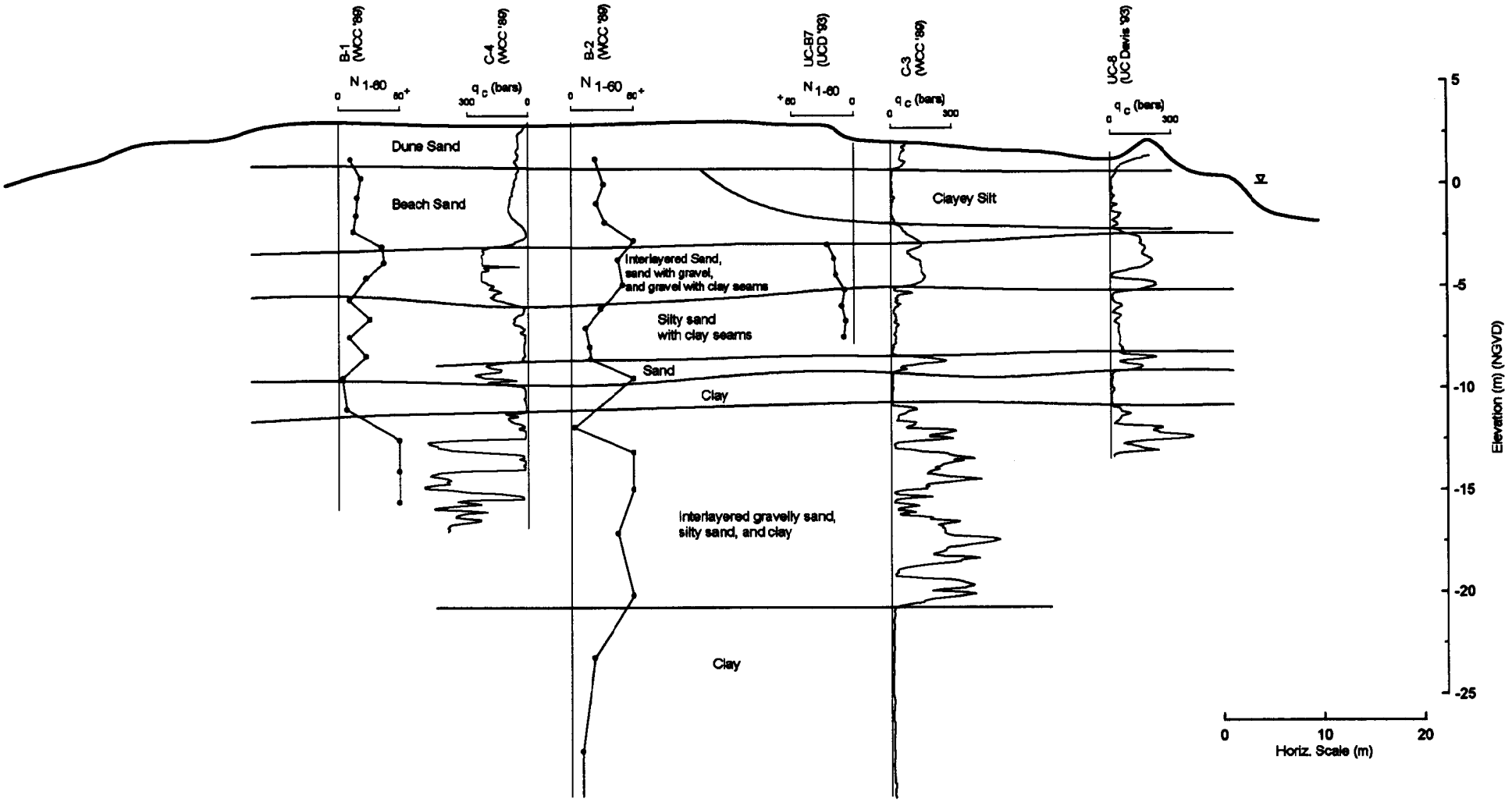


FIG. 9-5. Subsurface Conditions at Cross-Section A-A' Across the Southern Side of the Moss Landing Marine Laboratory Site

XSECT-98.GRF

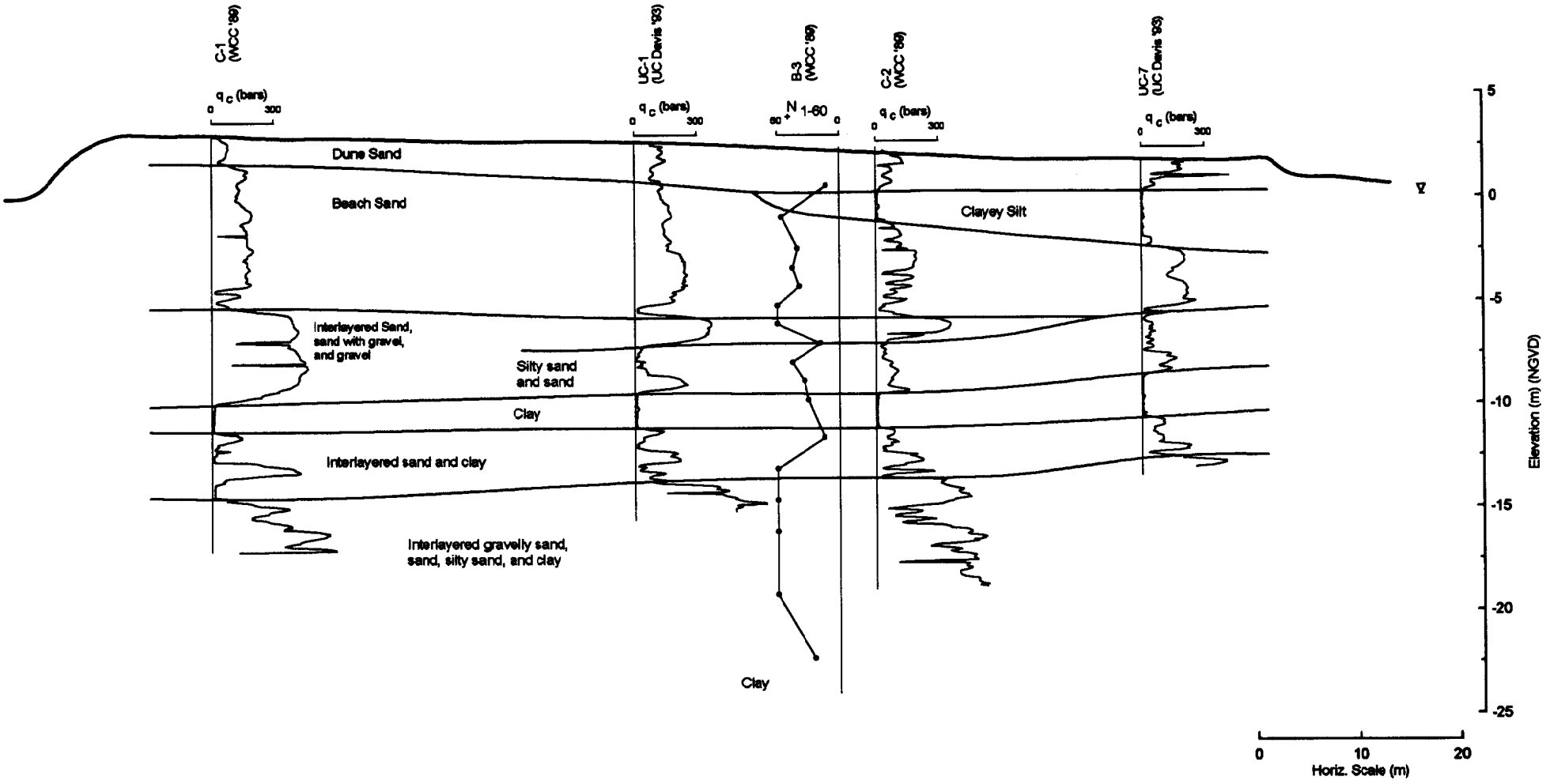


FIG. 9-6. Subsurface Conditions at Cross-Section B-B' Across the Northern Side of the Moss Landing Marine Laboratory Site

XSECT-AA.SRF

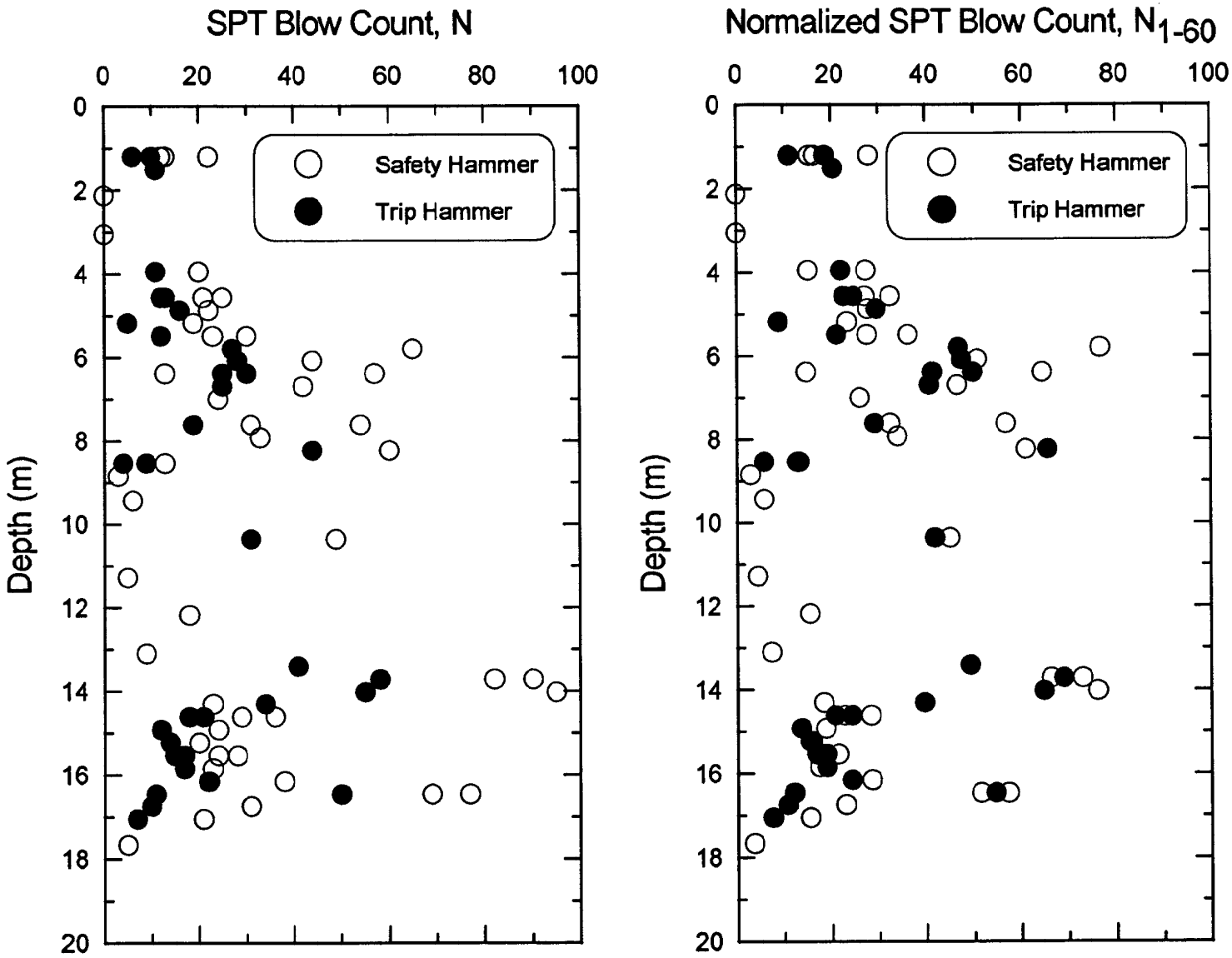


FIG. 9-7. Comparison of SPT Blow Counts Using Safety Versus Trip Hammers in a Grid of Eight Borings at Moss Landing Marine Lab (data by Fugro, Inc. 1980)

Fugro1.grf

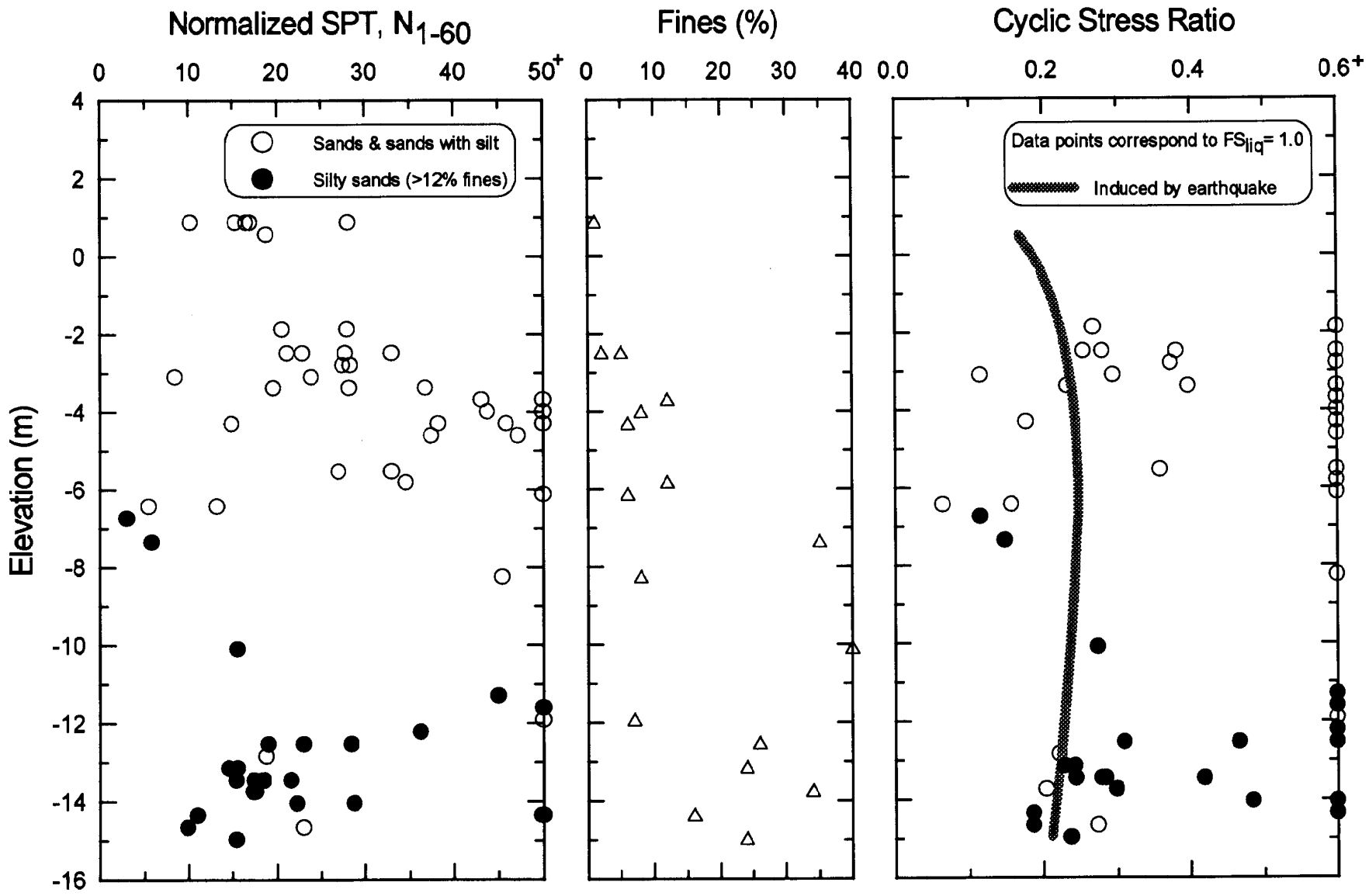


FIG. 9-8. Liquefaction Analysis of SPT Data From the Grid of Eight Borings at the Moss Landing Marine Lab (data by Fugro, Inc. 1980)

Fugliq1.grf

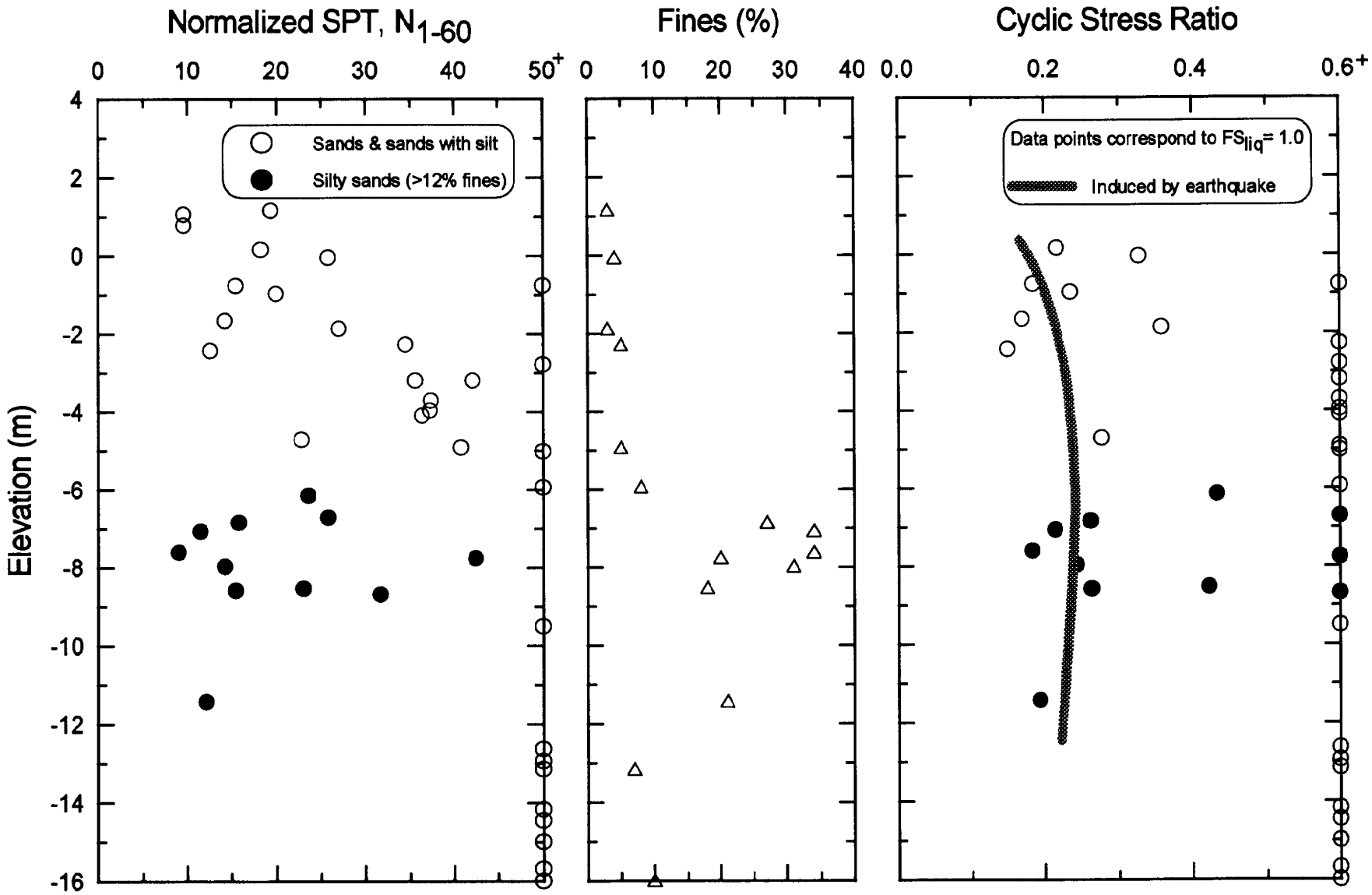


FIG. 9-9. Liquefaction Analysis of SPT Data From Borings B-1, B-2, and B-3 (by Woodward-Clyde) Consultants 1989) at the Moss Landing Marine Lab

WCCSPT1.grf

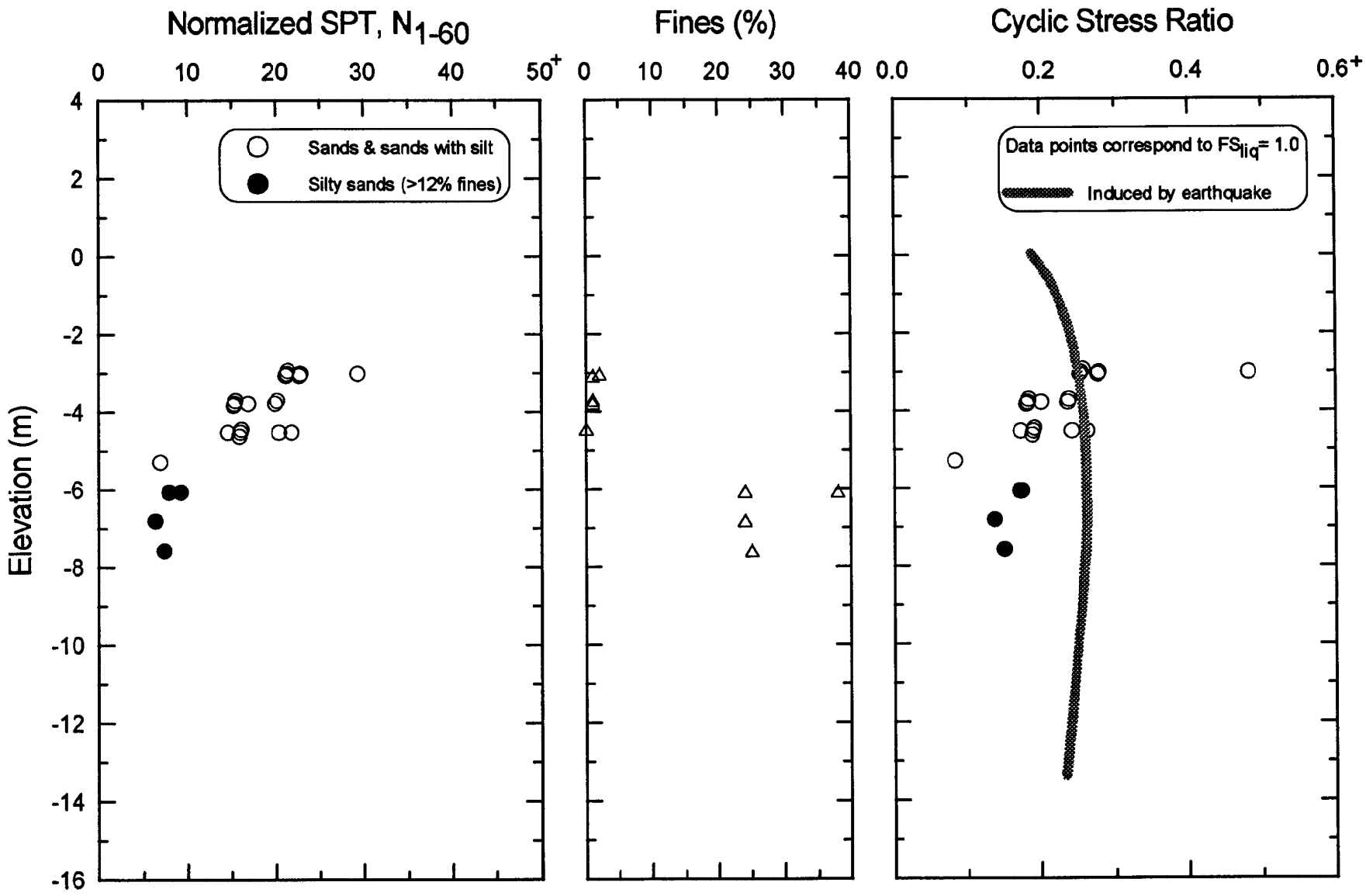


FIG. 9-10. Liquefaction Analysis of SPT Data From the Grid of Six Borings Near the Volley Ball Court at the Moss Landing Marine Lab

Volley1.grf

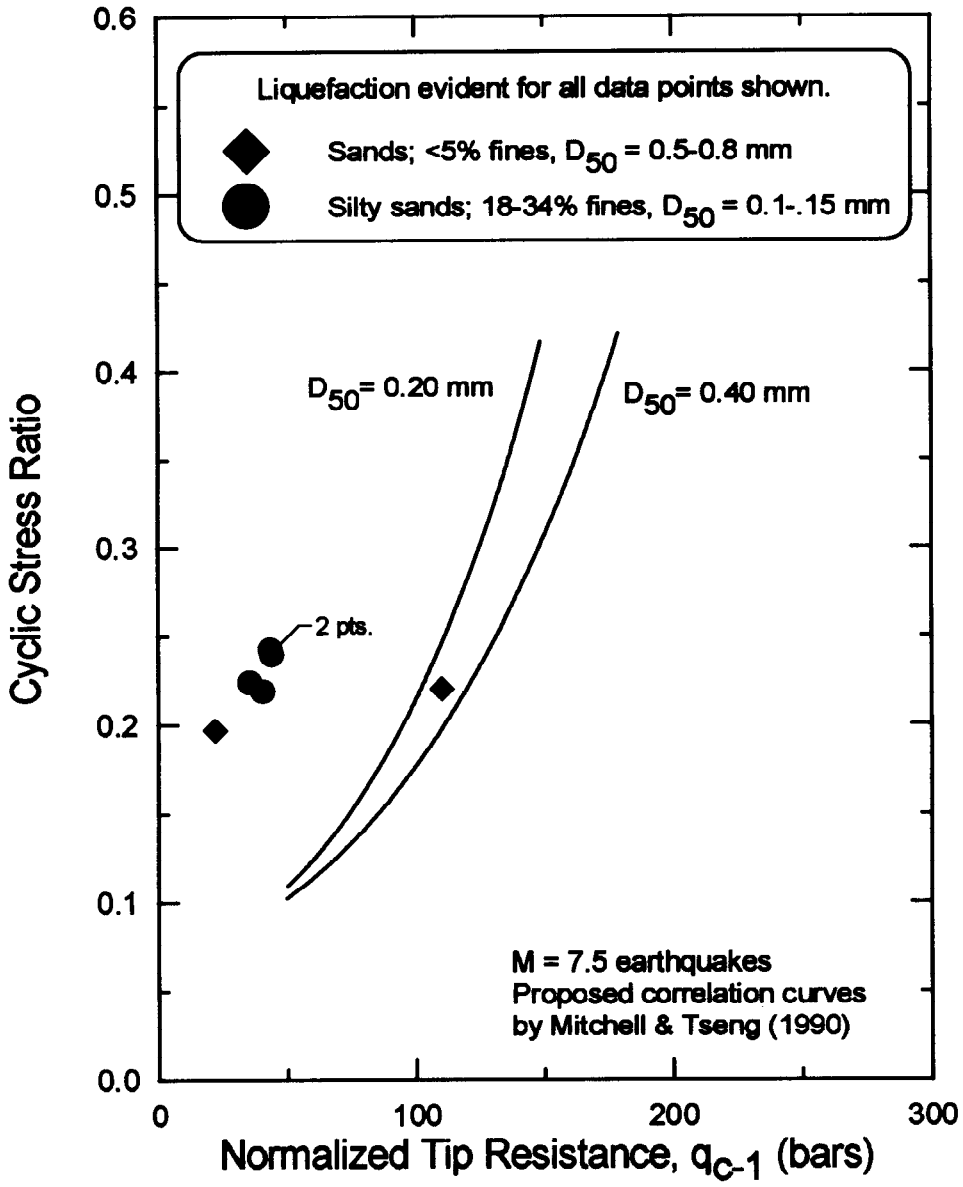


FIG. 9-11. Correlation of CPT Tip Resistance to Liquefaction Resistance at the Old Site of the Moss Landing Marine Laboratory

mlmlab-4.grf

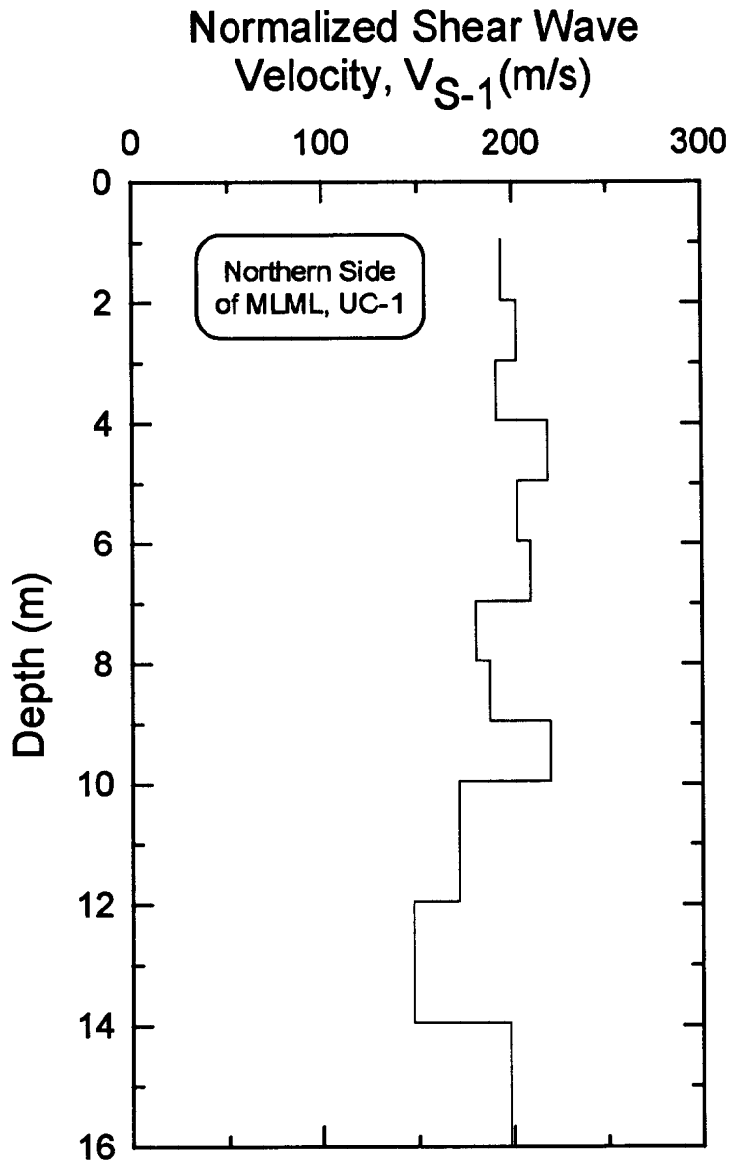


FIG. 9-12. Normalized Shear Wave Velocity Profile on Northern Side of the Moss Landing Marine Laboratory

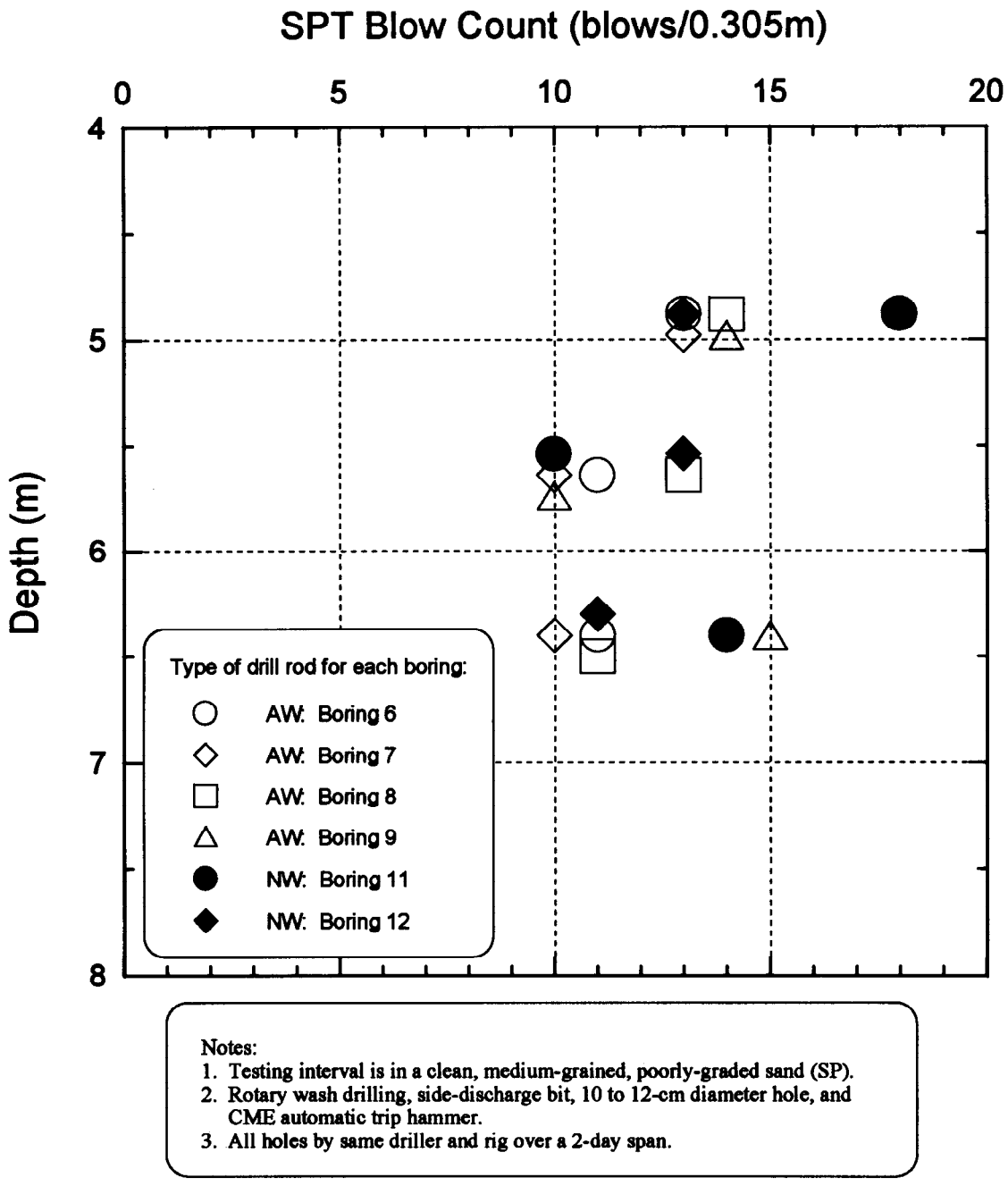


FIG. 9-13. Comparison of SPT Blow Counts Obtained With AW and NW Rods

## 10. OTHER SITES IN MOSS LANDING AREA

Ground deformations were observed at several additional sites in the Moss Landing area after the Loma Prieta earthquake. Reliable insitu test and site characterization data were not obtained at some of these additional sites for various reasons (i.e., accessibility, budget constraints, poorly defined exploration procedures for old data). Therefore, these sites will be only briefly described in this section.

The approach fills to the Highway No. 1 bridge across Elkhorn Slough were reported to have settled up to about 0.15 m, and thus was intermittently closed for repairs for a few days after the earthquake. Subsurface data along the alignment of the bridge are contained in the construction plans for the bridge (Caltrans 1985). The approach fills are underlain by a complex system of interlayered sand, silt, and clay. SPT blow counts are generally low in the shallower soils indicating relatively loose and soft soils. Liquefaction and earthquake-induced shear strains in these supporting soils beneath the approach fills would be reasonable consistent with established design methodologies. Unfortunately, details regarding the procedures used to perform the SPT tests are not generally available, and thus interpretation of the available data would be somewhat qualitative.

The 2,000 mW Pacific Gas and Electric Power Plant at Moss Landing suffered only minor damage during the Loma Prieta earthquake, and there was no evidence of liquefaction or significant soil movements near the main facilities. The large smoke stacks for Units 6 and 7 (Fig. 1-2) are visible in the background of Fig. 6-2. These large stacks are founded on piles 6 to 8 m long, while the generators and boilers are founded on thick concrete mats at elevations of about 0 m and 6.4 m, respectively. Subsurface data in this area were obtained from an engineering report by Dames and Moore (1963). The site is roughly flat at about elevation 8 m, and is underlain by medium-dense to dense sands to a depth of about 6 m, in turn underlain by dense- to very-dense gravelly sands with occasional thin layers of medium-stiff to stiff plastic clays and silts. The groundwater is generally at about elevation 0 m (i.e., close to mean sea level), and thus the upper 6 m of medium-dense to dense sands is likely not saturated. The apparent absence of liquefaction in the deeper dense- to very-dense gravelly sands is consistent with established design methodologies.

Large deformations were observed in the approach fills of the single-lane timber bridge that crosses the Old Salinas River providing access to the Moss Landing spit (Fig. 1-2). Liquefaction resulted in over 1 m of settlement and about 0.3 m of lateral deformations towards the river in the approach fill for the western end of the bridge. Near the west approach fill, the supporting timber piles for the bridge were displaced laterally at the mudline about 0.15 m on average. Referring to Figs. 2-1 and 2-2, it appears that the western approach fill is founded partially on fill placed in the river channel, and thus the subsurface conditions cannot be simply inferred from nearby explorations. Explorations at the location of the observed slumping were not possible because many utilities are buried in the approach fills and traffic accessibility to the businesses on the spit had to be always maintained. The eastern approach fill experienced settlements about 5 cm, but explorations were similarly not possible.

For a few hundred meters south of the MLML site, evidence of lateral spreading and liquefaction in the form of sinuous cracking and occasional graben-like features was observed. The south access road to the spit, beginning at the south tide gate to the Old Salinas River and joining

Sandholdt Road at the single-lane timber bridge across the river, was damaged because of settlement and lateral deformations associated with liquefaction.

North of the MBARI facilities, Pacific (Peninsula) Diesel, the old Fire Station, Gravelles' Boat Yard, and the north-east end of the Moss Landing spit were other notable cases of significant liquefaction-induced deformation and damage. Liquefaction-induced damage also occurred to the Moss Landing Harbor District's boat ramp located on the eastern side of the north harbor, requiring replacement of the boat ramp's precast concrete panel slabs.

# 11. DISCUSSION AND FINDINGS

## 11.1 General

Liquefaction appears to have primarily occurred in recent deposits at depths less than about 12 m. Liquefaction-induced deformations were often greatest along the shoreline of the harbor, which may be partly due to the presence of an exposed free-face and partly due to the sediments along the shoreline being the most recently deposited (as evidenced by historical shoreline location surveys summarized by Barminski 1993, and by aerial photographs).

Lateral deformation profiles obtained from the slope inclinometers located along Sandholdt Road suggest that deformations developed as relatively uniform shear strains over different strata, and not as deformations concentrated along individual failure planes. Slope inclinometers SI-2 and SI-5 along Sandholdt Road showed lateral deformations of 30 cm and 16 cm, respectively, developing as distributed shear strains over 2.5 m and 2.0 m thick intervals, respectively, of predominantly sand.

Thin strata of liquefiable soil were the source of significant deformations at some locations. Along Sandholdt Road, the 2.5 m and 2.0 m thick deformed intervals at slope inclinometers SI-2 and SI-5, respectively, both contained 0.5-0.6 m thick intervals having average normalized CPT tip resistances ($q_{c1}$) of 100-120 bars, while the remaining sands in the deformed intervals had substantially larger CPT tip resistances. Consequently, these 0.5-0.6 m thick intervals are believed to have had a dominant effect on the observed behavior of the slope, and contributed to deformations of the inclinometer tubes in the surrounding denser sands. At the Moss Landing Harbor District Facility, liquefaction of a 1 m thick layer of sand to sandy silt near Dock "C" resulted in deformations of about 15 cm horizontally and 30 cm vertically. These case histories show that significant ground deformations can develop due to liquefaction of relatively thin (0.5-1.0 m thick) continuous strata.

Behavior of fine-grained soils ranged from the apparent liquefaction of a clayey silt at the Moss Landing Marine Laboratory (MLML) to shear deformations of up to 0.7% in the silty clay and clayey silt strata along Sandholdt Road. Cyclic triaxial tests on Osterberg tube samples from the clayey silt stratum on the eastern side of the MLML site indicate that these soils are susceptible to developing significant strains and high residual excess pore pressures at the level of shaking experienced during the Loma Prieta earthquake, and thus likely contributed to the observed ground deformations (Meyers 1995). Along Sandholdt Road, data from the slope inclinometers showed: (1) the uppermost clayey silt layers, which intrude laterally from the harbor, experienced shear strains of 0% and 0.7% at the locations of SI-2 and SI-4, respectively; (2) the upper continuous stratum of soft- to medium-stiff, silty clay experienced shear strains of 0%, 0.3% and 0.3% at the locations of SI-2, SI-4 and SI-5, respectively; and (3) the lower continuous stratum of stiff- to very-stiff, silty clay experienced no deformations. These data may prove useful in further studies regarding the behavior of fine-grained soils during earthquake loading.

The type of construction was an important factor in the performance of pile-supported piers and docks along the Moss Landing spit. The Monterey Bay Aquarium Research Institute's (MBARI) pier, which is supported by reinforced concrete piles, performed very well, experiencing no measurable lateral or vertical displacements despite the 8-25 cm of lateral spreading deformations in

the adjacent roadway. In contrast, many older piers and docks supported on timber piles experienced large deformations because of lateral spreading deformations in the surrounding soils; e.g., timber piles supporting Gravelle's Boatyard dock displaced up to 0.4 m laterally at the waterline, and timber pile supports for the timber bridge across the Old Salinas River displaced laterally up to 0.15 m at the mudline.

## 11.2 Evaluation of Liquefaction Based on SPT and CPT Data

The SPT based approach of Seed et al. (1985) provided good agreement between the predicted occurrence/non-occurrence of liquefaction at the sites investigated, although the discrete sampling nature of the SPT provided insufficient detail at sites where the liquefiable strata were relatively thin (e.g., less than 1.5-m-thick).

The CPT based curves of Seed and De Alba (1986) did not always predict liquefaction where liquefaction was observed, which suggests that this procedure is not as inherently conservative as is often assumed by practicing engineers. Seed and De Alba's (1986) procedure was developed by applying $q_c/N_{60}$ ratios to the SPT based curves of Seed et al. (1985). While the SPT based curves of Seed et al. (1985) are generally considered a reasonably conservative enveloping of the empirical data, the inherent scatter of $q_c/N_{60}$ correlations about their mean (corresponding roughly to the values used by Seed and De Alba) introduces considerable scatter into the resulting CPT based procedure.

The CPT based curves of Mitchell and Tseng (1990) provided improved agreement with the occurrence/nonoccurrence of liquefaction in the Moss Landing area. The curves of Mitchell and Tseng (1990) are compared to the curves of Seed and De Alba (1986) in Fig. 11-1. For a given normalized CPT tip resistance, Mitchell and Tseng's curves for clean sand (<5% fines) would predict a lower cyclic strength than would be predicted by the curves of Seed and De Alba (1986).

Critical combinations of normalized CPT tip resistance and earthquake-induced cyclic stress ratio obtained in this study are summarized in Fig. 11-2 for clean sands and in Fig. 11-3 for silty sands. Mitchell and Tseng's (1990) curves for clean sand are also shown on these Figs. Earthquake-induced cyclic stress ratios were adjusted to equivalent cyclic stress ratios for M=7.5 earthquakes based on the ratios presented by Seed and Idriss (1982). In Figs. 11-2 and 11-3, the data points labelled as "medium-confidence" include those cases where: (1) the soil layer(s) responsible for observed ground deformations could not be conclusively identified based on the field evidence, and thus its selection involved considerable judgement; (2) the CPT tip resistance in the suspected critical layer was difficult to estimate due to insufficient layer thickness and/or the influence of contacts with soils of significantly different penetration resistances; and (3) a CPT location was labelled as "liquefied" or "nonliquefied" based on subjective field observations without the benefit of strong field evidence, such as provided by survey data or appropriate structural features, in its immediate vicinity. The two "liquefied" data points that plot below Mitchell and Tseng's curves in Fig. 11-2 are both "high-confidence," and correspond to the State Beach (near the beach pathway; $D_{50} \approx 0.4$ mm) and Sandholdt Road (adjacent to slope inclinometer SI-2; $D_{50} \approx 0.8$ mm). The remaining data are in good agreement with the curves of Mitchell and Tseng (1990).

In selecting the critical value of normalized CPT penetration resistance for each CPT sounding, several guidelines were adopted to reduce the potential differences in values that may be

obtained by different individuals. The first guideline was the use of a 0.6 m thick interval for averaging tip resistances in the critical layer, with the critical tip resistance being the lowest average; Additional guidelines regarding layers of insufficient thickness and the influence of contacts with softer soils are described in Section 1.3. Use of a 0.6 m continuous interval is consistent with the thicknesses of strata that were the source of significant deformations at slope inclinometers SI-2 and SI-5, and incidentally corresponds to the approximate minimum measurement interval of a SPT test.

The importance of establishing guidelines for determining critical tip resistances is illustrated in Fig. 11-4, which shows how the "critical tip resistance" can vary significantly with the "thickness of interval for averaging" for six different CPT soundings. In the extreme, critical tip resistances obtained with a 1.5 m averaging interval were up to 100% higher than those obtained with a 0.1 m averaging interval. Since CPT tip resistances are commonly recorded every 5 cm during penetration, a 0.1 m averaging interval only contains 2 measurements while a 1.5 m averaging interval contains 30 measurements. Over a more reasonable range of averaging interval thicknesses, the differences in critical tip resistance are not as significant. A reasonable upper limit for the averaging interval is probably about 0.6 m (as was used to generate Figs. 11-2 and 11-3) because continuous layers of this thickness can be a source of significant deformations. A lower limit for the averaging interval is more subjective, but 0.3 m may be considered a reasonable alternative to the 0.6 m averaging interval; Note that the guidelines would still provide for a smaller averaging interval to be used when evaluating thin sand lenses. For CPT tip resistance measurements taken every 5 cm during penetration, averaging intervals of 0.3 and 0.6 m would contain 6 and 12 measurements, respectively.

Subsequently, the data obtained in this study were re-evaluated using the guidelines in Section 1.3 but with a 0.3 m averaging interval. Critical CPT tip resistances obtained with the revised guidelines (0.3 m averaging interval) ranged from 0-22% lower, but most typically 5-15% lower, than those obtained using the original guidelines (0.6 m averaging interval). The re-evaluated data for clean sands, as summarized in Fig. 11-5, are also in reasonable agreement with the curves of Mitchell and Tseng (1990). While additional research is needed to evaluate the most appropriate set of guidelines for calculating critical tip resistances, it is essential that guidelines be established to provide a reasonable level of consistency between the development of semi-empirical correlations and their subsequent application in practice.

Pairing of CPT soundings with SPT borings was shown to provide considerably more valuable information for evaluating liquefaction potential than is obtained by either insitu testing method alone. CPT soundings identified SPT blow counts affected by overlying or underlying adjacent strata, and enabled more reliable characterization of relatively thin liquefiable strata. SPT samples, however, were essential for reliable interpretation of some strata's characteristics, and the blow count data were useful for developing site-specific $q_c/N_{60}$ ratios. This study provides additional examples of the long recognized and advocated advantages of pairing SPT and CPT field investigations (e.g., Seed and De Alba 1986).

## 11.3 Correlations of Shear Wave Velocity Data With Liquefaction Resistance

Shear wave velocity measurements using 1.0-2.0 m measurement intervals were ineffective in characterizing the critical strata at several locations because the measurement intervals crossed over two or more thin strata of significantly different characteristics. Consequently, critical values of

normalized shear wave velocity and cyclic stress ratio could only be calculated for locations where the measurement intervals coincided reasonably well with the suspected critical strata. This difficulty with characterizing strata less than 1 m thick is a significant limitation on the use of shear wave velocity correlations for predicting the occurrence of liquefaction, because liquefaction of such strata can result in significant deformations.

Data for those locations where measurements of shear wave velocity coincided reasonably well with the suspected critical strata are compared to the boundary curves proposed by Robertson et al. (1992) and Tokimatsu et al. (1991) in Fig. 11-6. Cyclic stress ratios are adjusted to equivalent cyclic stress ratios for M=7.5 earthquakes based on the ratios presented by Seed and Idriss (1982). As described in Section 1.3, the correlation proposed by Robertson et al. (Fig. 1.6) requires shear wave velocities to be normalized using

$$V_{s1} = V_s (P_a/\sigma_v')^{0.25}$$

while the correlation proposed by Tokimatsu et al. (Fig. 1-7) uses

$$V_{s1} = V_s (P_a/\sigma_m')^{0.33}$$

Mean effective stresses ($\sigma_m'$) were calculated based on a coefficient of earth pressure at rest ($K_o$) of 0.5 which is a reasonable value for these recent, and likely normally consolidated, deposits. For this value of $K_o$ and the range of effective overburden stresses involved ($\sigma_v'$ of 35-100 kPa), the $V_{s1}$ values calculated using Tokimatsu et al.'s method are 15-25% larger than the values calculated using Robertson et al.'s method. In Fig. 11-6, the data point corresponding to the "West side of Sandholdt Road" (CPT UC-6, across Sandholdt Road from slope inclinometer SI-5) is labelled as "medium-confidence" because its classification as "No liquefaction" is based on subjective field observations. The resulting data are in better agreement with the boundary curve proposed by Robertson et al. (1992), than with the boundary curve proposed by Tokimatsu et al. (1991).

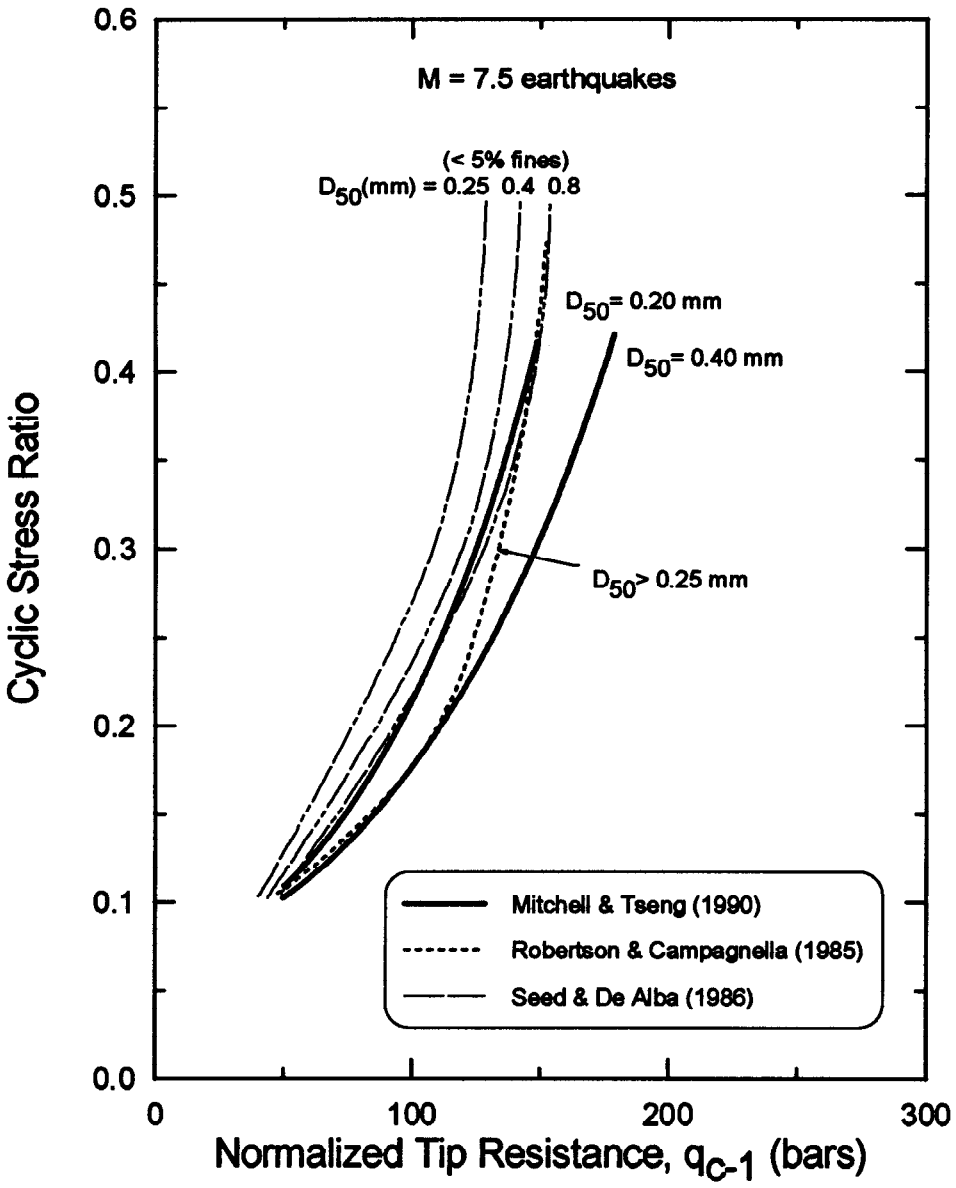


FIG. 11-1. Comparison of Proposed Boundary Curves for Liquefaction Resistance Evaluations Using CPT Data

qc-liq-1.grf

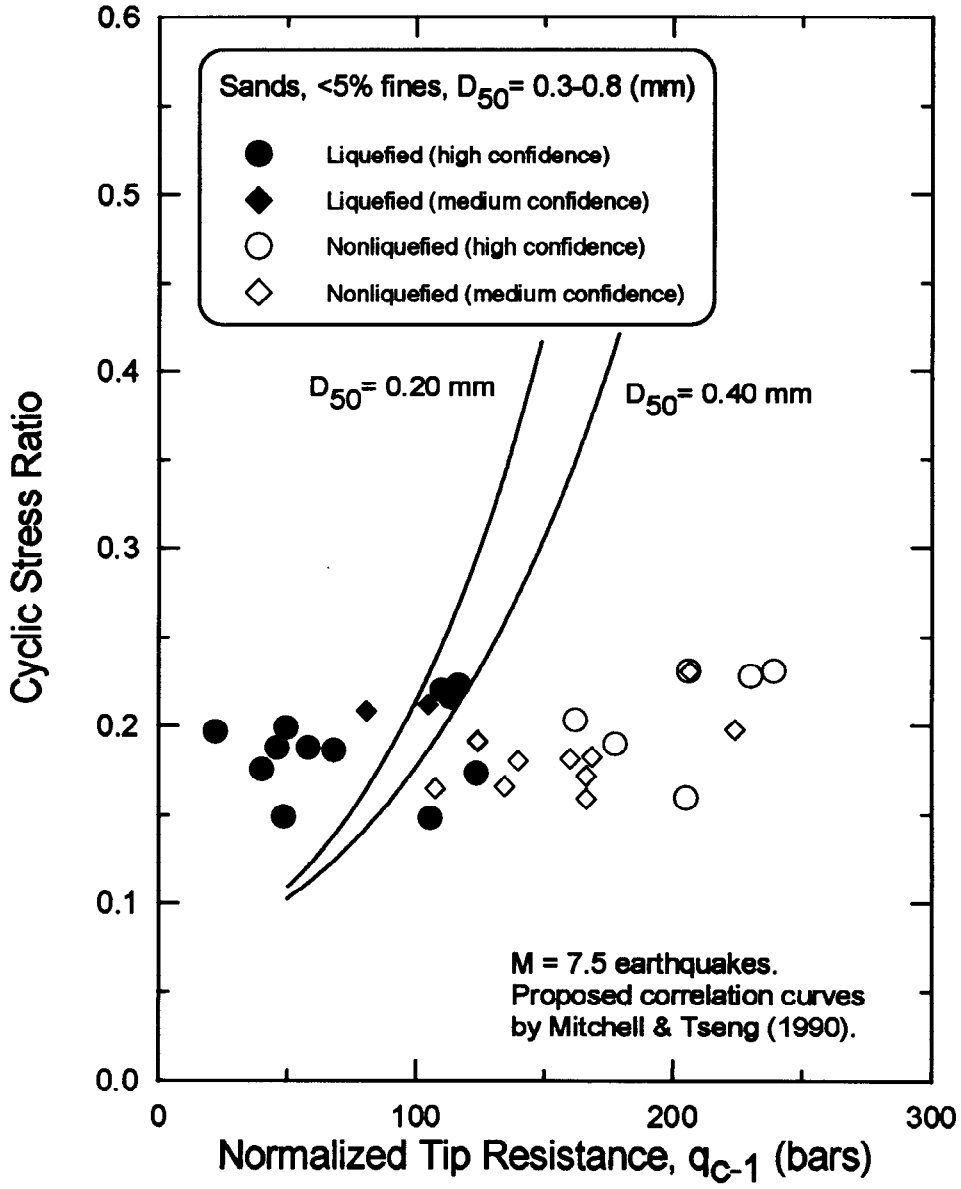


FIG. 11-2. Critical Combinations of CPT Tip Resistance and Cyclic Stress Ratio For Sands in the Moss Landing Area; Based on Guidelines With a 0.6 m Interval For Averaging of CPT Tip Resistances

CPTCOR1S.GRF

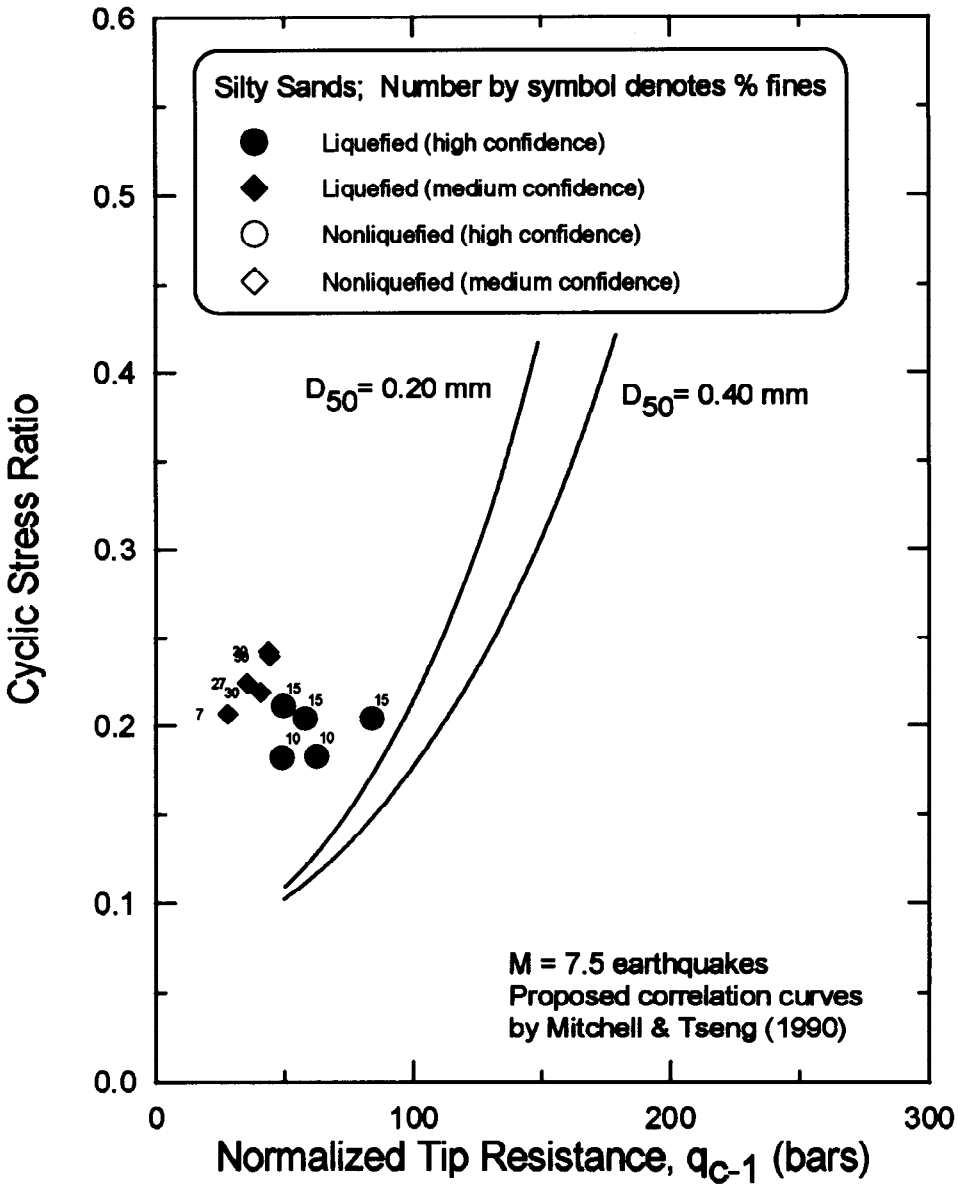


FIG. 11-3. Critical Combinations of CPT Tip Resistance and Cyclic Stress Ratio For Silty Sands in the Moss Landing Area; Based on Guidelines With a 0.6 m Interval For Averaging of CPT Tip Resistances

CPTCOR1M.GRF

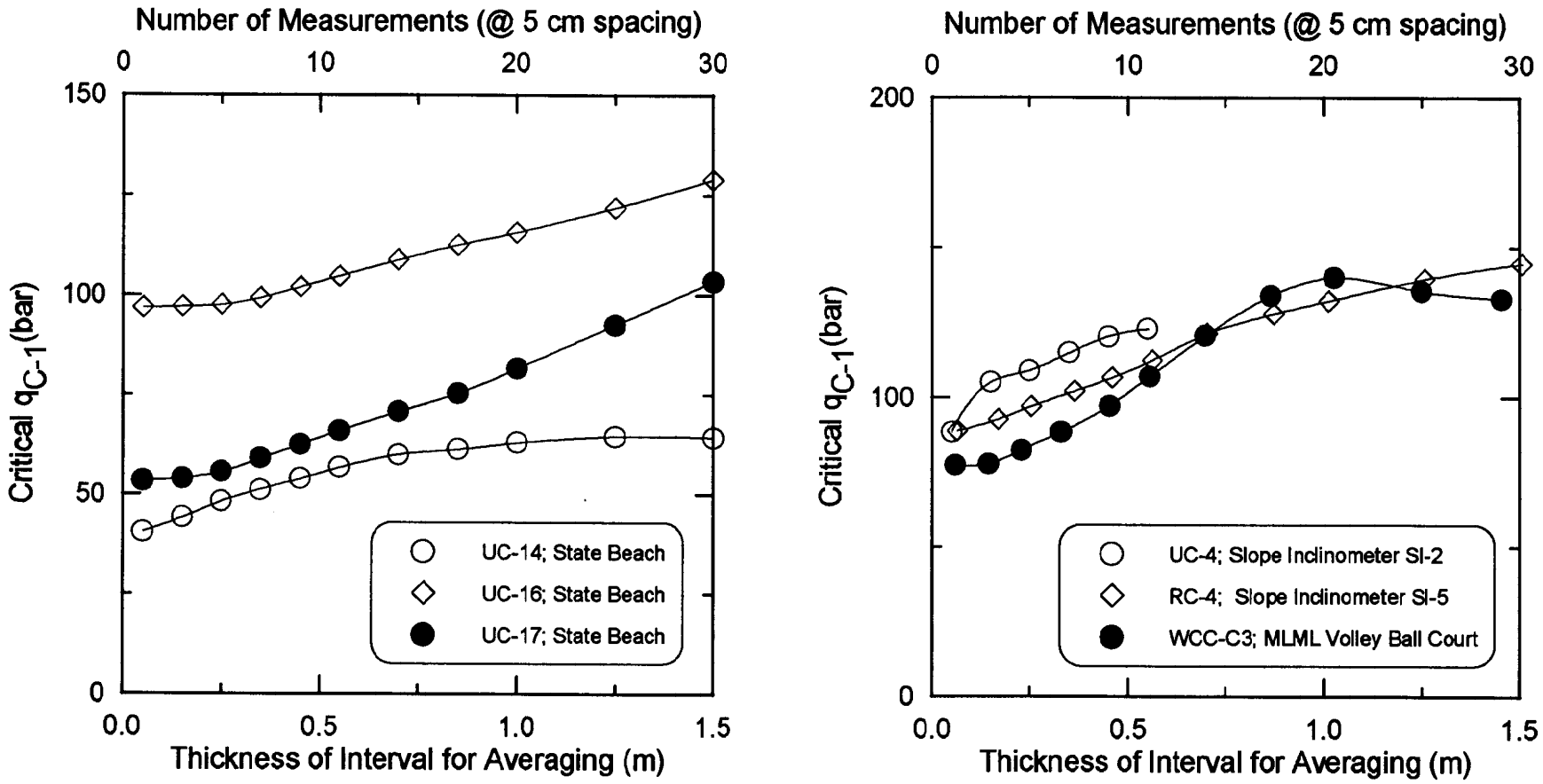


Fig. 11-4. Critical CPT Tip Resistance Versus the Thickness of the Interval Used For Averaging

InterSum.gr1

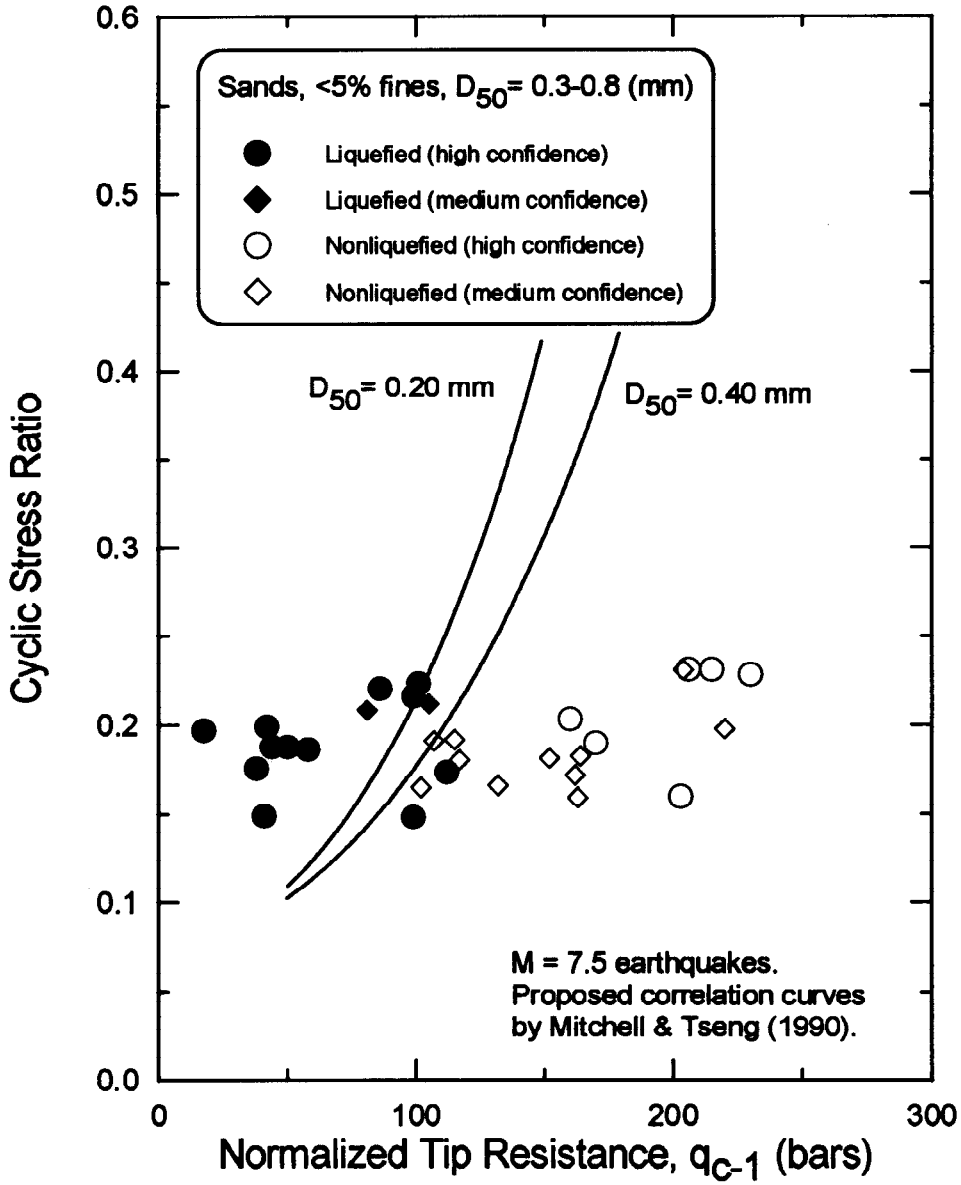


FIG. 11-5. Critical Combinations of CPT Tip Resistance and Cyclic Stress Ratio For Sands in the Moss Landing Area; Based on Guidelines With a 0.3 m Interval For Averaging of CPT Tip Resistances

CPTCOR2S.GRF

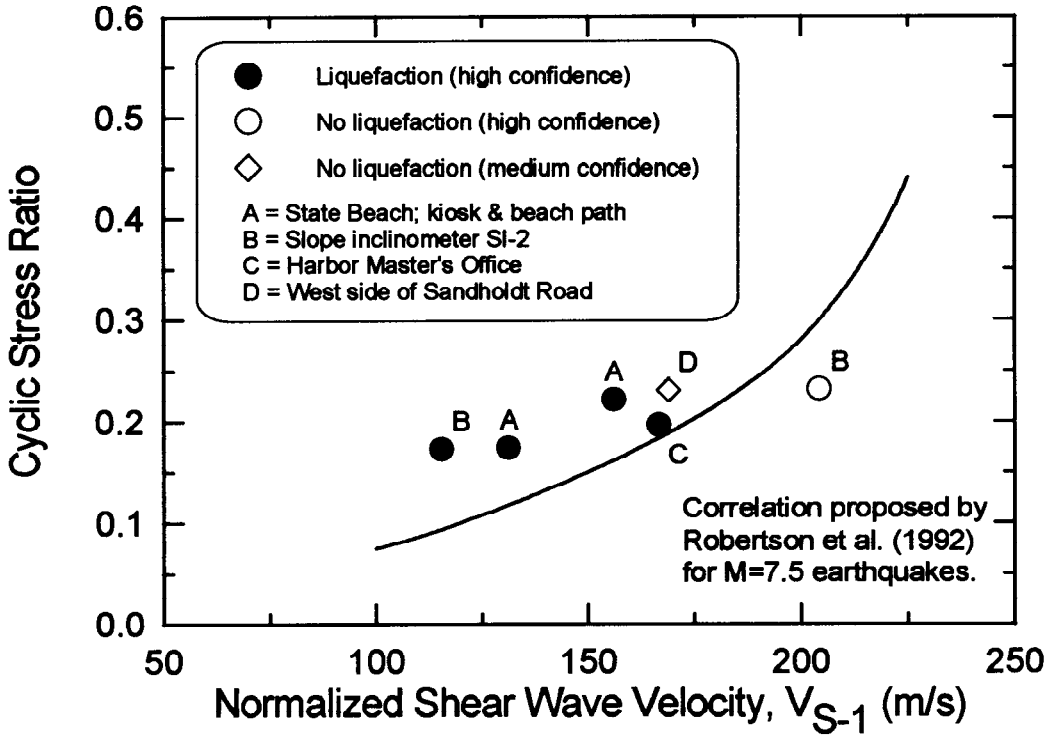


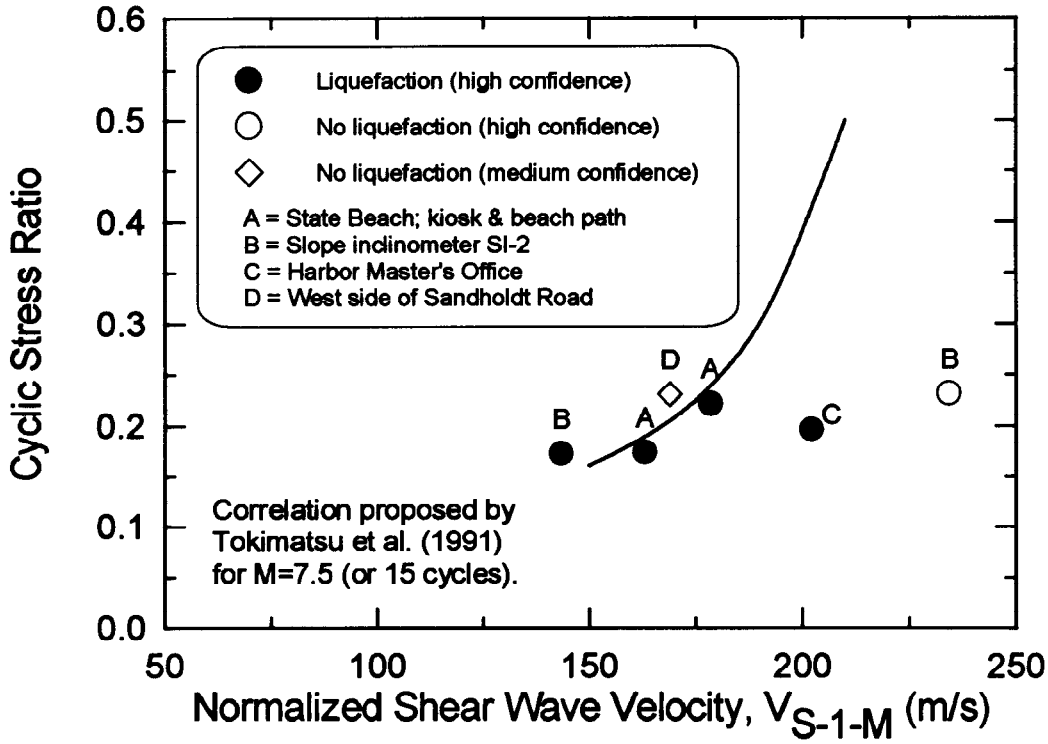


FIG. 11-6. Correlation Between Cyclic Stress Ratio and Normalized Shear Wave Velocity for Sands

# 12. CONCLUDING REMARKS

This report summarizes the results of an investigation and evaluation of liquefaction related ground displacements from several locations in the Moss Landing area during the Loma Prieta earthquake. Moss Landing, located midway between Santa Cruz and Monterey on the Monterey Bay, suffered widespread damage to structures and facilities because of liquefaction induced deformations, including the near collapse of the $6 million Moss Landing Marine Laboratory. This study provides information regarding the range of earthquake effects and ground displacements observed, the various soils encountered, detailed stratigraphy for several sites, the different insitu testing methods used, and a unique set of inclinometer data within a laterally spreading shoreline. Analyses of these data, presented herein, provide insight into the applicability/reliability of commonly used methodologies for predicting the occurrence and effects of earthquake-induced liquefaction.

It is hoped that the data and results presented in this report will provide a basis for further development of semi-empirical correlations for predicting the potential for liquefaction-related damage during earthquakes. Toward this goal, the data from this study were compared against selected semi-empirical correlations between liquefaction resistance and the results of SPT, CPT, or shear wave velocity tests. The results of this comparison and other specific findings of this study were discussed in Section 11. Ultimately, it is hoped that the data and findings of this study will contribute to the NERHP goal of earthquake hazards mitigation.

## REFERENCES


Abou-matar, H. and Goble, G. G. (1995). "Measurements on the standard penetration test." Accepted for publication by the Journal of Geotechnical Engineering, ASCE.

Brian Kangas Foulk, Inc. (1989). Post-earthquake survey, Moss Landing Marine Laboratories. Prepared for the California State University, San Jose, California, 1 pp.

Barminski, R. F., Jr. (1993). "Onshore and offshore effects of the 1989 Loma Prieta earthquake in the Moss Landing, California area." A Master of Science thesis presented to the Faculty of the Moss Landing Marine Laboratories, San Jose State University, December, 48 pp.

Caltrans (1985). Elkhorn Slough Bridge (No. 44-74), As-Built Plans, State of California, Department of Transportation, Sheets 12 and 13.

Coastland Consultants (1991). Woodward Marine, Project Plan, Moss Landing Harbor. Plans prepared 1-21-91, 4 sheets, by Coastland Consultants, Salinas, California.

Cooper Clark and Associates (1978). Preliminary Geotechnical Evaluation, Moss Landing Marine Laboratories. Prepared for California State University, San Jose, California, October 6.

Creegan and D'Angelo (1990). Moss Landing Harbor District, Harbor Master Parking Area: Earthquake Damage Repair. Plans prepared for the Moss Landing Harbor District Office, September 17, 5 sheets.

Dames and Moore (1963). Foundation Investigation, Moss Landing Power Plant Units 6 and 7, Moss Landing, California. Prepared for the Pacific Gas and Electric Company, November 21.

Department of Commerce (1988). Tide Tables 1989, High and Low Water Predictions, West Coast of North and South America. National Oceanic and Atmospheric Administration, U.S. Department of Commerce.

Dobry, R. and Baziar, M. H. (1992). "Modelling of lateral spreads in silty sands by sliding soil blocks." Proc., Stability and Performance of Slopes and Embankments - II, A 25-Year Perspective. Geotechnical. Special Pub. No. 31, Vol. 1, pp. 625-652.

Dupre and Tinsley (1980). Geology and liquefaction potential, northern Monterey and southern Santa Cruz Counties, California. U.S. Geological Survey Miscellaneous Field Studies Map MF-1199, 1:62,500.

EERI (1990). Loma Prieta Earthquake Reconnaissance Report. Earthquake Engineering Research Institute (EERI), Earthquake Spectra J., Supplement to Volume 6, May, pp. 448.

Fugro, Inc. (1980). Evaluation of the Cone Penetrometer for Liquefaction Hazard Assessment. Principal Investigators: G. R. Martin and B. J. Douglas. Prepared for the U. S. Department of the Interior, Geological Survey, Menlo Park, California, October.

Gordon, B. L. (1977). Monterey Bay Area: Natural History and Cultural Imprints. Boxwood Press, 321 pp.

Gray, Ken (1993). Department of Parks and Recreation. Personal communication.

Greene, H. G., Gardner-Taggart, J., Ledbetter, M. T., Barminski, R., Chase, T. E., Hicks, K. R., and Baxter, C. (1991). "Offshore and onshore liquefaction at Moss Landing spit, central California - Result of the October 17, 1989, Loma Prieta earthquake." Geology, Vol. 19, p. 945-949, September.

Griggs, G. B. (1990). "An evaluation of coastal hazards at Moss Landing Marine Laboratory Site." Prepared for Chancellor's Office of the California State University, February 15.

Harder, L. F. (1994). Department of Water Resources, State of California. Personal communication.

Harding Lawson Associates (1988). Geotechnical Investigation, Dredging and Slope Improvements, Moss Landing South Harbor. Prepared for the Moss Landing Harbor District, January 15.

Idriss, I. M. (1991). "Response of soft soil sites during earthquakes." H. Bolton Seed Memorial Symposium Proceedings, Editor J. M. Duncan, Vol. 2, pp. 273-289.

Idriss, I. M. (1991). Procedures for selecting earthquake ground motions at rock sites. A report to the National Institute of Standards and Technology, U. S. Department of Commerce, September: revised March 1993.

Ishihara, K. (1993). "Liquefaction and flow failure during earthquakes." Geotechnique 43, No. 3, pp. 351-415.

Jones, L. (1989). Moss Landing Marine Laboratory. Personal communication.

Khasali, G. (1993). Rutherford and Chekene. Personal communication.

Koester, J. P. (1992). "Cyclic strength and pore pressure generation characteristics of fine-grained soils." Ph.D. thesis for University of Colorado, November.

Kutter, B. L. (1994). University of California at Davis. Personal communication.

Lawson, A. C. (1908). The California earthquake of April 18, 1906: Report of the State Earthquake Investigation Commission, Carnegie Institution of Washington Publication 87, Washington, D.C., 3 Vols.

Liao, S. C. and Whitman, R. V. (1985). "Overburden correction factors for SPT in sand." Journal Geotechnical Engineering Division, ASCE, Vol. 112, No. 3, pp. 373-377.

Makdisi, F. I. and Seed, H. B. (1978). "Simplified procedure for estimating dam and embankment earthquake-induced deformations." Journal of the Geotechnical Engineering Division, ASCE, Vol. 104, No. GT7.

Mejia, L. H. (1992). "Liquefaction at Moss Landing." Submitted contribution to the NEHRP Report to Congress on the Loma Prieta, California, Earthquake of October 17, 1989, April.

Meyers, M. (1995). Behavior of a silt during the Loma Prieta earthquake. Masters thesis, University of California, Davis. In preparation.

Michael David Obele & Associates (1967). Soil investigation for Moss Landing Harbor Office Building. A report prepared for the Moss Landing Harbor District.

Mitchell, J. K. and Tseng, D.-J. (1990). "Assessment of liquefaction potential by cone penetration resistance." H. Bolton Seed Memorial Symposium Proceedings, Editor J. M. Duncan, Vol. 2, pp. 335-350.

Newmark, N. M. (1965) Effects of earthquakes on dams and embankments." Geotechnique, London, England, Vol. 5, No. 2, pp. 139-160.

Raggett, J. D. & Associates, Inc. (1989). Post-earthquake (10/17/89) Structural Survey, Moss Landing Marine Laboratory, California State University, Moss Landing, California. October 19.

Robertson, P. K., Woeller, D. J., and Finn, W. D. L. (1992). "Seismic cone penetration test for evaluating liquefaction potential under cyclic loading." Canadian Geotechnical Journal, Vol 29, No. 4, August, pp. 686-695.

Rutherford and Chekene (1987). Geotechnical Hazard Evaluation: Moss Landing Facility, Monterey Bay Aquarium Research Institute. Prepared for the Monterey Bay Aquarium Research Institute, December 30.

Rutherford and Chekene (1988). Geotechnical Investigation: Moss Landing Facility (Technology Building), Monterey Bay Aquarium Research Institute. Prepared for the Monterey Bay Aquarium Research Institute, April 11.

Rutherford and Chekene (1993). Geologic Hazards Evaluation/Geotechnical Investigation: Monterey Bay Aquarium Research Institute Buildings 3 and 4. Prepared for the Monterey Bay Aquarium Research Institute, February 16.

Seed, H. B., and De Alba, P. (1986). "Use of SPT and CPT tests for evaluating the liquefaction resistance of sands." Use of In Situ Tests in Geotechnical Engineering, Geotechnical Special Publication No. 6, Virginia Tech, Blacksburg, Virginia, June 23-25.

Seed, H. B. and Idriss, I. M. (1971). "Simplified procedure for evaluating soil liquefaction potential." Journal Soil Mechanics and Foundations Division, ASCE, 97:SM9, Sept., pp. 1249-1273.

Seed, H. B., Tokimatsu, K., Harder, L. F., and Chung, R. M. (1985). "Influence of SPT procedures in soil liquefaction resistance evaluations." Journal Geotechnical Engineering Division, ASCE, Vol. 111, No. 12.

Seed, R. B. and Harder, L. F. (199). "SPT-based analysis of cyclic pore pressure generation and undrained shear strength." H. Bolton Seed Memorial Symposium Proceedings, Editor J. M. Duncan, Vol. 2, pp. 351-376.

Shakal, A., Huang, M., Reichle, M., Ventura, C., Cao, T., Sherburne, R., Savage, M., Darragh, R., and Petersen, C. (1989). "CSMIP strong-motion records from the Santa Cruz Mountains (Loma Prieta), California earthquake of 17, October 1989." Report No. OSMS 89-06, California Strong Motion Instrumentation Program, Division of Mines and Geology, California Department of Conservation, Sacramento, California, November 17, 184 p.

Souza, Ron (1993). Assistant Harbor Manager, Moss Landing Harbor. Personal communication.

State of California (1990). Moss Landing State Beach, General Plan, September 1990. Department of Parks and Recreation, Sacramento, California.

Sumerville and Yoshimura (1990). "Strong motion modeling of the October 17, 1989 Loma Prieta earthquake. AGU Abstract.

Taber, F. (1994). Taber Consultants, West Sacramento. Personal communication.

Tillis, K. (1990). Harding Lawson and Associates. Personal communication.

Tinsley, J. C. (1993). U. S. Geological Survey. Personal communication.

Tokimatsu, K., Kuwayama, S. and Tamura, S. (1991). "Liquefaction potential evaluation based on Rayleigh wave investigation and its comparison with field behavior." Proc., Second International Conference on Recent Advances in Geotechnical Earthquake Engineering and Soil Dynamics, March 11-15, St. Louis, Missouri, Paper No. 3.8.

Tuttle, M., Cowie, P., Tinsley, J., Bennett, M., and Berrill, J. (1990). "Liquefaction and foundation failure of Chevron oil and gasoline tanks at Moss Landing, California." Geophysical Research Letters, Vol. 17, No. 4, pp. 56-74.

Wang, W. S. (1979). "Some findings in soil liquefaction." Research Institute of Water Conservancy and Hydroelectric Power, Beijing, China, August.

Wald, D. J., Burdick, L. J., and Somerville, P. G. (1988). "Simulation of acceleration time histories close to large earthquakes." Proceedings of specialty conference, Earthquake Engineering and Soil Dynamics II - Recent Advances in Ground-Motion Evaluation. Geotechnical Engineering Division, ASCE.

Waterman & Kuska Architects (1967). Office for the Moss Landing Harbor District. Plans prepared for the Moss Landing Harbor District. Courtesy of Moss Landing Harbor District Office.

Woodward-Clyde Consultants (1990). Phase I - Geotechnical Study, Marine Biology Laboratory, California State University, Moss Landing California. Prepared for the California State University, January.

Youd, T. L. and Bennett, M. (1983). "Liquefaction sites - Imperial Valley, California." Journal of Geotechnical Engineering, ASCE, 109(3), 440-457.

Youd, T. L. and Hoose, S. N. (1978). "Historic ground failures in northern California triggered by earthquakes." U.S. Geological Survey Profession Paper 993, U.S.G.S., Denver, CO, 177 p.